博士論文

New bioactive sponge metabolites discovered through cell-based assays

（培養細胞系アッセイによってカイメンから見いだした新規生物活性物質に関する研究）

Laboratory of Aquatic Natural Products Chemistry

Graduate School of Agricultural and Life Sciences

The University of Tokyo

Supervisor: Professor Shigeki Matsunaga

Yuki Hitora

人羅　勇気

Table of Contents

Acknowledgments.

I am grateful Professor Shigeki Matsunaga for providing me a chance to join the laboratory of aquatic natural products chemistry, and great support for my research. I would like to express my gratitude to Associate Professor Shigeru Okada and Assistant Professor Kentaro Takada for giving me insightful suggestions and discussions during the research. I am particularly grateful for the supports given by my lab members.

I would like to thank Assistant Professor Yuji Ise for identifying the marine sponges. I thank Professor Makoto Fujita, Department of Applied Chemistry, The University of Tokyo, and Professor Kenji Mori, Professor Emeritus, The University of Tokyo, for valuable discussion about the absolute configuration of miyakosyne A.

I thank the crew of R/V Natushima, for collecting a sponge *Petrosia* sp. and unidentified sponges S09-1060-01 and S09-1061-002. I thank Professor Susumu Otsuka and the crew of Toyoshio-maru in Hiroshima University for collecting an unidentified marine sponge S13-013. I thank Dr. Y. Ito, JEOL, for valuable advice about the measurement of tandem FABMS.

I would also like to express my gratitude to JSPS for the financial support.

List of Abbreviations

AcOH	acetic acid
^{1}H	proton
^{13}C	carbon thirteen
COSY	correlation spectroscopy
DMSO	dimethyl sulfoxide
DQF-COSY	double quantum filtered-COSY
FABMS	fast atom bombardment mass spectrometry
FDA	Food and Drug Administration
Fucci	fluorescent ubiquitination-based cell cycle Indicator
HMBC	heteronuclear multiple bond coherence spectroscopy
HSQC	heteronuclear multiple quantum coherence spectroscopy
MeCN	acetonitrile
MeOH	methanol
MTT	3-(4,5-Dimethyl-2-thiazolyl)-2,5-diphenyl-2H-tetrazolium bromide
NMR	nuclear magnetic resonance
NOESY	nuclear Overhauser enhancement spectroscopy
PI	propidium iodide
ROESY	rotating frame nuclear Overhauser enhancement spectroscopy
TOCSY	total correlation spectroscopy

Chapter 1.

General Introduction

The dawn of marine natural product chemistry goes back to the 1950s with the discovery of nucleoside analogues from a marine sponge.[1] Continuing study of metabolites of marine organisms led to the discovery of a large number of fascinating bioactive compounds from various marine flora and fauna, including sponges, corals, ascidians, sea weeds, and marine bacteria.[2] Marine sponges are known to be particularly rich sources of bioactive metabolites, and more than 25,000 metabolites have been identified so far.[3] The driving force that motivates scientists to discover new compounds from marine organisms is their structural diversity and unique bioactivity.[4]

The potential of marine natural products has been verified as leads for drug development, and the importance of identification of novel bioactive compounds from marine organisms has been increasing. Recent technological breakthroughs permitted us to access deeper fields of marine natural products chemistry and accelerated the discovery of bioactive marine natural products.[3] For example, development of

mass-sensitive NMR techniques enabled the structure analysis of submilligram samples and made it easier to access rare minor constituents of marine organisms.[5] Moreover, improvements of sensitivity of mass spectrometer resulted in the development of new research fields: metabolomics and molecular networking of natural product.[6, 7] The innovative research of X-ray crystallography demonstrated its potential as new effective methodology for the structure elucidation of small molecules.[8] A technological improvements in collecting marine organisms made it possible to access uncommon marine organisms inhabiting at deep-sea or unexplored sea area.[9] Consequently, the number of newly isolated compounds from marine organisms per decade continues increasing.

Together with the technological breakthroughs and renaissance of marine natural product chemistry, new scientific fields are evolving from marine natural product chemistry; genetics, chemical biology, chemical genetics and chemical ecology.[10] These translational researches activate the marine natural products chemistry, and attract a great deal of attention to marine natural products as a tool for the scientific research and leads for drug discovery.[11]

Recently, several marine natural product derived drugs have been approved by the Food and Drug Administration (FDA) and European Agency for the Evaluation of

Medicinal Products (EMA), and approximately 20 compounds are either in Phase I, Phase II, or Phase III clinical trials.[12] Most of these therapeutically important marine natural products have been discovered through cell-based assays (Table 1-1). The detail of several representative marine natural products and marine-derived drugs are introduced below.

Table 1-1. List of marine-derived drug leads identified by cell-based assay

Compound Name	Chemical Class	Marine Organisms
Ecteinascidin 743[13]	Alkaloid	Tunicate
Halichondrin B[14]	Macrolide	Sponge
Dolastatin 10[15]	Peptide	Bacterium
Dolastatin 15[15]	Peptide	Bacterium
Kahalalide F[16]	Depsipeptide	Mollusk
Plitidepsin[17]	Depsipeptide	Tunicate
Jorumycin[18]	Alkaloid	Nudibranch
Pseudopterosin[19]	Diterpene glycoside	Soft coral
Bryostatin-1[20]	Polyketide	Bryozoa
Hemiasterlin[21]	Tripeptide	Sponge
Salinosporamide A[22]	β-Lactone-γ-lactone	Bacterium
Bengamide B[23]	Amino acid derivative	Sponge
Discodermolide[24]	Lactone	Sponge
Spisulosine[25]	Lipid	Mollusk

Approved marine-derived anticancer drugs

Spongothymidine was isolated from the Caribbean marine sponge *Tethyacrypta* in the 1950s, and consists of an arabinose sugar and thymine.[1] Spongothymidine and cytarabine, a synthetic analogue of spongothymidine, are nucleoside analogues,[26] and they inhibit DNA polymerase and DNA synthesis by competing with cellular nucleoside.[27] Cytarabine was approved as the anticancer drug by FDA in 1969, the first marine-derived drug, and used in the treatment of acute lymphocytic leukemia, acute myelocytic leukemia and blast and meningeal leukemia.[28]

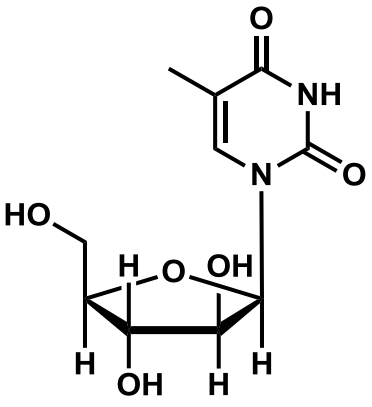

Spongothymidine

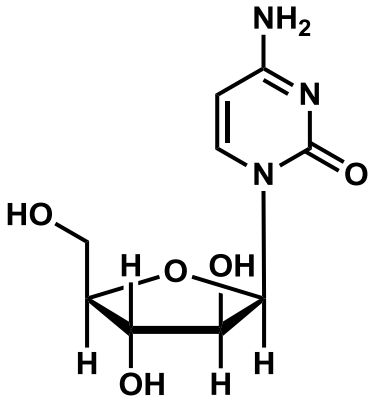

Cytarabine

A tetrahydroisoquinoline alkaloid, trabectedin, another name being ecteinascidin 743, was isolated from the Caribbean tunicate, *Ecteinascidia turbinate*.[13] Trabectedin is composed of three tetrahydroisoquinoline units and 10-membered lactone ring bearing a thioether bridge. This compound exhibits potent toxicity against a broad spectrum of tumor types. The mechanism of action of trabectedin is still unclear, but it is known to form a covalent bond to the DNA minor groove, and interacts with the nucleotide excision repair system.[29] It induces mitotic arrest and apoptosis. Trabectedin inhibits the gene expression of MDR1 gene, which encodes a P-glycoprotein, and keeps the drug susceptibility of tumor cells.[30] It was approved as the anticancer drug for ovarian cancer.

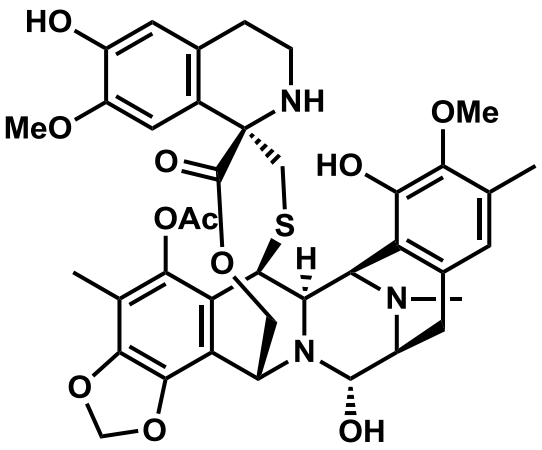

Trabectedin (ET-743)

Halichondrin B, a polyether macrolide was originally isolated from the marine sponge *Halichondria okadai* in 1986.[14] It showed very potent cytotoxicity against L1210 murine leukemia cells with an IC_{50} value of 0.3 nM, and induced cell cycle arrest at G2/M phase by inhibition of tubulin polymerization. Halichondrin B is known to interact with vinca domain of tubulin, a region located at the interface of tubulin heterodimers.[31] Its molecular mechanism of action is distinct from other tubulin-targeting agents such as taxane and vincas.[32] Eribulin mesylate, a structurally simplified synthetic Halichondrin B analogue, was developed by Eisai.[33] Eribulin mesylate was approved by FDA for the treatment of metastatic breast cancer.[34]

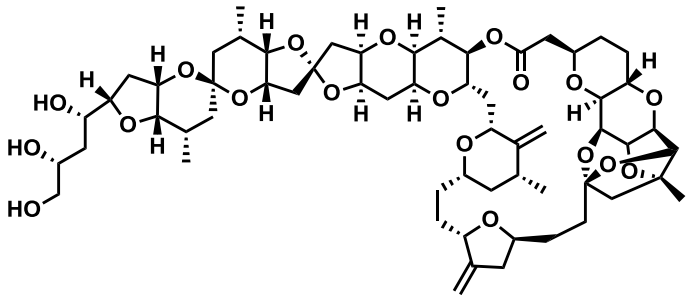

Halichondrin B

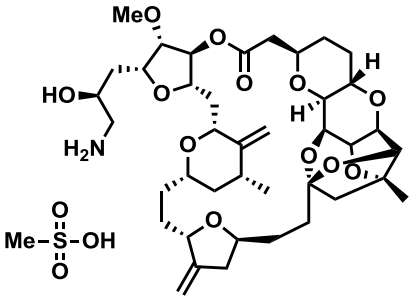

Eribulin mesylate

Dolastatin 10 was discovered from the sea hare *Dolabella auricularia* as a potent antineoplastic compound in 1972.[15] The cyanobacteria *Symploca hydnoides* and *Lyngbya majuscule* were later revealed to be the producers of dolastatin 10.[35] Dolastatin 10 binds to the vinca domain of tubulin and inhibits the assembly of tubulin.[31, 32] Investigation of the structure activity relationship of synthetic analogues of dolastatin 10 resulted in the development of monomethyl auristatin E.[36] Seattle Genetics developed a technology to couple this compound to monoclonal antibodies.[37] This antibody-drug conjugate, named brentuximabvedotin binds to the antigen, CD30, expressed on the cancer cell surface, and monomethyl auristatin E exhibits toxicity against cancer cells. Brentuximabvedotin was approved by FDA in 2011 for the treatment of Hodgkin's lymphoma or systemic anaplastic large cell lymphoma.

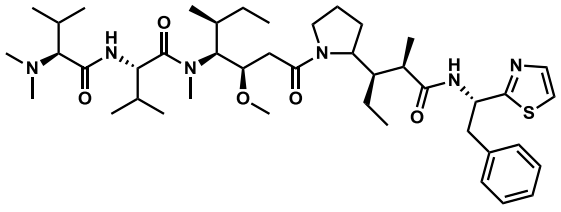

Dolastatin 10

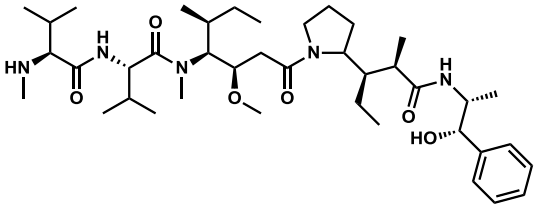

Monomethyl Auristatin E

Marine-derived anticancer drugs in clinical trials

Plitidepsin, didemnin B homologue, is a depsipeptide isolated from the Mediterranean Sea tunicate *Aplidium albicans*.[17] The chemical structure of plitidepsin is very close to that of didemnin B, the only difference being in the lactate residue.[38] It shows potent antitumor activity against SK-MEL-28, human melanoma cells, with an IC_{50} value of 12 nM. It induces cell cycle arrest at G1 and G2/M phase and apoptosis by the activation of Rac1/ c-Jun NH_2-terminal kinase pathway.[39] It has proceeded to the Phase I and II clinical trials in combination with other active agents, bortezomib and dexamethasone for the treatment of patients with relapsed and refractory myeloma.

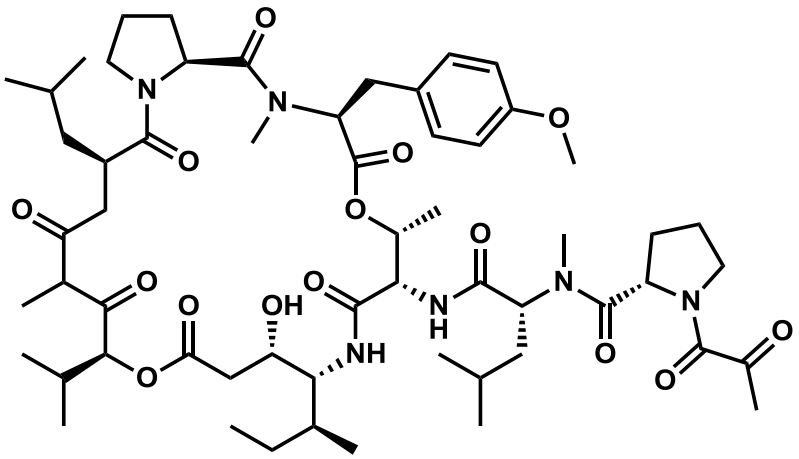

Plitidepsin (Aplidin)

Hemiasterlin is a cytotoxic tripeptide, originally isolated from the sponge *Hemiasterella minor*.[40] E7974 is the synthetic analogue of hemiasterlin developed by Eisai Inc. Substitution of the N-terminal amino acid residue of hemiasterlin conquered the susceptibility of p-glycoprotein mediated efflux and enhanced the potency.[41] E7974 exhibits antimitotic activity, disruption of spindle formation, and induction of caspase-3 mediated apoptosis. It binds to the β-tubulin and inhibits the tubulin polymerization.[41] E7974 has been assessed in the Phase I clinical trial for the treatment of the colon cancer.[42]

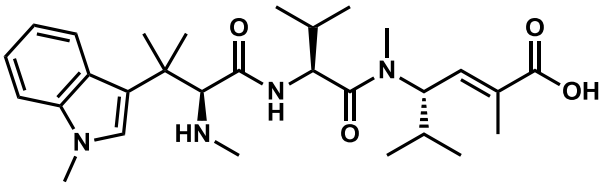

Hemiasterlin

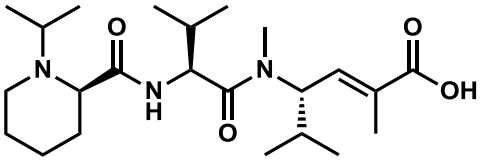

E7974

Cell-based assay has advantages of its reproducibility and simplicity.[43] It is robust enough to be applied to the high throughput screening, and it can screen membrane permeable compounds, targeting a wide variety of the cellular components.[44] A variety of cell-based assays are developed that measure cell proliferation, toxicity, activation of specific signaling pathways and changes in morphology.[45] Cell viability assay is one of the basic and effective techniques to evaluate cytotoxicity and anti-proliferative activity. Furthermore, cell viability assays against a panel of multiple cancer cell lines can predict the molecular mechanism of the bioactive compounds.[46] Reporter gene assays, which screen bioactive compounds that modulate the expression level of the specific gene, is sensitive enough to be applied for the high-throughput screening of the compound libraries.[47] Cell morphology-based assays can identify bioactive compounds modulating cellular processes, and provide insights into the molecular mechanisms of them.[48] Therefore, I searched for novel sponge metabolites that showed potent bioactivity against cancer cells by using cell-based assays.

The subjects described in this doctoral thesis are the studies on the novel bioactive marine natural products discovered through cell-based assays. Second chapter dscribes the studies of cytotoxic acetylenes, (-)-durynes and miyakosynes. Third chapter deals with the study of cytotoxic macrolactams, poecillastrin C and its analogue. And

the fourth chapter is concerned with the identification of the cell cycle arrest inducers discovered through the time-lapse imaging of HeLa/Fucci2 cells.

Chapter 2

Cytotoxic acetylenes isolated from a deep-sea marine sponge *Petrosia* sp.

2.1. Isolation and structure elucidation of (-)-durynes and miyakosynes.

2.1.1. Introduction

Linear acetylene compounds are prominent constituents of the order *Haplosclerida*.[1] Sponge-derived linear acetylenes share the terminal acetylene moiety consisting of a terminal alkyne, a secondary hydroxyl group, and an olefin. Even though their molecular mechanisms are yet to be disclosed, their diverse biological activities, including antitumor, antimicrobial, antifungal, and antiviral activities are of interest for the new drug development.[2]

In the course of the cytotoxicity screening, the crude extract of a deep-sea marine sponge *Petrosia* sp. exhibited potent activity against HeLa human cervical carcinoma cells. Bioassay-guided fractionation of the extract afforded two groups of acetylene compounds, (-)-durynes and miyakosynes. Duryne was originally isolated from the Bahamian sponge *Cribrochalina dura*,[3] and its absolute configuration was

determined by the total synthesis.[4] In this study, we isolated the enantiomer of duryne, termed (-)-duryne (**2-1**), and its homologues (-)-duryne B-F (**2-2** – **2-6**), and miyakosynes A-F (**2-7** – **2-12**). (-)-Durynes consisted of one or two double bonds around the center of the molecules, whereas miyakosynes had a branched methyl instead of the olefin. In this chapter, isolation and structure elucidation of the (-)-duryne (**2-1**), (-)-durynes B-F (**2-2** – **2-6**), and miyakosynes A-F (**2-7** – **2-12**) are described below.

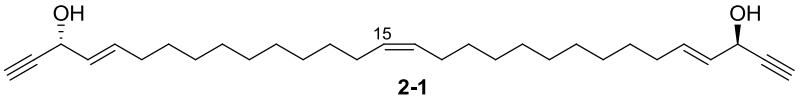

2-1

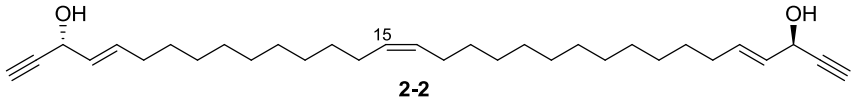

2-2

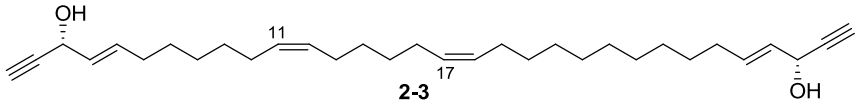

2-3

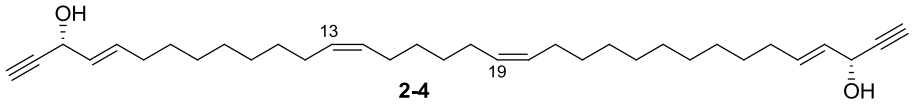

2-4

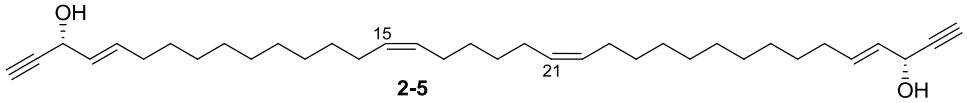

2-5

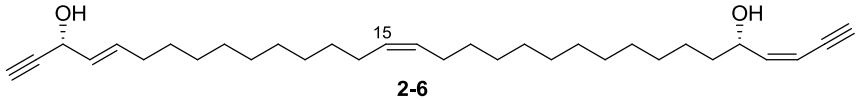

2-6

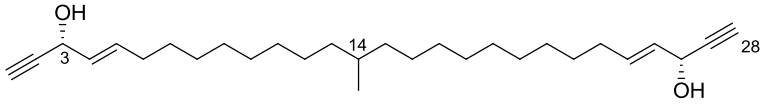

2-7

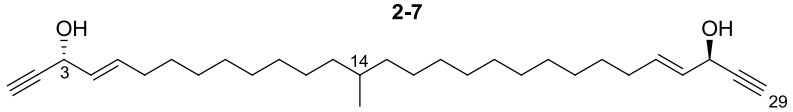

2-8

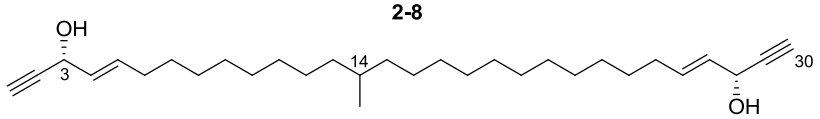

2-9

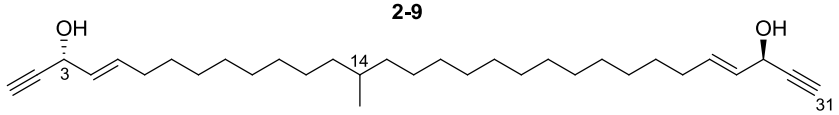

2-10

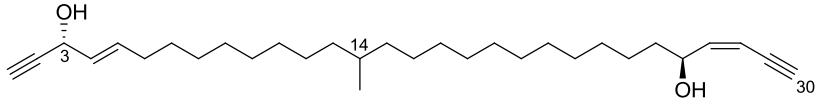

2-11

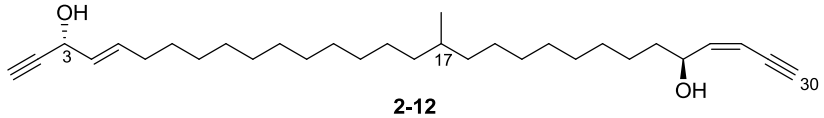

2-12

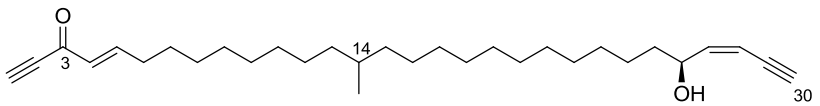

2-13

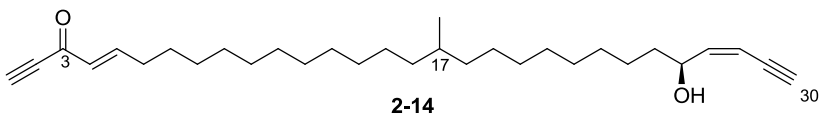

2-14

2.1.2. Results and Discussion

The sponge *Petrosia* sp. was collected by a remotely operated vehicle at Miyako sea-knoll. The sponge specimen was extracted with EtOH and MeOH/$CHCl_3$ (1:1), and the combined extracts were concentrated and partitioned between $CHCl_3$ and H_2O. The $CHCl_3$ layer was further partitioned between 90% MeOH and *n*-hexane. Bioassay-guided fractionation of the 90% MeOH fraction by ODS column chromatography, silica gel column chromatography, and reversed-phase HPLC afforded twelve cytotoxic compounds (**2-1** – **2-12**).

Compound **2-1**, which analyzed for $C_{30}H_{48}O_2$ by HRESIMS, exhibited ^1H NMR signals characteristic of the terminal structure of sponge-derived acetylenes, [δ 2.57 (d, *J*=2.1 Hz; H-1, H-30), δ 4.84 (brd, *J*=6.4 Hz; H-3, H-28), δ 5.61 (dd, *J*=15.1, 6.4 Hz; H-4, H-27), and 5.92 (dt, *J*=15.1, 6.9 Hz; H-5, H-26)]. A literature search showed that the ^1H and ^{13}C NMR data of **2-1** (Table 2-1) were identical with those of duryne and the position of the central olefin was confirmed by tandem FABMS (Figure 2-1). However, an opposite sign with a similar magnitude for the specific rotation ($[\alpha]_D$ = -19) showed that **2-1** was the enantiomer of the previously reported duryne ($[\alpha]_D$ = +29).[3,4] The modified Mosher's analysis of **2-1** supported this assignment (Figure 2-2).[5] Therefore, we named **2-1** was firmly established to be (-)-duryne.[6]

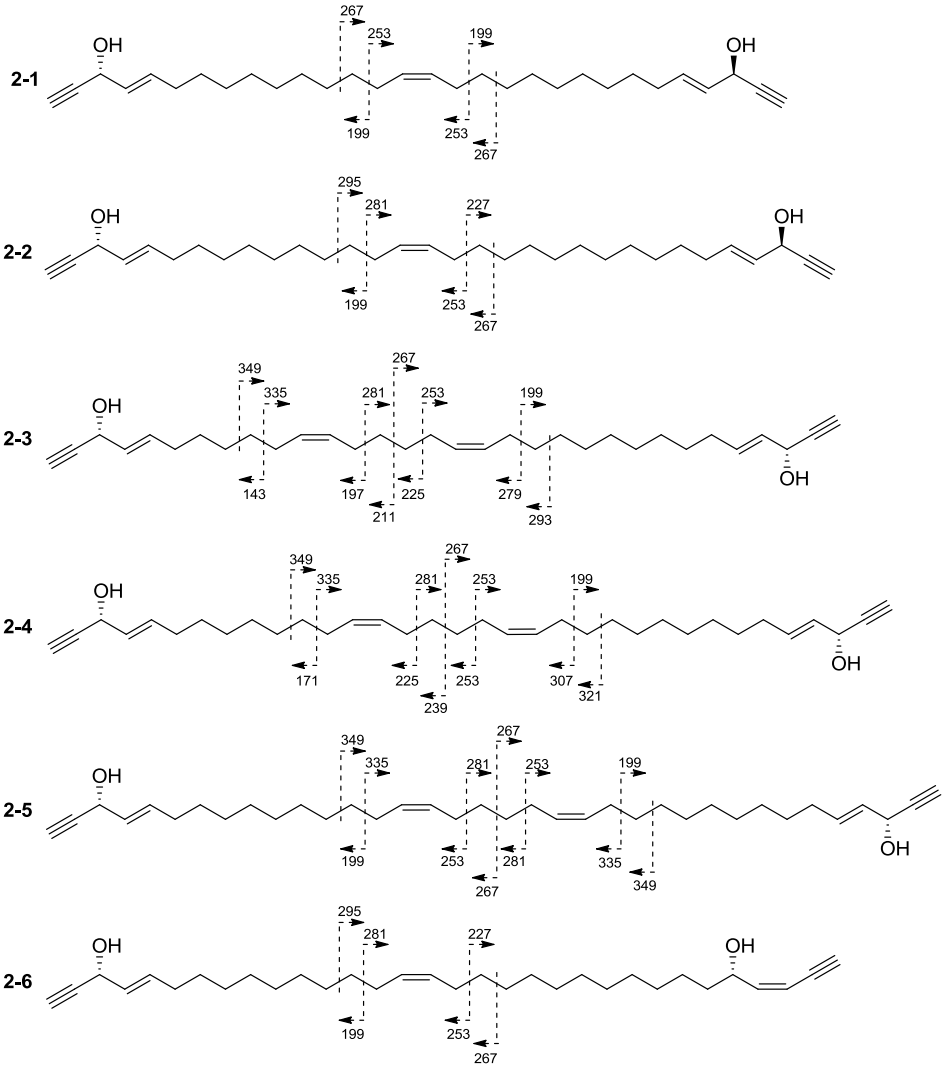

Figure 2-1. Key tandem FABMS fragmentationsfor **2-1** – **2-6** by using the $[M+Li]^+$ ion as the precursor.

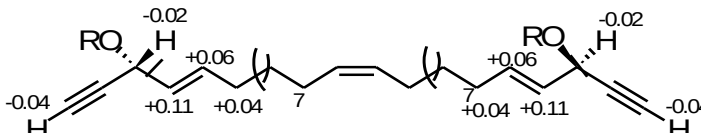

2-1a: R=(*R*)-MTPA**, 2-1b**: R=(*S*)-MTPA

Figure 2-2. Modified Mosher analysis for **2-1**. $\Delta\delta$ (δ_S-δ_R) values are shown**.**

(-)-Duryne B (**2-2**) had the molecular formula of $C_{32}H_{52}O_2$ as assigned by HRESIMS. The ^{1}H and ^{13}C NMR spectra of **2-2** were identical with those of **2-1** except for the integration of the methylene region (Table 2-1), suggesting that they differ only in the length of the aliphatic chains. The position of the *Z*-olefin in the middle of the chain was assigned by tandem FABMS to be between C-15 and C-16 (Figure 2-1). The geometry of the Δ^{15}-double bond was assigned by the chemical shifts of 27.4 ppm for C-14 and C-17.[7] The positions of the double bonds were confirmed by ozonolysis with oxidative work-up, which gave FABMS ions at *m*/*z* 215 and 243 $[M-H]^-$, consistent with the formation of undecanedioic acid and tridecanedioic acid, respectively (Scheme 2-1). The configurations of the two secondary alcohols were both determined to be *R* by the modified Mosher's method.[5]

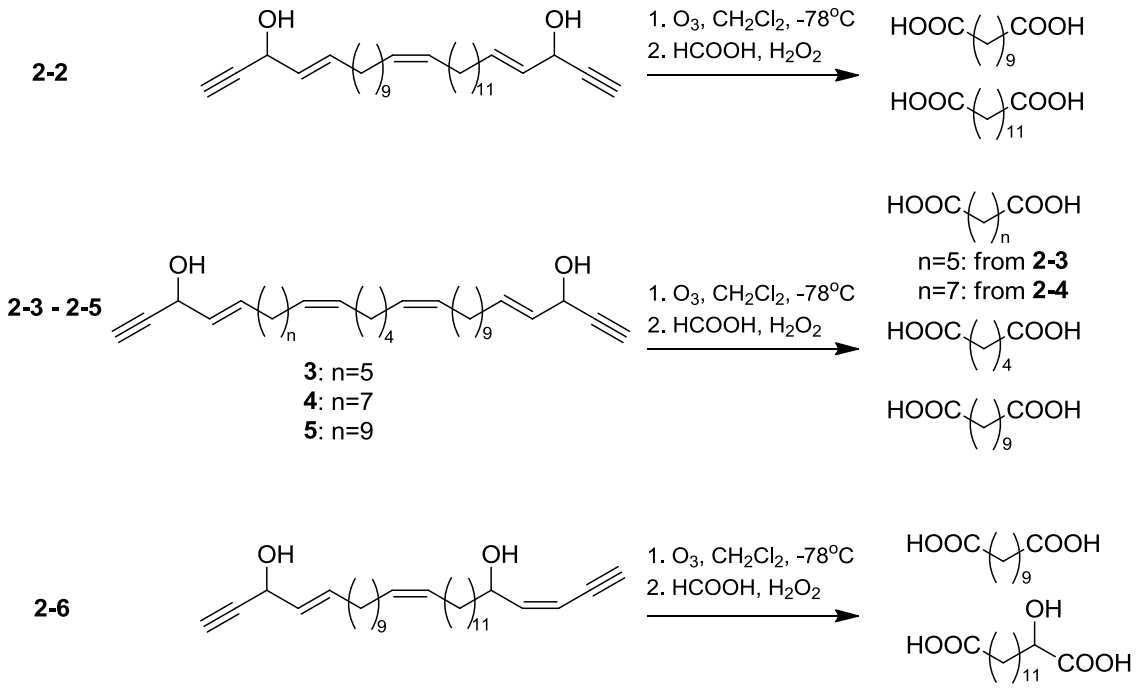

Scheme 2-1. Ozonolysis of **2-2** – **2-6**.

(-)-Durynes C-E (**2-3** - **2-5**) had molecular formulas of $C_{32}H_{50}O_2$, $C_{34}H_{54}O_2$, and $C_{36}H_{58}O_2$, respectively, as assigned by HRESIMS. The ^{1}H NMR data of **2-3** - **2-5** were identical with those of **2-1**, except for doubled olefinic and allylic proton peaks representing the central double bonds and an increased methylene peak at δ 1.27-1.34, suggesting that **3**-**5** have longer aliphatic chains and one additional double bond in their chains (Table 2-2). The geometries of the olefins in the middle of the chain in **2-3** - **2-5** were all assigned as *Z* judging from the chemical shifts of the allylic carbons.[7] The locations of the two *Z*-olefins were assigned by tandem FABMS to be $\Delta^{11,17}$ for **2-3**,

$\Delta^{13,19}$for **2-4**, and $\Delta^{15,21}$ for **2-5** (Figure 2-1). These assignments were confirmed by the ozonolysis experiments (Scheme 2-1). Ozonolysis of **2-3**, **2-4**, and **2-5** followed by oxidative work-up afforded common FABMS ion peaks at *m/z* 145 and 215 which suggested the formation of adipic acid and undecanedioic acid, respectively. Additional ions were observed at *m/z* 159 and *m/z* 187 in the ozonolysis products of **2-3** and **2-4**, respectively, consistent with the formation of heptanedioic acid and nonanedioic acid. The absolute configurations of the secondary alcohols in the three compounds were all determined as *R* by the modified Mosher's method.[5]

HRESIMS showed that (-)-duryne F (**2-6**) was an isomer of **2-4**. The structure of one end was identical with those in the other compounds as judged from the ^{1}H and ^{13}C NMR data (Table 2-1), whereas in the other end, an acetylenic proton (δ 3.14, *J*=2.5 Hz, H-32) was coupled to a *Z*-olefinic proton (δ 5.54, *J*=11.0, 2.5 Hz; H-30) which was then coupled to another olefinic proton (δ 6.00, *J*=11.0, 8.9 Hz; H-29). This latter proton, H-29, was further coupled to an oxymethine proton (δ 4.68, H-28), indicating a rearranged terminus relative to the commonly observed motif. There was a degenerate olefinic signal integrating for 2H, which was assumed as a *Z*-olefin in the middle of the chain. The *Z*-geometry was again assigned by the chemical shifts of the allylic carbons.[7] Tandem FABMS data were not sufficient to locate the double bond, because it was not

possible to distinguish the two termini by the MS data. Again we resorted to an ozonolysis experiment which afforded a reaction mixture with FABMS ion peaks at *m/z* 215 and 273, consistent with the formation of undecanoic acid and 2-hydroxytetradecanoic acid, respectively, demonstrating the location of the double bond between C-15 and C-16 (Scheme 2-1). The absolute configuration was determined to be 3*R*, 28*S* by the modified Mosher's method.[5]

Table 2-1. ^{1}H and ^{13}C NMR data of (-)-Duryne (**2-1**), (-)-Duryne B (**2-2**), and (-)-Duryne F (**2-6**) in $CDCl_3$.

(-)-duryne (**2-1**)			(-)-duryne B (**2-2**)			(-)-duryne F (**2-6**)		
position	δ_C[a]	δ_H (*J* in Hz)	position	δ_C[b]	δ_H (*J* in Hz)	position	δ_C[b]	δ_H (*J* in Hz)
1, 30	74.1	2.57, d (2.1)	1	73.9	2.57, d (2.1)	1	74.1	2.57, d (2.1)
2, 29	83.5		2	83.4		2	83.4	
3, 28	63	4.84, d (6.4)	3	62.8	4.84, brd (6.2)	3	62.8	4.84, brd (6.2)
4, 27	128.3	5.61, dd (15.1, 6.4)	4	128.3	5.61, dd (15.3, 6.2)	4	128.1	5.62, dd (15.1, 6.2)
5, 26	134.8	5.92, dt (15.1, 6.9)	5	134.5	5.92, dt (15.3, 6.9)	5	134.4	5.92, dt (15.1, 6.9)
6, 25	32.1	2.07, m	6	31.9	2.07, m	6	31.8	2.07, m
7, 24	30.0[c]	1.40, m	7	28.7	1.40, m	7	28.9	1.40, m
8-12, 19-23	29.4-29.8[c]	1.27-1.30, m	8-13	28.7-29.7	1.27-1.36	8-13	28.7-30.0	1.27-1.34
13, 18	29.0[c]	1.32, m	14	27.4	2.02, m	14	27.3	2.01, m
14, 17	27.4	2.02, m	15	129.9	5.35, m	15	129.9	5.36, m
15, 16	129.9	5.35, m	16	129.9	5.35, m	16	129.9	5.36, m
			17	27.4	2.02, m	17	27.3	2.01, m
			18-25	28.7-29.7	1.27-1.36	18-26	28.7-30.0	1.27-1.34
			26	28.7	1.40, m	27α	36.3	1.63, m
			27	31.9	2.07, m	27β		1.52, m
			28	134.5	5.92, dt (15.3, 6.9)	28	70	4.68, m
			29	128.3	5.61, dd (15.3, 6.2)	29	147.5	6.00, dd (11.0, 8.9)
			30	62.8	4.84, brd (6.2)	30	108.7	5.54, dd (11.0, 2.5)
			31	83.4		31	82.4	
			32	73.9	2.57, d (2.1)	32	79.5	3.14, d (2.5)

[a] ^{13}C NMR spectrum was measured at 150 MHz. [b] Chemical shifts were assigned from the HSQC data.

[c] Assignments with the same superscript in the same column may be interchangeable.

Table 2-2. ^{1}H and ^{13}C NMR data of (-)-Duryne C-E (**2-3 - 2-5**) in $CDCl_3$.

(-)-duryne C (**2-3**)			(-)-duryne D (**2-4**)			(-)-duryne E (**2-5**)		
position	δ_C [b]	δ_H (*J* in Hz)	position	δ_C [a]	δ_H (*J* in Hz)	position	δ_C [b]	δ_H (*J* in Hz)
1	73.9	2.57, d (2.1)	1	74.1	2.57, d (2.1)	1, 36	74.1	2.57, d (2.2)
2	83.3		2	83.6		2, 35	83.2	
3	62.8	4.84, brd (6.2)	3	62.9	4.84, brd (6.2)	3, 34	62.8	4.84, brd (6.2)
4	128.4	5.61, dd (15.1, 6.2)	4	128.6	5.61, dd (15.1, 6.2)	4, 33	128.2	5.61, dd (15.1, 6.2)
5	134.5	5.92, dt (15.1, 6.9)	5	134.7	5.92, dt (15.1, 6.9)	5, 32	134.5	5.93, dt (15.1,6.9)
6	31.9	2.07, m	6	32.1	2.07, m	6, 31	31.9	2.07, m
7	28.7	1.40, m	7	29	1.40, m	7, 30	28.7	1.40, m
8	29.1-29.4	1.28-1.33	8-10	29.3-29.9	1.28-1.32	8-12, 25-29	28.7-29.7	1.27-1.34
9	29.4	1.36,m	11	29.5	1.36, m	13, 24	29.4	1.36, m
10	27.1	2.02, m	12	27.1	2.03, m	14, 23	27.1	2.03, m
11	130	5.36, m	13	129.9	5.35, m	15, 22	129.7	5.36, m
12	130	5.36, m	14	130.2[d]	5.35, m	16, 21	129.7	5.36, m
13	27.1	2.02, m	15	27.1	2.03, m	17, 20	27.1	2.03, m
14	29.4	1.36, m	16	29.5	1.36, m	18, 19	29.4	1.36, m
15	29.4	1.36, m	17	29.5	1.36, m			
16	27.1	2.02, m	18	27.1	2.03, m			
17	130	5.36, m	19	130.1[d]	5.35, m			
18	130	5.36, m	20	129.9	5.35, m			
19	27.1	2.02, m	21	27.1	2.03, m			
20	29.4	1.36, m	22	29.5	1.36, m			
21-25	29.1-29.4	1.28-1.33	23-27	29.3-29.9	1.28-1.32			
26	28.7	1.40, m	28	29	1.40, m			
27	31.9	2.07, m	29	32.1	2.07, m			
28	134.5	5.92, dt (15.1, 6.9)	30	134.7	5.92, dt (15.1, 6.9)			
29	128.4	5.61, dd (15.1, 6.2)	31	128.6	5.61, dd (15.1, 6.2)			
30	62.8	4.84, brd (6.2)	32	62.9	4.84, brd (6.2)			
31	83.3		33	83.6				
32	73.9	2.57, d (2.1)	34	74.1	2.57, d (2.1)			

[a] ^{13}C NMR spectrum was measured at 150 MHz. [b] Chemical shifts were assigned from the HSQC data.
[d] Assignments with the same superscript in the same column may be interchangeable.

Miyakosyne A (**2-7**) had the molecular formula of $C_{29}H_{48}O_2$ as assigned by HRESIMS. An interesting feature of the ^{1}H NMR spectrum was that a methyl doublet (δ 0.84, *J*=6.7 Hz) was integrated for 1.5 H compared to other isolated ^{1}H signals. This observation was accounted for by the presence of one methyl group in otherwise symmetrical structure. The ^{1}H NMR and HSQC data showed the presence of characteristic terminal structure comprised of terminal acetylene, carbinol, and *E*-olefin, in this order, as found in duryne and petrosynol (Table 2-3).[8,9] The molecular formula and NMR data indicated that the two termini were linked through a saturated linear aliphatic chain with one methyl branch. The branched methyl group was shown not to be located near the termini by interpretation of HMBC spectrum. The position of the methyl branch was investigated by analysis of tandem FABMS data. Because the molecule has an identical polar group placed at both ends, it is likely that each end comprises the charged site with the same probability. Therefore, we considered the tandem FABMS data as a summation of product ion spectra with each end charged. When a methyl branch is present, the regularity of the appearance of product ions separated by 14 units, corresponding to the C-C bond cleavages in the aliphatic chain, is broken by the absence of one peak, resulting in the separation of two adjacent ions by 28 units.[10] In the tandem FABMS of **2-7**, such phenomenon was not observed. Instead,

significant fluctuation in the intensities of the ion peaks at *m/z* 199, 213, 227, and 241 was observed, while the intensity changes of larger or smaller ions (e.g. *m/z* 171, 185, 255, and 269) were within statistical errors (Figure 2-3). In the tandem FABMS of methyl branched fatty acids, the incidence of cleavage between α-carbon and β-carbon of the branching points is twice as that between the neighboring methylene carbons.[10] With this tendency in mind, we can predict the relative intensity of product ions for a specific methyl branch (Figure 2-4, Table 2-4). In the spectrum with C-13 methyl branch, the ratio of ion peaks at *m/z* 185, 199, 213, 227, 241, and 255 was expected to be 3:1:3:3:1:3, whereas that with C-14 methyl branch in a ratio of 2:3:2:2:3:2 (Table 2-4), the latter ratio being matched well with the observed value (Figure 2-3). Compounds with methyl branch at C-11 and C-12 would give different ratios from the observed value (Table 2-4). Therefore, we concluded that **2-7** had C-14 methyl branch. Because of the limited precision of the analysis, it is not possible to eliminate the possibility of the presence of small amounts of other positional isomers. The absolute configurations of the carbinol carbons were determined as *R*, because the ^{1}H NMR data of the terminal portions of the (*R*)-MTPA esters of **2-7** were superimposable on those of the (*S*)-MTPA ester of petrocortyne A:[11] petrocortyne A contains the corresponding terminal moiety with the *S*-configuration. The configuration of the branched methyl

group is discussed in secion 2.2.

Table 2-3. ^{1}H and ^{13}C NMR data of Miyakosynes A-D (**2-7** - **2-10**) in $CDCl_3$.

	miyakosyne A (**2-7**)		miyakosyne B (**2-8**)		miyakosyne C (**2-9**)		miyakosyne D (**2-10**)	
No.	δ_H, mult.	$^{a}\delta_C$	δ_H, mult.	$^{a}\delta_C$	δ_H, mult.	$^{b}\delta_C$	δ_H, mult.	$^{b}\delta_C$
1	2.57, d (2.1)	74.2	2.56, d (2.2)	74.1	2.56, d (2.1)	74.0	2.57, d (2.1)	74.0
2		83.5		83.6		83.4		83.4
3	4.84, brd (6.2)	63.0	4.83, brd (6.2)	62.9	4.84, brd (6.2)	62.8	4.84, brd (6.1)	62.9
4	5.61, dd (15.1, 6.2)	128.5	5.61, dd (15.4, 6.2)	128.5	5.61, dd (15.1, 6.2)	128.3	5.62, dd (15.3, 6.1)	128.4
5	5.92, dt (15.1, 6.9)	134.9	5.91, dt (15.4,6.9)	134.7	5.91, dt (15.1, 6.8)	134.5	5.93, dt (15.3, 6.9)	134.7
6	2.07, m	32.2	2.07, m	32.1	2.07, m	31.9	2.07, m	31.9
7	1.39, m	29.0	1.39, m	29.0	1.39, m	29.0	1.40, m	28.9
8-12	1.24 - 1.31	29.3 - 30.2	1.23 - 1.30	29.3 - 30.2	1.23 - 1.30	29.0 - 30.2	1.23 - 1.30	29.0 - 30.2
13	1.08, m	37.3	1.07, m	37.3	1.07, m	37.0	1.08, m	37.1
14	1.36, m	32.9	1.35, m	32.9	1.35, m	32.7	1.35, m	32.8
15	1.08, m	37.3	1.07, m	37.3	1.07, m	37.0	1.08, m	37.1
16-21	1.24 - 1.31	29.3 - 30.2	1.23 - 1.30	29.3 - 30.2	1.23 - 1.30	29.0 - 30.2	1.23 - 1.30	29.0 - 30.2
22	1.39, m	29.0	1.23 - 1.30	29.3 - 30.2	1.23 - 1.30	29.0 - 30.2	1.23 - 1.30	29.0 - 30.2
23	2.07, m	32.2	1.39, m	29.0	1.23 - 1.30	29.0 - 30.2	1.23 - 1.30	29.0 - 30.2
24	5.92, dt (15.1, 6.9)	134.9	2.07, m	32.1	1.39, m	29.0	1.23 - 1.30	29.0 - 30.2
25	5.61, dd (15.1, 6.2)	128.5	5.91, dt (15.4,6.9)	134.7	2.07, m	31.9	1.40, m	28.9
26	4.84, brd (6.2)	63.0	5.61, dd (15.4, 6.2)	128.5	5.91, dt (15.1, 6.8)	134.5	2.07, m	31.9
27		83.5	4.83, brd (6.2)	62.9	5.61, dd (15.1, 6.2)	128.3	5.93, dt (15.3, 6.9)	134.7
28	2.57, d (2.1)	74.2		83.6	4.84, brd (6.2)	62.8	5.62, dd (15.3, 6.1)	128.4
29			2.56, d (2.2)	74.1		83.4	4.84, brd (6.1)	62.9
30					2.56, d (2.1)	74.0		83.4
31							2.57, d (2.1)	74.0
14-Me	0.84, d (6.7)	19.9	0.84, d (6.6)	19.9	0.84, d (6.6)	19.7	0.84, d (6.6)	19.8

a ^{13}C NMR was measured at 150 MHz. *b* ^{13}C NMR chemical shifts were determined by HSQC data.

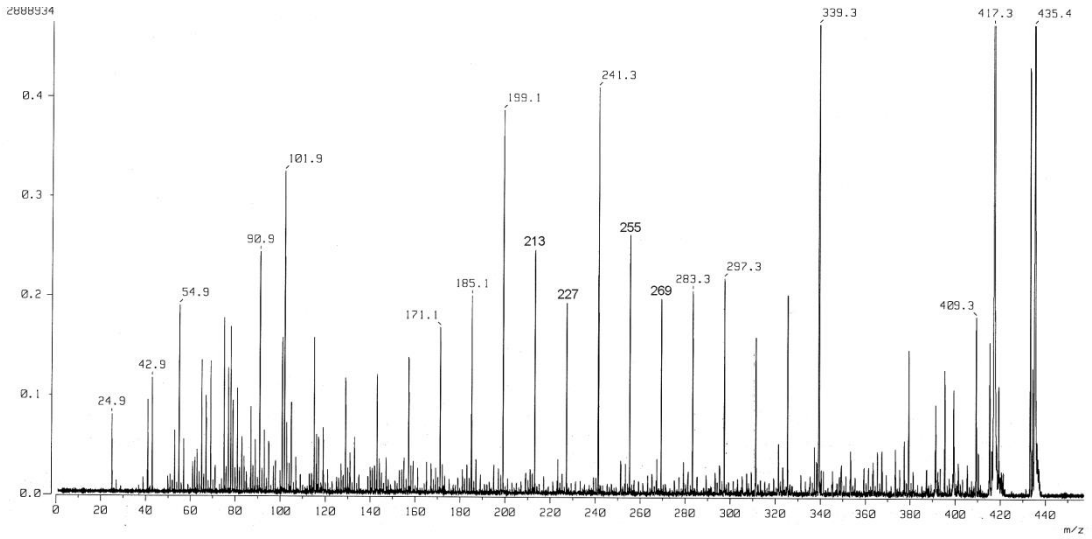

Figure 2-3. Tandem FAB mass spectrum of miyakosyne A (**2-7**).

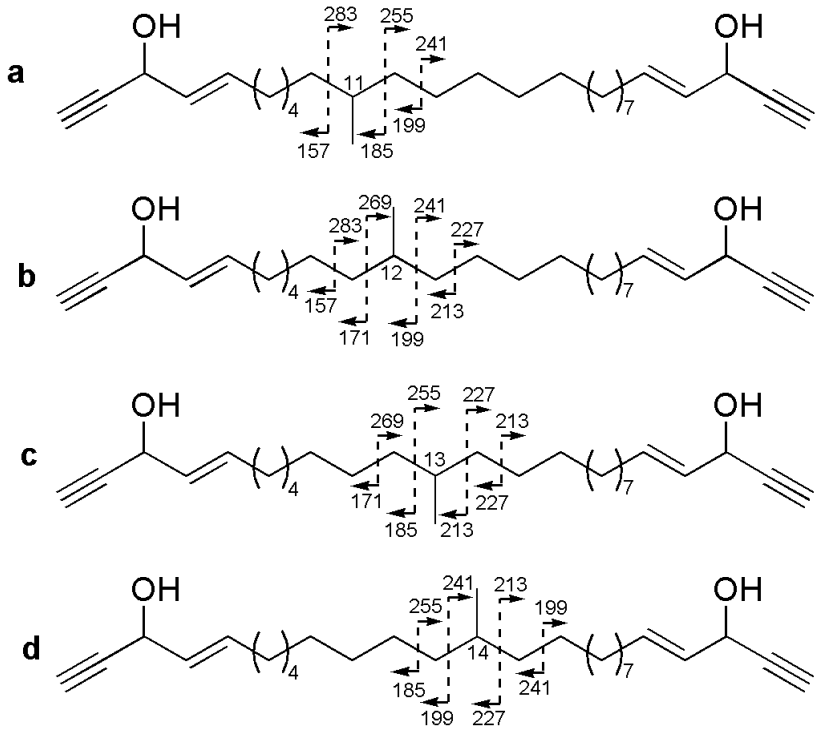

Figure 2-4. Mass numbers of product ions in the tandem FABMS for **2-7** with a methyl branch at C-11 (**a**), C-12 (**b**), C-13 (**c**), and C-14 (**d**).

Table 2-4. Predicted relative intensities of ions for methyl branches at C-11 (a), C-12 (b), C-13 (c), and C-14 (d) in **2-7**.

m/z	157	171	185	199	213	227	241	255	269	283
a: C-11	+++	+	+++	++	++	++	++	+++	+	+++
b: C-12	++	+++	+	+++	++	++	+++	+	+++	++
c: C-13	++	++	+++	+	+++	+++	+	+++	++	++
d: C-14	++	++	++	+++	++	++	+++	++	++	++

Miyakosynes B-D (**2-8** - **2-10**) had molecular formulas of $C_{30}H_{50}O_2$, $C_{31}H_{52}O_2$, and $C_{32}H_{54}O_2$, respectively, as assigned by HRESIMS. ^1H and ^{13}C NMR data of **8**-**10** were almost identical with those for **2-7**, indicating that **2-8** - **2-10** have the common terminal structures and a methyl branch (Table 2-3). This was confirmed by analyses of 2D NMR data. The positions of the methyl branch in **2-8** - **2-10** were all assigned to be at C-14 by application of similar arguments on interpretation of tandem FABMS data as described above. The absolute configurations of the carbinol carbons in all these compounds were determined as *R* by interpretation of the ^1H NMR spectra of the bis-(*R*)-MTPA esters as described above.

Table 2-5. ^{1}H and ^{13}C NMR data of Miyakosynes E (**2-11**) and F (**2-12**) in $CDCl_3$.

miyakosynes E (**2-11**) and F (**2-12**)		
No.	δ_H, mult.	[a] δ_C
1	2.57, d (2.1)	74.0
2		83.3
3	4.84, brd (6.2)	62.8
4	5.62, dd (15.1, 6.2)	128.3
5	5.92, dt (15.1, 6.9)	134.7
6	2.07, m	31.9
7	1.40, m	28.7
8-12 (8-15)[b]	1.23 - 1.30	29.0 - 30.2
13 (16)[b]	1.08, m	37.0
14 (17)[b]	1.35, m	32.7
15 (18)[b]	1.08, m	37.0
16-24 (16-19)[b]	1.23 - 1.30	29.0 - 30.2
25α	1.63, m	36.5
25β	1.53, m	
26	4.68, m	70.0
27	6.00, dd (11.0, 8.3)	147.5
28	5.54, dd (11.0, 1.4)	108.8
29		82.7
30	3.14, d (1.4)	79.4
14-Me (17-Me)	0.84, d (6.6)	19.7

[a] ^{13}C NMR chemical shifts were determined by HSQC data.
[b] Parenthetic carbon numbers were assigned for **2-11**.

Miyakosynes E (**2-11**) and F (**2-12**), obtained as an inseparable mixture, were both isomeric with **2-9**. ^{1}H NMR spectrum of the mixture showed one set of resonances for the common terminal structure and its rearranged form comprised of an conjugated enyne system linked to an allylic secondary alcohol, with a *Z*-olefin ($J_{H27,H26}$=11.0 Hz, Table 2-5). There was a branched methyl group in this molecule as well. The mixture of **2-11** and **2-12** gave the tandem FABMS spectrum almost identical with that of **2-9**, allowing us to locate the methyl group in the aliphatic chain, but it was not possible to

differentiate the two terminal polar groups which had identical compositions. Fortunately, the reactivity of the two secondary alcohols was different: allylic propargylic alcohol was much more susceptible to oxidation. DDQ oxidation of the mixture afforded a mixture of keto-alcohols (**2-13** and **2-14**), which was derivatized with Girard's T reagent[12] and subjected to the tandem FABMS analysis. In the Girard's T derivatives, the newly introduced positive charge was considered as the sole ionization site. The fixed charged site allowed the tandem FABMS data to be interpreted unambiguously. We expected the disruption of the regularity of fragments of 14 mass units differences by the presence of a branched methyl. Such a disruption was not observed. Instead, intensities of ions at *m/z* 318 and 360 were weaker than their neighboring ions, implying that **2-11** and **2-12** were a mixture of two compounds with a branched methyl group at either C-14 or C-17 (Figure 2-5). The absolute configurations of **2-11** and **2-12** were both determined to be (3*R*, 26*S*) by the modified Mosher's method (Figure 2-6).

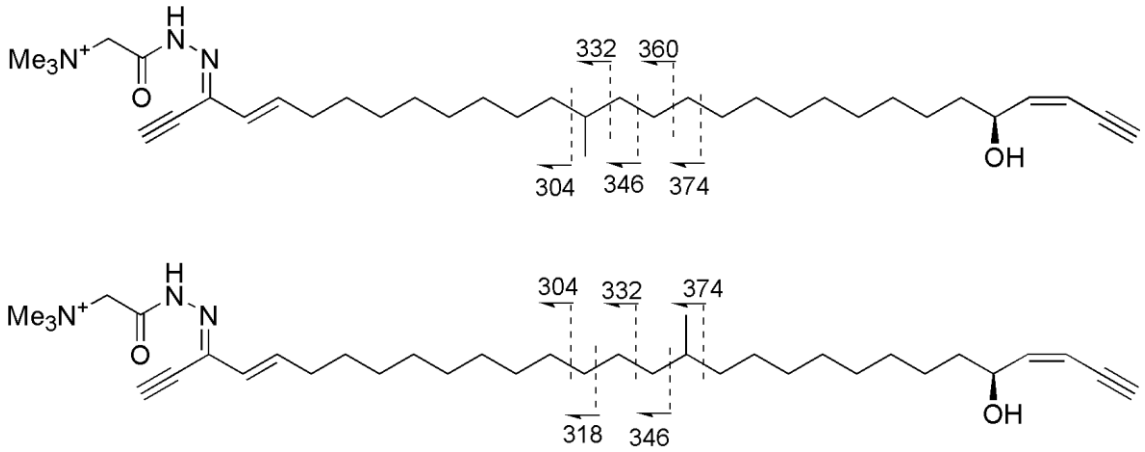

Figure 2-5. Diagnostic tandem FABMS fragment ions for the Girard's T derivatives of a mixture of **2-13** and **2-14**.

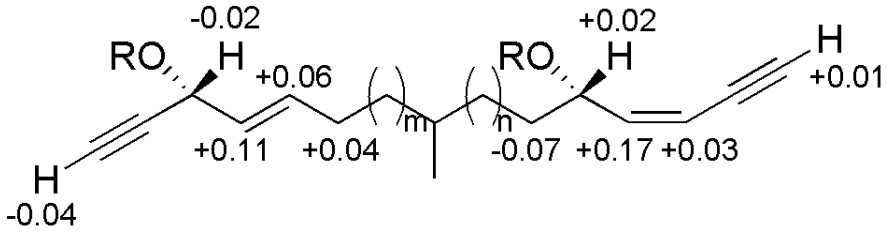

Figure 2-6. Result of the modified Mosher's method for the MTPA ester of **2-11** (m=7, n=10) and **2-12** (m=10, n=7). $\Delta\delta$ (δ_S-δ_R) values are shown.

(-)-Duryne (**2-1**) and (-)-durynes B-F (**2-2** - **2-6**) showed cytotoxic activity against HeLa cells with IC_{50} values of 0.50, 0.26, 0.26, 0.10, 0.08, and 0.34 μM, respectively. They are equipotent to duryne, whose reported IC_{50} values are 0.16-0.23 μM against P388, HCT-8, A549, and MCF7 cell lines.[3] Miyakosynes A-D (**2-7** - **2-10**) and a mixture of miyakosynes E (**2-11**) and F (**2-12**) exhibited cytotoxic activity against

HeLa cells with IC_{50} values of 0.23, 0.29, 0.88, 0.30, and 0.66 μM, respectively. The configuration of the allylic propargylic alcohol is variable among acetylenes from *Petrosia*. Only the *S*-isomers were reported for the petrosynols,[13, 14] adociacetylenes,[15]duryne,[3] petroformynes,[16] neopetroformynes,[17] petrocortynes,[18, 19] and the petroformynic acids.[20] They invariably exhibit a positive sign of optical rotation. However, the *R*-configuration was assigned for the corresponding carbinol carbons in the triangulynes, all of which showed a negative sign of optical rotation.[21] Curiously scalemic C_{30}-acetylenes were isolated from a Korean *Petrosia* sp.[22, 23] It is interesting to note that (-)-duryne was equipotent to its enantiomer, suggesting that the cellular targets of these metabolites do not recognize the configuration of the two secondary alcohols. Furthermore, miyakosynes were also equipotent to (-)-durynes, therefore, we reason that neither methyl branch nor the central olefin is indispensable for the potent cytotoxicity of this class of metabolites.

2.1.3. Experimental Section

2.1.3.1. General Experimental Procedures.

Optical rotations were measured on a JASCO DIP-1000 digital polarimeter. UV spectra were measured on a Shimadzu Biospec 1600. IR spectra were measured with a JASCO FT-IR-230 spectrophotometer. NMR spectra were recorded on a JEOL alpha 600 NMR spectrometer at 300 K. Chemical shifts were referenced to solvent peaks: δ_H7.27 and δ_c 77.2 for $CDCl_3$. ESI mass spectra were measured on a JEOL JMS-T100LC. FABMS and FABMSMS were measured on a JEOL JMS-700T. HPLC was carried out on the Shimadzu LC 20AT with a SCL-10Avp controller and a SPD-10Avp detector.

2.1.3.2. Animal Material.

The sponge *Petrosia* sp. was collected at Miyako sea-knoll, southwestern Japan, 25º25.64′N, 125º42.48′E, at a depth of 415 m, during a cruise of R/V Natsushima, by using the Remotely Operated Vehicle ‘Hyper-Dolphin’ in October 2009.A subglobular sponge with an optically smooth surface. A single large oscule with a peripheral sleeve opened on top of the body. Color beige. Consistency hard and crumbly. The ectosomal

skeleton is different from the choanosomal skeleton, consisting of a tangential unispicular network. The choanosomal skeleton consists of an isotropic network. Megascleresstrongyles in two size classes, with few oxeas. Microscleresabsent. The comparable species are *P. spheroida* Tanita, 1967 and *P. solusstrongyla* Hoshino, 1981 based on its external morphology. *P. spheroida* is distinguished from the present species by its bean-shaped microstrongyles. *P. solusstrongyla* has strongyles only, and the form and size of strongyles are variable. Habitat of the present species is also different from the two species. *P. spheroida* is reported from the shallow water of southwestern region of Japan Sea and *P. solusstrongyla*is reported from the subtidal zone to a depth of 15 m in Kagoshima. The specimen used for the identification (NSMT-Po1954) was deposited at National Museum of Nature and Science, Tokyo.

2.1.3.3. Extraction and Isolation.

The sponge was frozen after collection and kept frozen until extraction. The sponge (130 g, wet weight) was homogenized and extracted with EtOH (350 mL x 3) and $CHCl_3$/MeOH (1:1) (350 mL). The combined extracts were concentrated, and partitioned between H_2O (200 mL) and $CHCl_3$ (200 mL x 3). The $CHCl_3$ layer (IC_{50} value against HeLa cells 0.4 μg/mL) was further partitioned between *n*-hexane (100

mL) and 90% MeOH (100 mL). The 90% MeOH layer (IC_{50} 0.4 μg/mL) was concentrated and subjected to ODS column chromatography eluting with 50 % MeOH, 70 % MeOH (IC_{50} 10 μg/mL), 90% MeOH (IC_{50} 10 μg/mL), MeOH (IC_{50} 0.4 μg/mL), and $CHCl_3$/MeOH/H_2O (6:4:1, IC_{50} 22 μg/mL). The MeOH eluate was concentrated and subjected to silica gel column chromatography eluting with $CHCl_3$ (IC_{50} 0.4 μg/mL), $CHCl_3$/MeOH (98:2, IC_{50} 4.5 μg/mL), $CHCl_3$/MeOH (95:5, IC_{50} 4.5 μg/mL), $CHCl_3$/MeOH (9:1), $CHCl_3$/MeOH/H_2O (8:2:0.1), and $CHCl_3$/MeOH/H_2O (7:3:0.5). The $CHCl_3$ eluate was subjected to silica gel column chromatography eluting with *n*-hexane/EtOAc (9:1, IC_{50} 4.5 μg/mL), *n*-hexane/EtOAc (8:2, IC_{50} 0.4 μg/mL), and *n*-hexane/EtOAc (1:1, IC_{50} 4.5 μg/mL). The *n*-hexane/EtOAc (8:2) eluate was concentrated and separated by ODS HPLC (Cosmosil AR-II; 10 x 250 mm) with 90% - 100% MeOH to afford 14 fractions. The second fraction was purified by ODS HPLC (Cosmosil MS-II; 10 x 250 mm) with 85% MeCN to afford **2-1** (6.3 mg), **2-7** (21.6 mg), **2-9** (37 mg). The third fraction was purified by ODS HPLC with 86% MeCN to afford **2-3** (2.0 mg). The fifth fraction was purified by ODS HPLC with 90% MeCN to afford **2-8** (66 mg). The sixth fraction was purified by ODS HPLC with 90% MeCN to afford **2-6** (1.8 mg). The seventh fraction was purified by ODS HPLC with 85% MeCN to afford **2-2** (15.6 mg), **2-11** and **2-12** (7.2 mg). The eighth fraction was purified by ODS

HPLC with 90% MeCN to afford **2-4** (16.0 mg). The ninth fraction was purified by ODS HPLC with 90% MeCN to afford **2-10** (8.6 mg). The thirteenth fraction was purified by ODS HPLC with 93% MeCN to afford **2-5** (1.2 mg).

2.1.3.3.1. (-)-duryne (2-1): white solids; $[\alpha]^{17}_{D}$ -19 (*c* 0.27, $CHCl_3$); IR (film) ν_{max} 3400-3360 (br), 3282, 2917, 2852, 2118, 1654, 1467, 1088, 962 cm^{-1};^{1}H NMR data ($CDCl_3$), see Table 1; ^{13}C NMR data ($CDCl_3$), see Table 1; HRESIMS *m/z* 463.3524 $[M+Na]^+$ (calcd for $C_{30}H_{48}O_2Na$, 463.3552)

2.1.3.3.2. (-)-duryne B (2-2): white solids; $[\alpha]^{26}_{D}$ -17 (*c* 0.34, $CHCl_3$); UV (MeOH) λ_{max}(log ε) 206 (3.57); IR (film) ν_{max} 3440-3400 (br), 2916, 2849, 2121, 1647, 1468, 1215 cm^{-1}; ^{1}H NMR data ($CDCl_3$), see Table 1; ^{13}C NMR data ($CDCl_3$), see Table 1; HRESIMS *m/z* 491.3857 $[M+Na]^+$ (calcd for $C_{32}H_{52}O_2Na$, 491.3865)

2.1.3.3.3. (-)-duryne C (2-3): white solids; $[\alpha]^{25}_{D}$ -61 (*c* 0.05, $CHCl_3$); UV (MeOH) λ_{max}(log ε) 207 (3.60); IR (film) ν_{max} 3400-3360 (br), 3307, 3005, 2925, 2853, 2118, 1655, 1459, 1012, 968 cm^{-1};^{1}H NMR data ($CDCl_3$), see Table 2; ^{13}C NMR data ($CDCl_3$), see Table 2; HRESIMS *m/z* 489.3706 $[M+Na]^+$ (calcd for $C_{32}H_{50}O_2Na$, 489.3708).

2.1.3.3.4. (-)-duryne D (2-4): white solids; $[\alpha]^{26}_{D}$ -38 (*c* 0.22, $CHCl_3$); UV (MeOH) λ_{max}(log ε) 206 (3.59); IR (film) ν_{max} 3400-3340 (br), 3290, 2997, 2920, 2849, 2120, 1654, 1459, 1215, 964 cm^{-1};^{1}H NMR data ($CDCl_3$), see Table 2; ^{13}C NMR data ($CDCl_3$),

see Table 2; HRESIMS *m/z* 517.3986 $[M+Na]^+$ (calcd for $C_{34}H_{54}O_2Na$, 517.4021).

2.1.3.3.5. (-)-duryne E (2-5): white solids; $[\alpha]^{26}_D$ -120 (*c* 0.02, MeOH); UV (MeOH) λ_{max}(log ε) 210 (3.73); ^{1}H NMR data ($CDCl_3$), see Table 2; ^{13}C NMR data ($CDCl_3$), see Table 2; HRESIMS *m/z* 545.4351 $[M+Na]^+$ (calcd for $C_{36}H_{58}O_2Na$, 545.4334)

2.1.3.3.6. (-)-duryne F (2-6): white solids; $[\alpha]^{26}_D$ -32 (*c* 0.04, $CHCl_3$); UV (MeOH) λ_{max}(log ε) 225 (3.76); IR (film) ν_{max} 3400-3360 (br), 3308, 2922, 2851, 2120, 1655, 1459, 1014, 968 cm^{-1};^{1}H NMR data ($CDCl_3$), see Table 1; ^{13}C NMR data ($CDCl_3$), see Table 1; HRESIMS *m/z* 491.3846 $[M+Na]^+$ (calcd for $C_{32}H_{52}O_2Na$, 491.3865)

2.1.3.3.7. miyakosyne A (2-7)

Colorless solid; $[\alpha]_D^{24}$ -28 (*c* 0.42, MeOH); HRESIMS $(M+Na)^+$*m/z* 451.3548 (calcd for $C_{29}H_{48}O_2Na^+$, 451.3547); ^{1}H NMR ($CDCl_3$) and ^{13}C NMR ($CDCl_3$) data, see table 1.

2.1.3.3.8. miyakosyne B (2-8)

Colorless solid; $[\alpha]_D^{26}$ -27 (*c* 0.60, MeOH); HRESIMS $(M+Na)^+$*m/z* 465.3735 (calcd for $C_{30}H_{50}O_2Na^+$, 465.3704); ^{1}H NMR ($CDCl_3$) and ^{13}C NMR ($CDCl_3$) data, see table 1.

2.1.3.3.9. miyakosyne C (2-9)

Colorless solid; $[\alpha]_D^{24}$ -28 (*c* 0.72, MeOH); HRESIMS $(M+Na)^+$*m/z* 479.3856 (calcd for $C_{31}H_{52}O_2Na^+$, 479.3860); ^{1}H NMR ($CDCl_3$) and ^{13}C NMR ($CDCl_3$) data, see table 1.

2.1.3.3.10. miyakosyne D (2-10)

Colorless solid; $[\alpha]_D^{26}$ -25 (*c* 0.35, MeOH); HRESIMS $(M+Na)^+$ *m/z* 493.4036 (calcd for $C_{32}H_{54}O_2Na^+$, 493.4017); ^1H NMR ($CDCl_3$) and ^{13}C NMR ($CDCl_3$) data, see table 1.

2.1.3.3.11. miyakosynes E and F (2-11, 2-12)

Colorless oil; $[\alpha]_D^{25}$ -34 (*c* 0.32, MeOH); HRESIMS $(M+Na)^+$ *m/z* 479.3882 (calcd for $C_{31}H_{52}O_2Na^+$,479.3860); ^1H NMR ($CDCl_3$) and ^{13}C NMR ($CDCl_3$) data, see Table 3.

2.1.3.4. Preparation of MTPA Esters.

To solutions of samples **2-1** - **2-12** (0.1 mg each) in dry pyridine (10 μL) was added (*S*)-MTPACl (2 μL). The solutions were left at room temperature for 4 h-15 h, and the reaction mixtures were diluted with H_2O and extracted with $CHCl_3$. The organic layers were purified by reversed-phase HPLC to afford the (*R*)-MTPA esters. (*S*)-MTPA esters of **2-1** - **2-6, 2-11** - **2-12** were prepared in a similar way using (*R*)-MTPACl.

2.1.3.4.1. (*R*)-MTPA Ester of 2-1 (2-1a): ^1H NMR ($CDCl_3$) δ 6.04 (H-3, H-28), 6.02 (H-5, H-26), 5.50 (H-4, H-27), 5.35 (H-15, H-16), 2.64 (H-1, H-30), 2.05 (H-6, H-25), 2.02 (H-14, H-17), 1.26 - 1.36 (H-7 - H-13, H-18 - H-24): ESIMS *m/z* 895 $[M+Na]^+$

2.1.3.4.2. (*S*)-MTPA Ester of 2-1 (2-1b): ^1H NMR ($CDCl_3$) δ6.08 (H-5, H-26), 6.02 (H-3, H-28), 5.61 (H-4, H-27), 5.35 (H-15, H-16), 2.60 (H-1, H-30), 2.09 (H-6, H-25), 2.02 (H-14, H-17), 1.27 - 1.39 (H-7 - H-13, H-18 -H-24): ESIMS *m/z* 895 $[M+Na]^+$

2.1.3.4.3. (*R*)-MTPA Ester of 2-2 (2-2a): ^{1}H NMR ($CDCl_3$) δ 6.04 (H-3, H-30), 6.02 (H-5, H-28), 5.50 (H-4, H-29), 5.35 (H-15, H-16), 2.64 (H-1, H-32), 2.05 (H-6, H-27), 2.02 (H-14, H-17), 1.26 - 1.37 (H-7 -H-13, H-18 - H-26); ESIMS *m/z* 923 $[M+Na]^+$

2.1.3.4.4. (*S*)-MTPA Ester of 2-2 (2-2b): ^{1}H NMR ($CDCl_3$) δ 6.08 (H-5, H-28), 6.02 (H-3, H-30), 5.61 (H-4, H-29), 5.35 (H-15, H-16), 2.60 (H-1, H-32), 2.09 (H-6, H-27), 2.02 (H-14, H-17), 1.27 - 1.40 (H-7 - H-13, H-18 -H-26); ESIMS *m/z* 923 $[M+Na]^+$

2.1.3.4.5. (*R*)-MTPA Ester of 2-3 (2-3a): ^{1}H NMR ($CDCl_3$) δ 6.04 (H-3, H-30), 6.02 (H-5, H-28), 5.50 (H-4, H-29), 5.35 (H-11, H-12, H-17, H-18), 2.64 (H-1, H-32), 2.05 (H-6, H-27), 2.02 (H-10, H-13, H-16, H-19), 1.27 - 1.38 (H-7 - H-9, H-14 - H-15, H-20 - H-26); ESIMS *m/z* 921 $[M+Na]^+$

2.1.3.4.6. (*S*)-MTPA Ester of 2-3 (2-3b): ^{1}H NMR ($CDCl_3$) δ 6.08 (H-5, H-28), 6.02 (H-3, H-30), 5.61 (H-4, H-29), 5.35 (H-11, H-12, H-17, H-18), 2.60 (H-1, H-32), 2.09 (H-6, H-27), 2.02 (H-10, H-13, H-16, H-19), 1.27 - 1.40 (H-7 - H-9, H-14 - H-15, H-20 - H-26); ESIMS *m/z* 921 $[M+Na]^+$

2.1.3.4.7. (*R*)-MTPA Ester of 2-4 (2-4a): ^{1}H NMR ($CDCl_3$) δ 6.04 (H-3, H-32), 6.02 (H-5, H-30), 5.50 (H-4, H-31), 5.35 (H-13, H-14, H-19, H-20), 2.64 (H-1, H-34), 2.05 (H-6, H-29), 2.02 (H-12, H-15, H-18, H-21), 1.26 - 1.36 (H-7 - H-11, H-16 - H-17, H-22 - H-28); ESIMS *m/z* 949 $[M+Na]^+$

2.1.3.4.8. (*S*)-MTPA Ester of 2-4 (2-4b): ^{1}H NMR ($CDCl_3$) δ 6.08 (H-5, H-30), 6.02 (H-3, H-32), 5.61 (H-4, H-31), 5.35 (H-13, H-14, H-19, H-20), 2.60 (H-1, H-34), 2.09 (H-6, H-29), 2.02 (H-12, H-15, H-18, H-21), 1.26 - 1.39 (H-7 - H-11, H-16 - H-17, H-22 - H-28); ESIMS *m/z* 949 $[M+Na]^+$

2.1.3.4.9. (*R*)-MTPA Ester of 2-5 (2-5a):^{1}H NMR ($CDCl_3$) δ 6.04 (H-3, H-34), 6.02 (H-5, H-32), 5.50 (H-4, H-33), 5.35 (H-15, H-16, H-21, H-22), 2.64 (H-1, H-36), 2.05 (H-6, H-31), 2.02 (H-14, H-17, H-20, H-23), 1.26 - 1.37 (H-7 - H-13, H-18 - H-19, H-24 - H-30); ESIMS *m/z* 977 $[M+Na]^+$

2.1.3.4.10. (*S*)-MTPA Ester of 2-5 (2-5b):^{1}H NMR ($CDCl_3$) δ 6.08 (H-5, H-32), 6.02 (H-3, H-34), 5.61 (H-4, H-33), 5.35 (H-15, H-16, H-21, H-22), 2.60 (H-1, H-36), 2.09 (H-6, H-31), 2.02 (H-14, H-17, H-20, H-23), 1.27 - 1.41 (H-7 - H-13, H-18 - H-19, H-24 - H-30) ESIMS *m/z* 977 $[M+Na]^+$

2.1.3.4.11. (*R*)-MTPA Ester of 2-6 (2-6a):^{1}H NMR ($CDCl_3$) δ 6.04 (H-3), 6.02 (H-5), 5.95 (H-28), 5.83 (H-29), 5.64 (H-30), 5.36 (H-15, H-16), 5.50 (H-4), 3.25 (H-32), 2.64 (H-1), 2.05 (H-6), 2.02 (H-14, H-17), 1.81 (H-27α), 1.68 (H-27β), 1.26 - 1.36 (H-7 - H-13, H-18 - H-26); ESIMS *m/z* 923 $[M+Na]^+$

2.1.3.4.12. (*S*)-MTPA Ester of 2-6 (2-6b):^{1}H NMR ($CDCl_3$) δ 6.08 (H-5), 6.02 (H-3), 6.00 (H-29), 5.96 (H-28), 5.67 (H-30), 5.61 (H-4), 5.36 (H-15, H-16), 3.26 (H-32), 2.60

(H-1), 2.09 (H-6), 2.02 (H-14, H-17), 1.74 (H-27α), 1.23 - 1.61 (H-7 - H-13, H-18 - H-26, H-27β); ESIMS *m/z* 923 $[M+Na]^+$

2.1.3.4.13. (*R*)-MTPA ester of 2-7: ^{1}H NMR ($CDCl_3$) δ 6.04 (H-3, H-26), 6.02 (H-5, H-24), 5.50 (H-4, H-25), 2.64 (H-1, H-28), 2.05 (H-6, H-23), 1.24-1.64 (H-7 - H-12, H-16 - H-22), 1.36 (H-14), 1.08 (H-13, H-15), 0.84 (14-Me); ESIMS *m/z* 899 $(M+Na)^+$

2.1.3.4.14. (*R*)-MTPA ester of 2-8: ^{1}H NMR ($CDCl_3$) δ 6.04 (H-3, H-27), 6.02 (H-5, H-25), 5.50 (H-4, H-26), 2.64 (H-1, H-29), 2.05 (H-6, H-24), 1.24-1.64 (H-7 - H-12, H-16 - H-23), 1.35 (H-14), 1.08 (H-13, H-15), 0.84 (14-Me); ESIMS *m/z* 913 $(M+Na)^+$

2.1.3.4.15. (*R*)-MTPA ester of 2-9: ^{1}H NMR ($CDCl_3$) δ 6.04 (H-3, H-28), 6.02 (H-5, H-26), 5.50 (H-4, H-27), 2.64 (H-1, H-30), 2.05 (H-6, H-25), 1.24-1.64 (H-7 - H-12, H-16 - H-24), 1.35 (H-14), 1.08 (H-13, H-15), 0.84 (14-Me); ESIMS *m/z* 927 $(M+Na)^+$

2.1.3.4.16. (*R*)-MTPA ester of 2-10: ^{1}H NMR ($CDCl_3$) δ 6.04 (H-3, H-29), 6.02 (H-5, H-27), 5.50 (H-4, H-28), 2.64 (H-1, H-31), 2.05 (H-6, H-26), 1.24-1.64 (H-7 - H-12, H-16 - H-25), 1.35 (H-14), 1.08 (H-13, H-15), 0.84 (14-Me); ESIMS *m/z* 941 $(M+Na)^+$

2.1.3.4.17. (*R*)-MTPA ester of 2-11 and 2-12: ^{1}H NMR for (*R*)-MTPA ester of **5** and **6** ($CDCl_3$) δ 6.04 (H-3), 6.02 (H-5), 5.95 (H-26), 5.83 (H-27), 5.64 (H-28), 5.50 (H-4), 3.26 (H-30), 2.64 (H-1), 2.05 (H-6), 1.81 (H-25α): (*R*)-MTPA ester of **11** 1.25-1.68 (H-7 - H-12, H-16 - H-24, H-25β), 1.35 (H-14), 1.08 (H-13, H-15), 0.84 (14-Me); (*R*)-MTPA

ester of **12** 1.25-1.68 (H-7 - H-15, H-19 - H-24, H-25β), 1.35 (H-17), 1.08 (H-16, H-18), 0.84 (17-Me); ESIMS *m/z* 911 $(M+Na)^+$

2.1.3.4.18. (*S*)-MTPA ester of 2-11 and 2-12: ^{1}H NMR for (*S*)-MTPA ester of **11** and **12** ($CDCl_3$) δ 6.08 (H-5), 6.02 (H-3), 6.00 (H-27), 5.97 (H-26), 5.67 (H-28), 5.61 (H-4), 3.27 (H-30), 2.60 (H-1), 2.05 (H-6), 1.74 (H-25α): (*S*)-MTPA ester of **5** 1.23-1.63 (H-7 - H-12, H-16 - H-24, H-25β), 1.36 (H-14), 1.08 (H-13, H-15), 0.84 (14-Me); (*S*)-MTPA ester of **6** 1.23-1.63 (H-7 - H-15, H-19 - H-24, H-25β), 1.36 (H-17), 1.08 (H-16, H-18), 0.84 (17-Me); ESIMS *m/z* 911 $(M+Na)^+$

2.1.3.5. Ozonolysis of 2-2 - 2-6. Separately solution of acetylenes, **2-2** - **2-6** (0.5 mg each) in CH_2Cl_2 (1 mL) were treated with O_3 at -78ºC for 15 min. After excess O_3 was removed by a stream of N_2, the reaction mixtures were treated with 90% HCOOH/35% H_2O_2 (2:1, 1 mL) at room temperature for 15 min. The products were concentrated and subjected to FABMS without further separation.

2.1.3.6. keto-alcohols 2-13 and 2-14

To a mixture of **2-11** and **2-12** (0.5 mg) was added DDQ solution in dioxane (15 mg/mL, 20 μL). The solution was left at room temperature for a week, and the reaction mixture

was purified by silica gel column chromatography eluted with *n*-hexane/EtOAc (95:5) to afford a mixture of keto-alcohols **2-13** and **2-14**(0.2 mg)

2.1.3.6.1. keto-alcohols 2-13 and 2-14

Colorless oil; HRESIMS $(M+Na)^+$ *m/z* 477.3698 (calcd for $C_{31}H_{50}O_2Na^+$, 477.3704); ^1H NMR of keto-alcohol **2-13** and **2-14** ($CDCl_3$) δ 7.26 (m, H-5), 6.19 (d, *J*=15.6, H-4), 6.00 (dd, *J*=11.0, 8.3, H-27), 5.54 (dd, *J*=11.0, 1.4, H-28), 4.68 (m, H-26), 3.22 (s, H-1), 3.14 (d, *J*=1.4, H-30), 2.32 (m, H-6), 1.63 (m, H-25α), 1.53 (m, H-25β): **2-13** 1.35 (m, H-14), 1.08 - 1.40 (H-7 - H-13, H-15 - H-24), 0.84 (d, *J*=6.6, 14-Me); **2-14**1.35 (m, H-17), 1.08 - 1.40 (H-7 - H-16, H-18 - H-24), 0.84 (d, *J*=6.6, 17-Me)

2.1.3.7. Preparation of Girard's T derivatives of 2-13 and 2-14.

To a portion of a mixture of **2-13** and **2-14** (0.1 mg) was added Girard's reagent T in AcOH (50 mg/mL, 20 μL) and the solution was kept at 70 ºC for 30 min. The reaction mixture was evaporated by a stream of dry nitrogen and diluted with MeOH (5 μL) before application to tandem FABMS analysis.

2.1.3.8. Cytotoxicity Assay.

The cytotoxicities of **2-1** - **2-12** against HeLa cells were evaluated by an MTT assay.[24]

HeLa human cervical cancer cells were cultured in Dulbecco's modified Eagle's medium containing 10% fetal bovine serum, 2 μg/mL gentamycin, and 2 μg/mL antibiotic-antimicotic (Gibco) at 37°C under an atomosphere of 5% CO_2. To each well of a 96-well microplate containing 200 μL of tumor cell suspension (1 x 10^4 cells/mL) was added a sample after 24 h preincubation, and the plate was incubated for 72 h. After addition of 3-(4,5-dimethylthiazol-2-yl)-2,5-diphenyltetrazolium bromide (MTT) saline solution (1 mg/mL, 50 μL) to each well, the plate was incubated for 3 h. After the incubation, the supernatant was discarded and DMSO (150 μL) was added. The absorbance was measured to determine IC_{50} values. In this assay, adriamycin was used as a positive control (IC_{50} 1.64 μM).

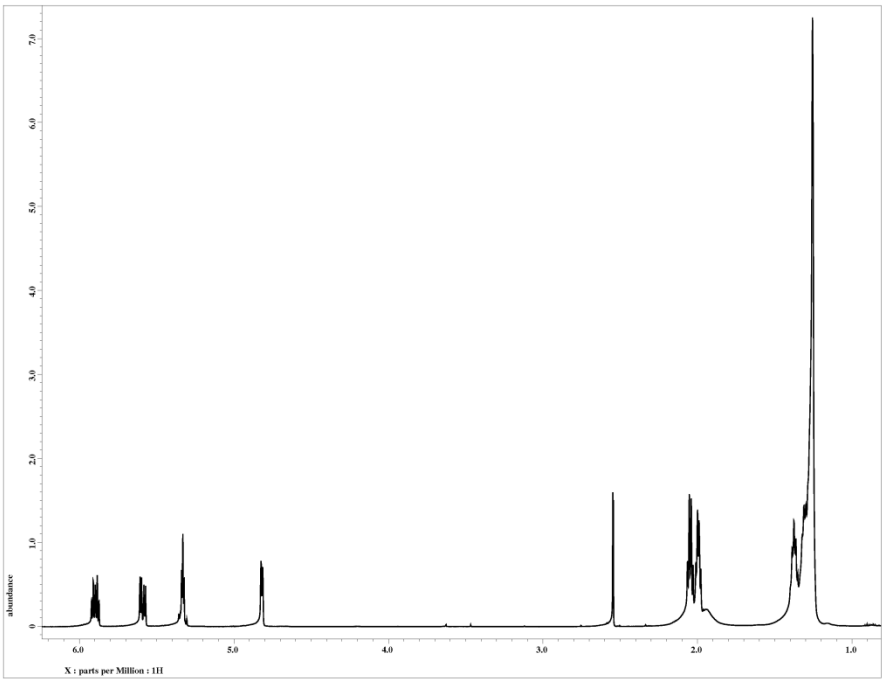

Figure S2-1-1. ^{1}H NMR spectrum of (-)-duryne (**2-1**) in $CDCl_3$

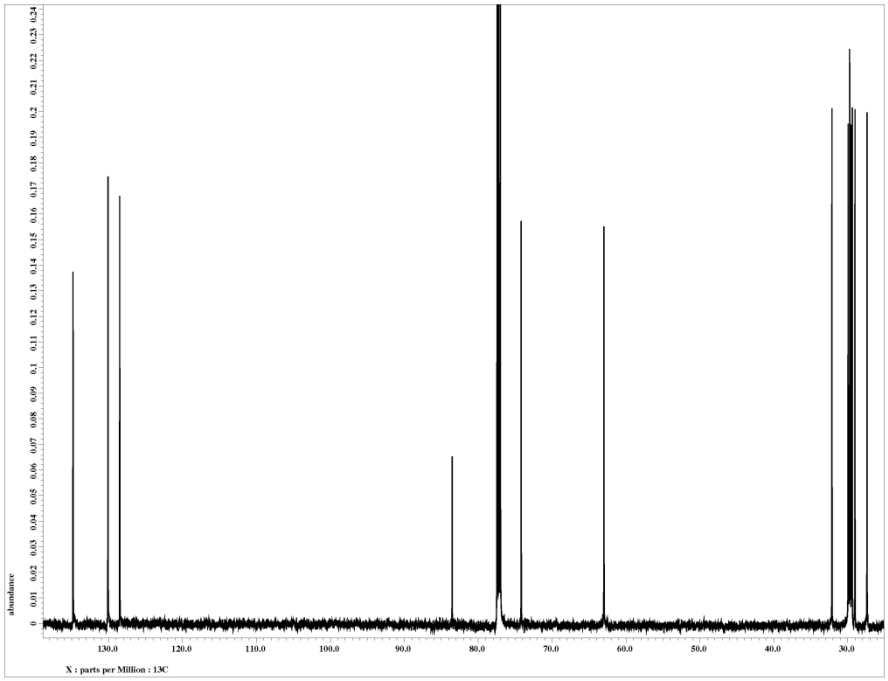

Figure S2-1-2. ^{13}C NMR spectrum of (-)-duryne (**2-1**) in $CDCl_3$

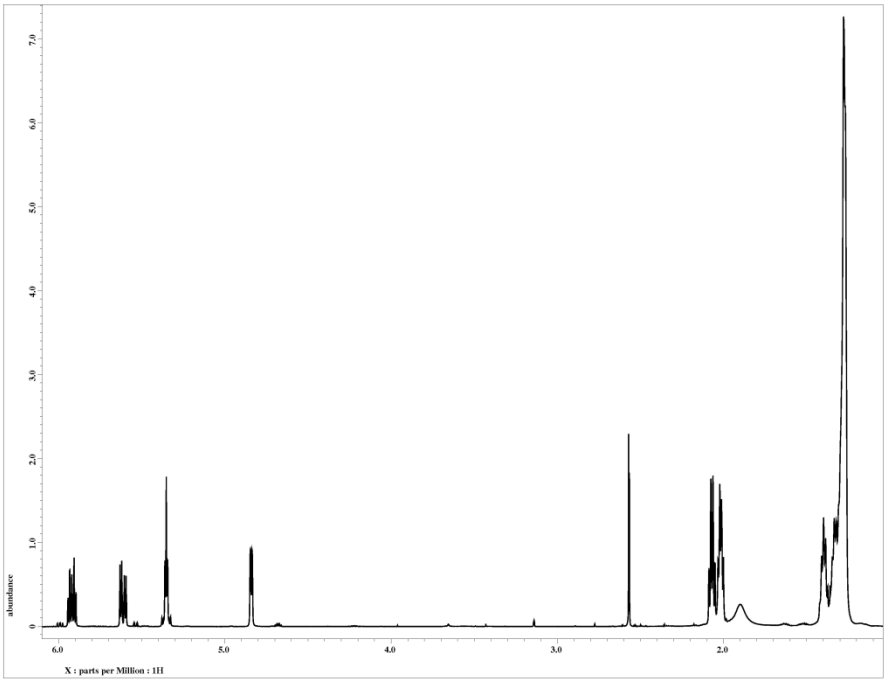

Figure S2-1-3. ^{1}H NMR spectrum of (-)-duryne B (**2-2**) in $CDCl_3$

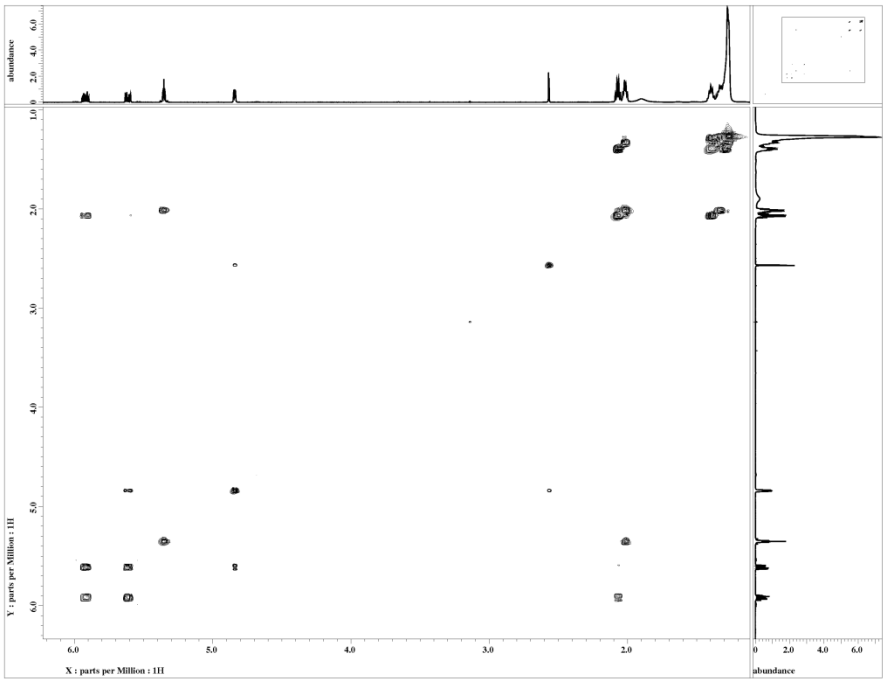

Figure S2-1-4. COSY spectrum of (-)-duryne B (**2-2**) in $CDCl_3$

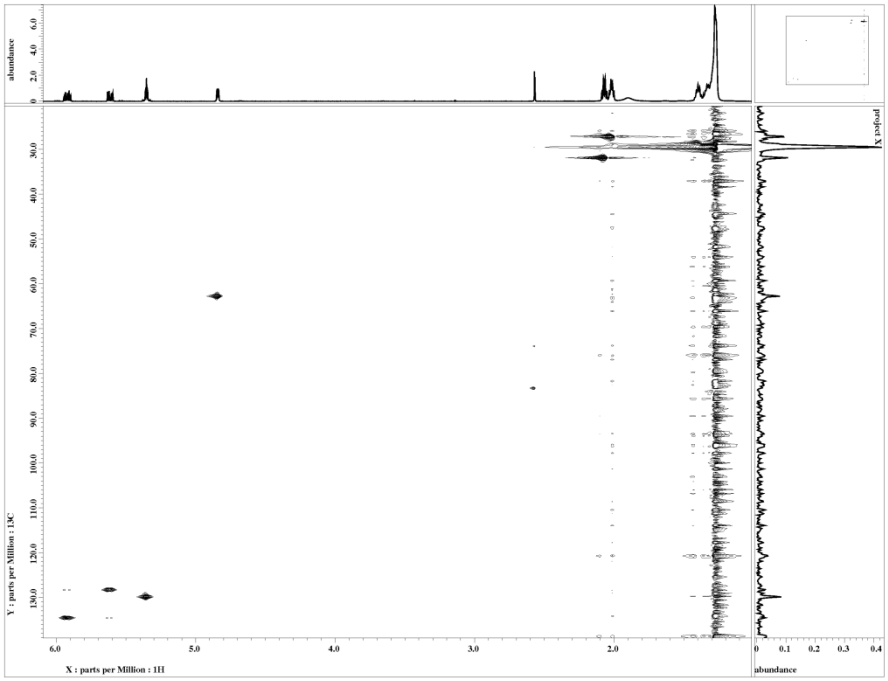

Figure S2-1-5. HSQC spectrum of (-)-duryne B (**2-2**) in $CDCl_3$

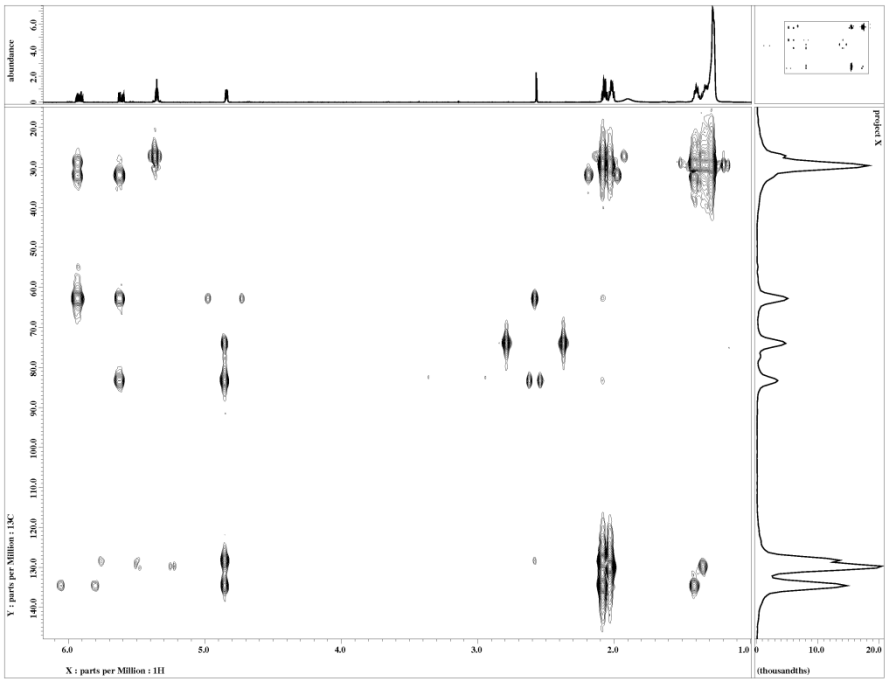

Figure S2-1-6. HMBC spectrum of (-)-duryne B (**2-2**) in $CDCl_3$

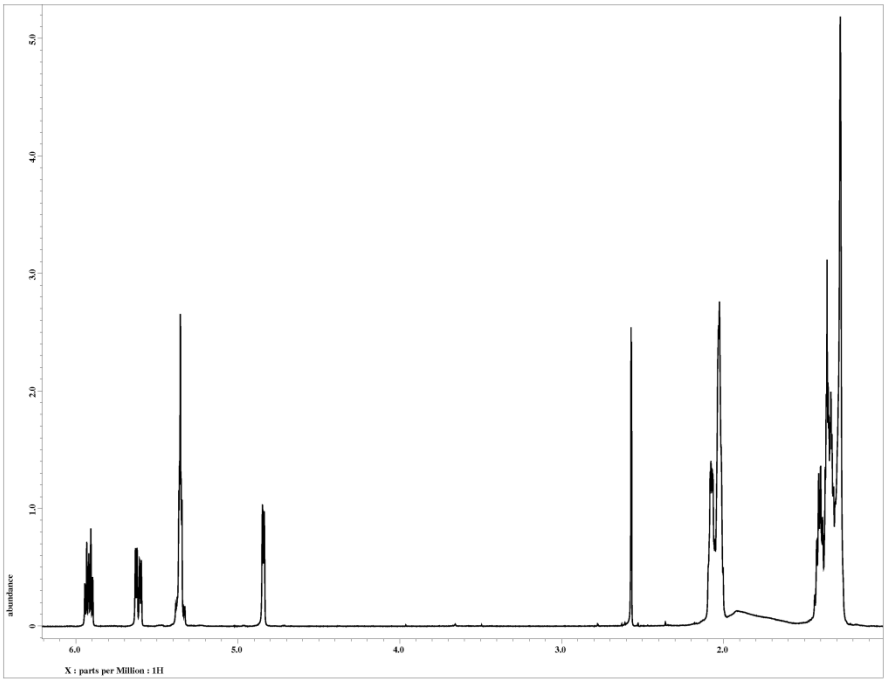

Figure S2-1-7. ^{1}H NMR spectrum of (-)-duryne C (**2-3**) in $CDCl_3$

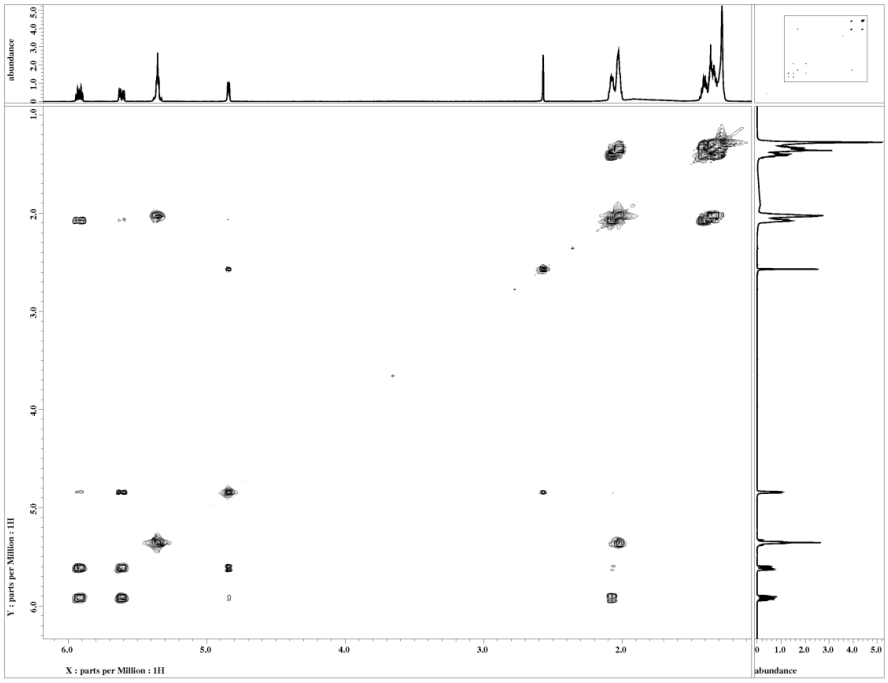

Figure S2-1-8. COSY spectrum of (-)-duryne C (**2-3**) in $CDCl_3$

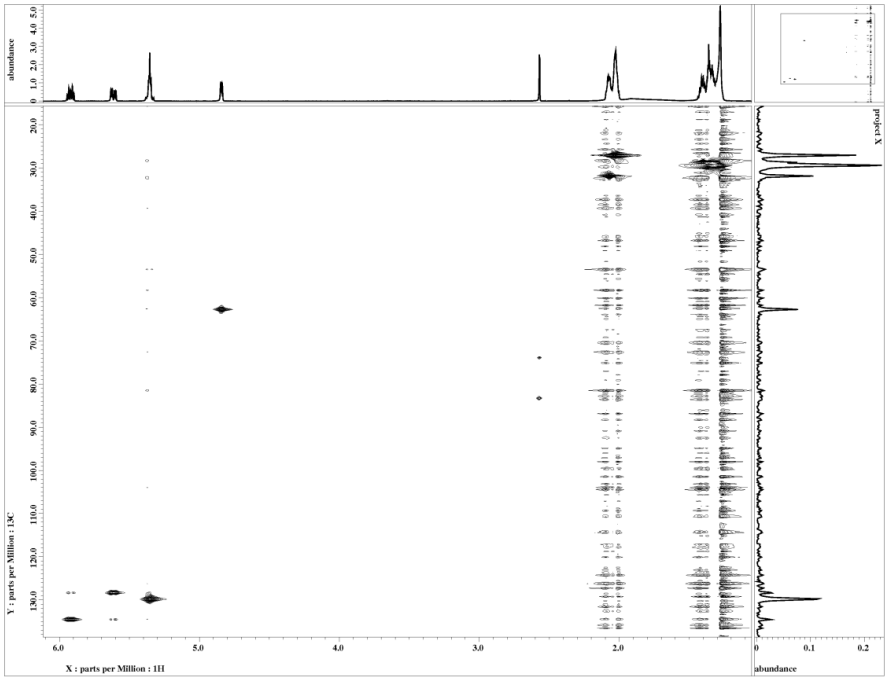

Figure S2-1-9. HSQC spectrum of (-)-duryne C (**2-3**) in $CDCl_3$

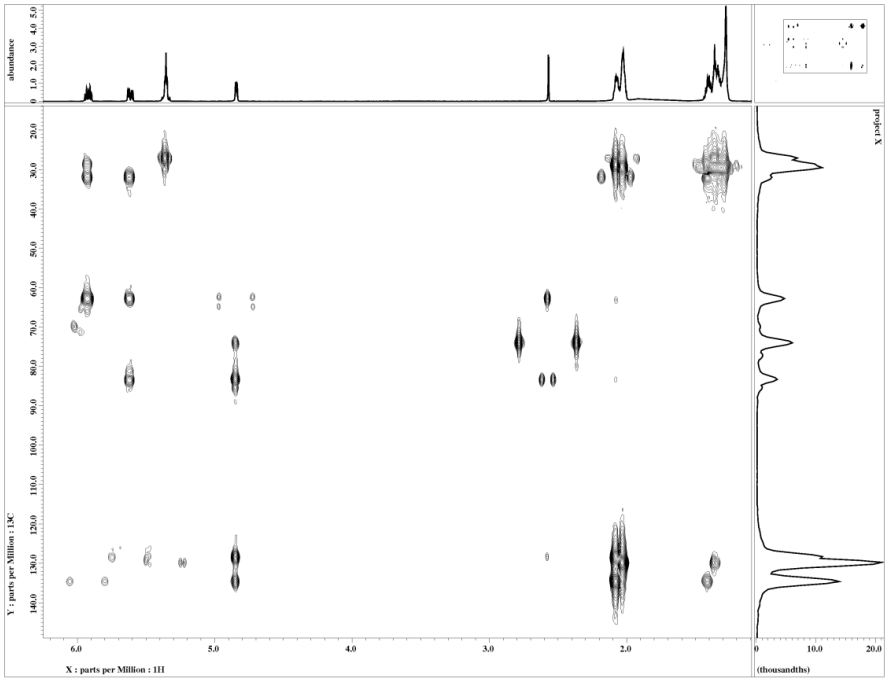

Figure S2-1-10. HMBC spectrum of (-)-duryne C (**2-3**) in $CDCl_3$

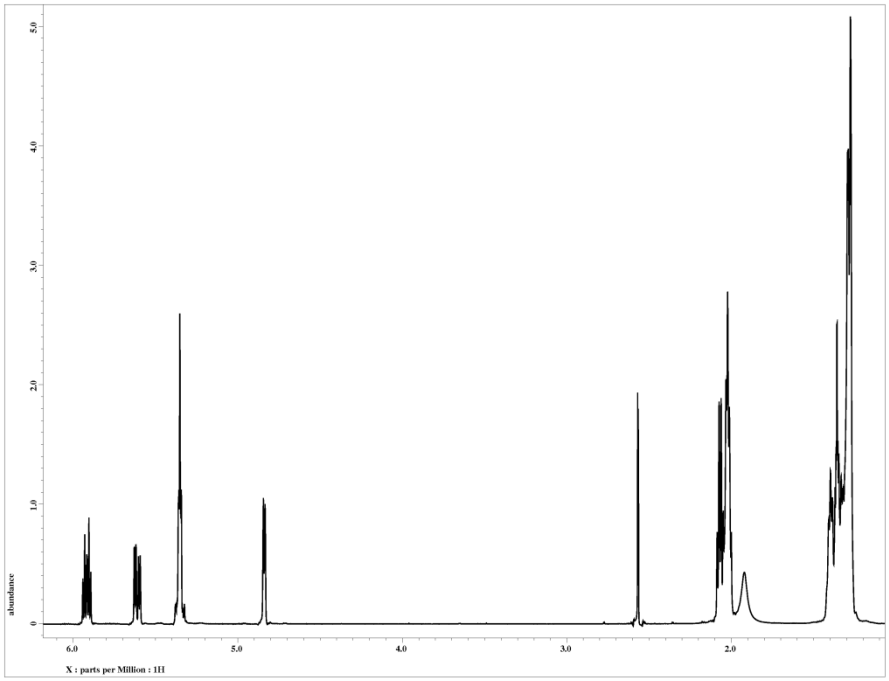

Figure S2-1-11. ^{1}H NMR spectrum of (-)-duryne D (**2-4**) in $CDCl_3$

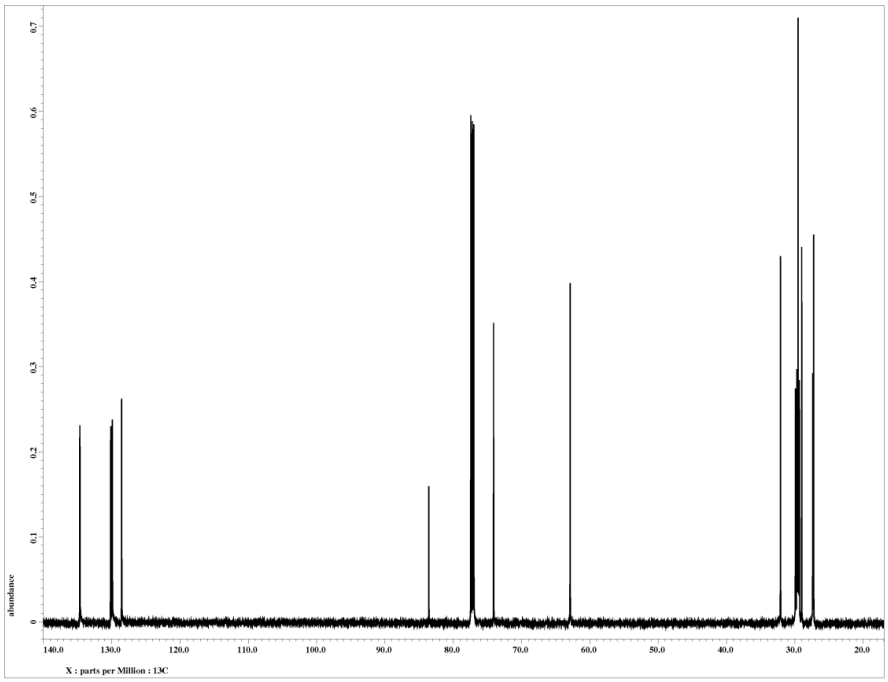

Figure S2-1-12. ^{13}C NMR spectrum of (-)-duryne D (**2-4**) in $CDCl_3$

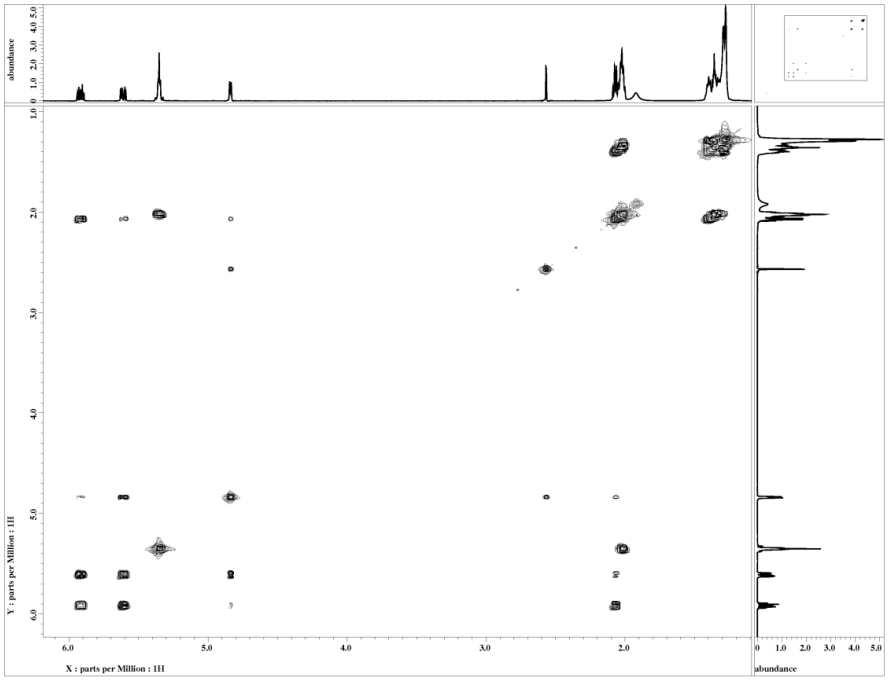

Figure S2-1-13. COSY spectrum of (-)-duryne D (**2-4**) in $CDCl_3$

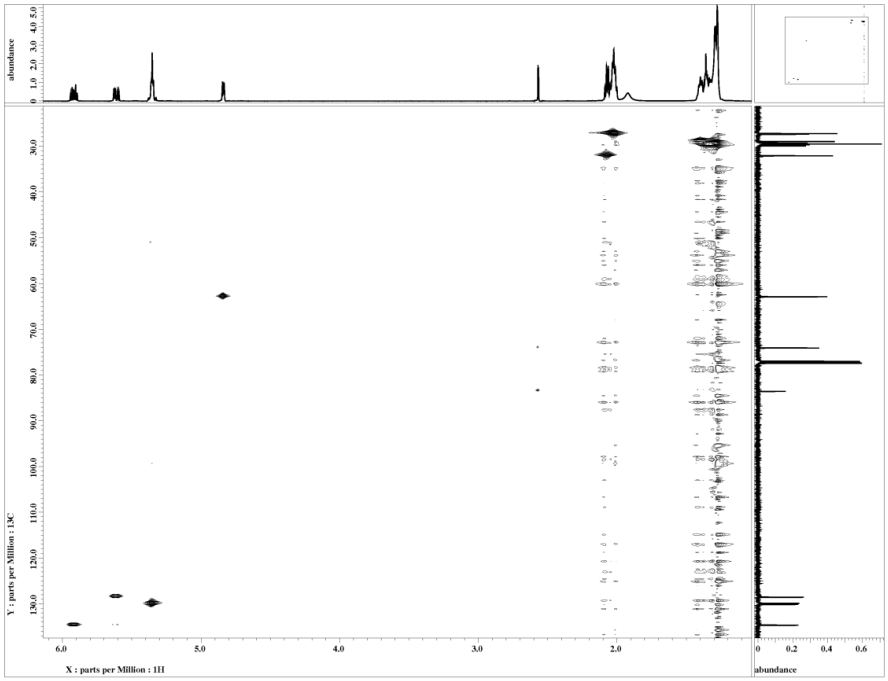

Figure S2-1-14. HSQC spectrum of (-)-duryne D (**2-4**) in $CDCl_3$

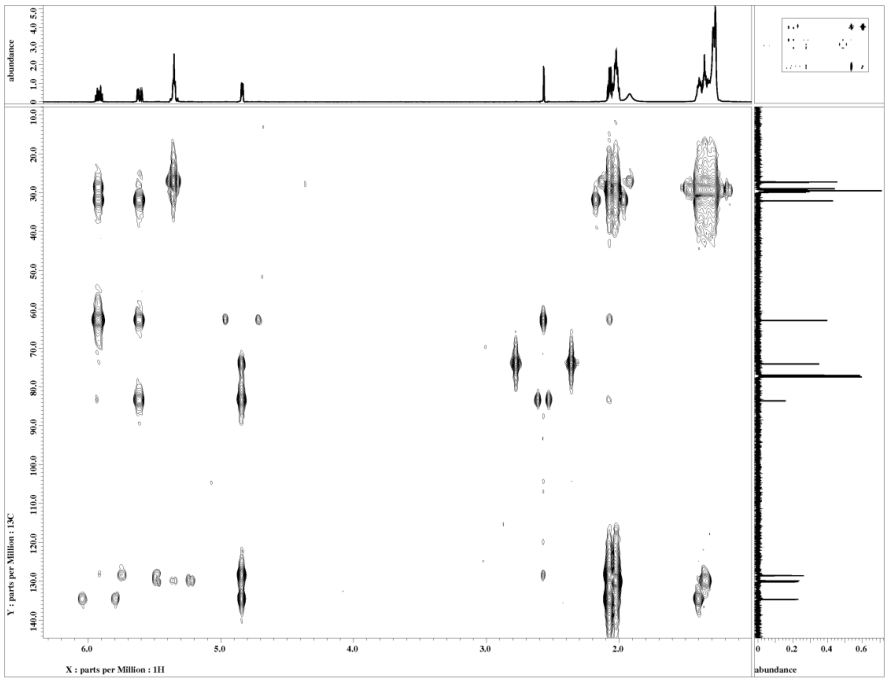

Figure S2-1-15. HMBC spectrum of (-)-duryne D (**2-4**) in $CDCl_3$

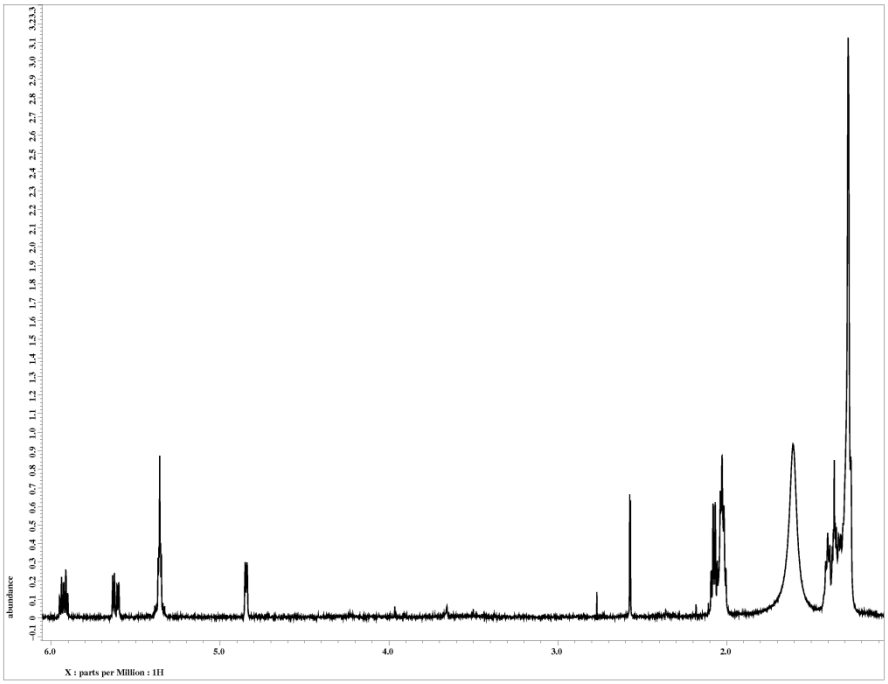

Figure S2-1-16. ^{1}H NMR spectrum of (-)-duryne E (**2-5**) in $CDCl_3$

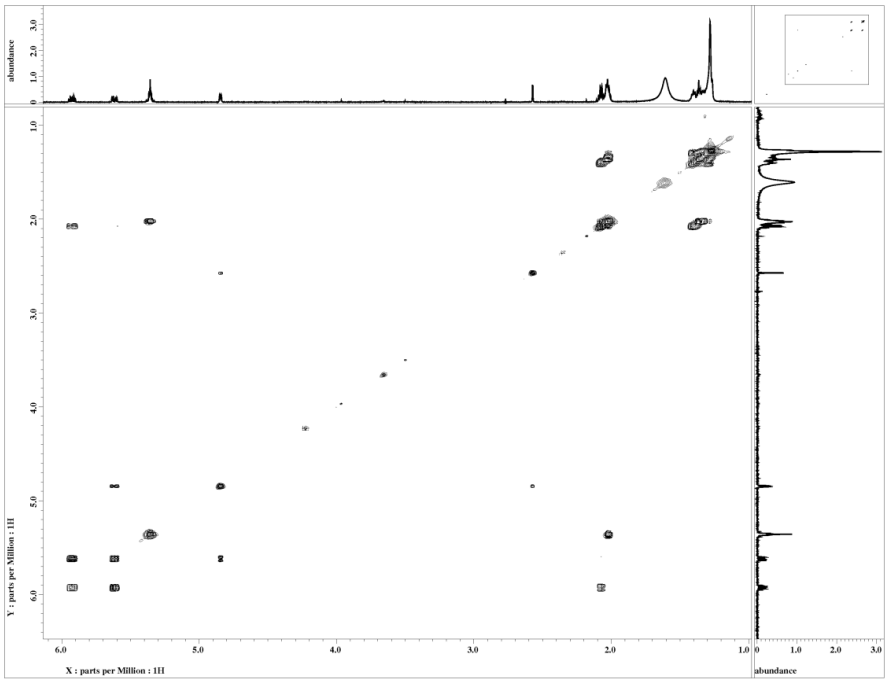

Figure S2-1-17. COSY spectrum of (-)-duryne E (**2-5**) in $CDCl_3$

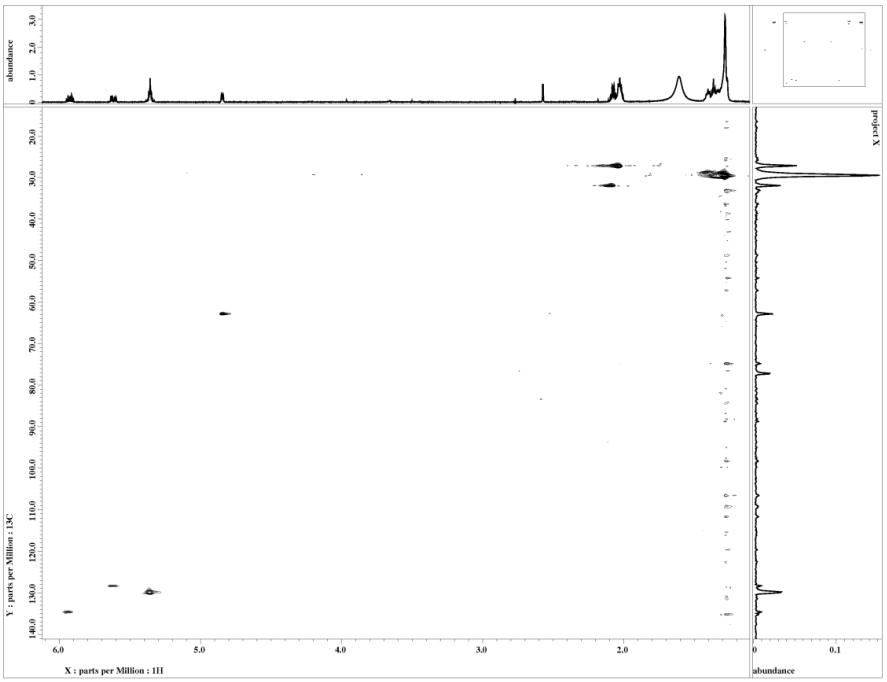

Figure S2-1-18. HSQC spectrum of (-)-duryne E (**2-5**) in $CDCl_3$

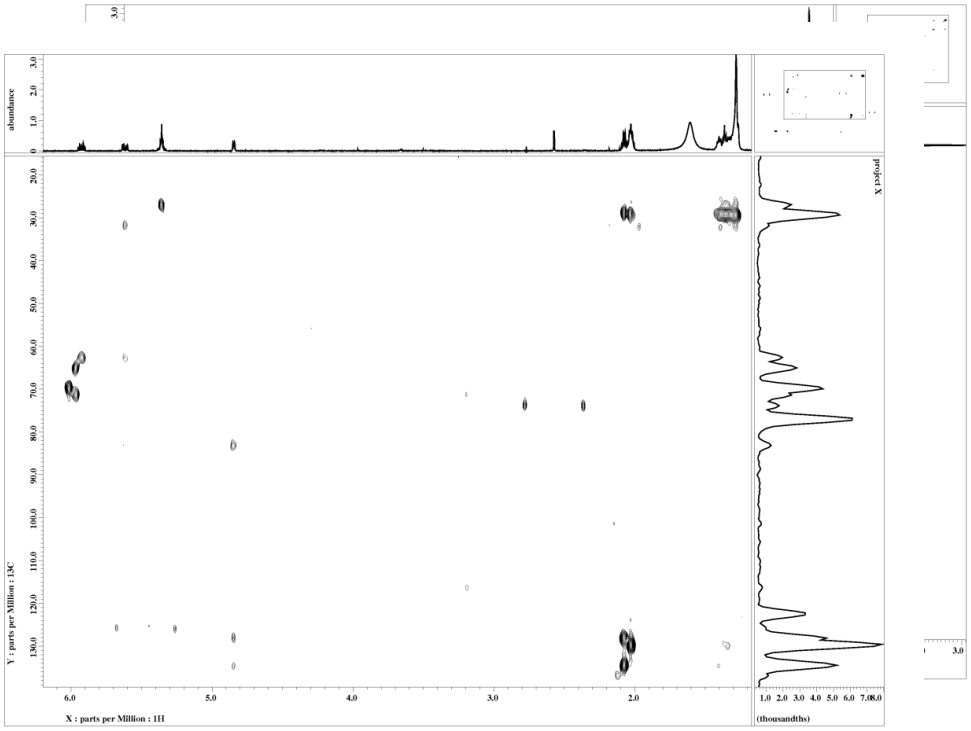

Figure S2-1-19. HMBC spectrum of (-)-duryne E (**2-5**) in $CDCl_3$

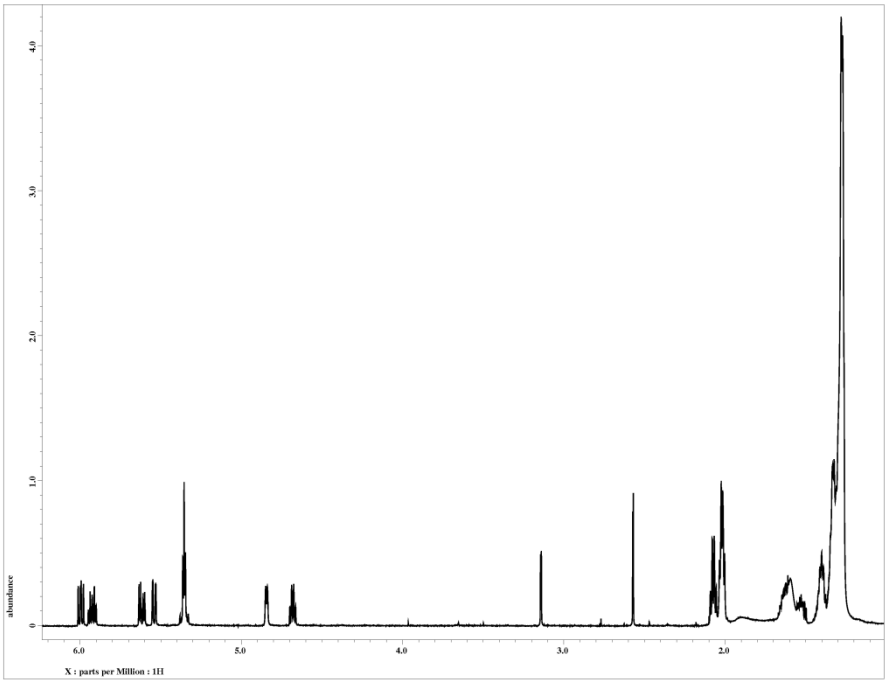

Figure S2-1-20. ^{1}H NMR spectrum of (-)-duryne F (**2-6**) in $CDCl_3$

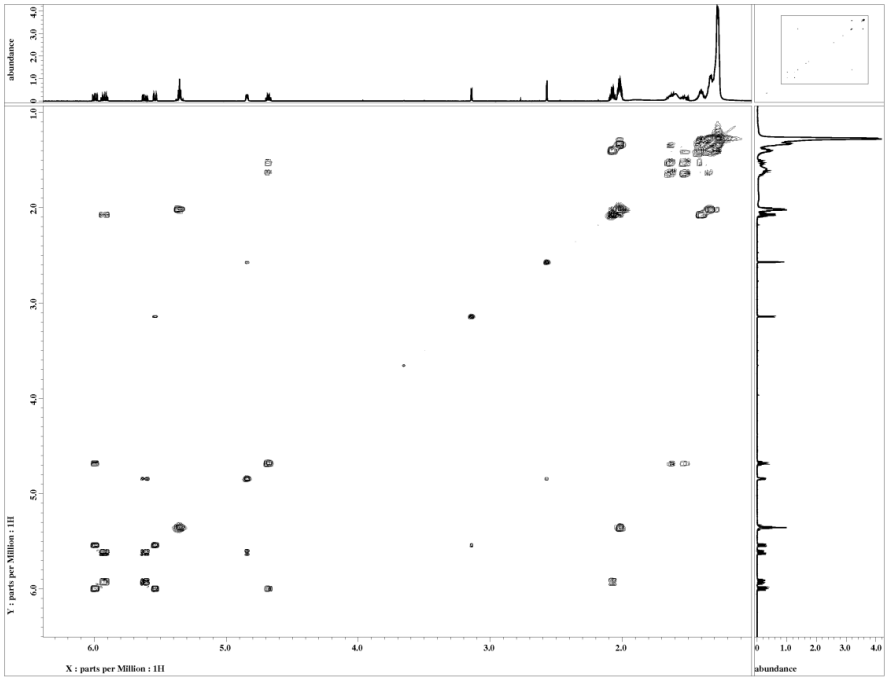

Figure S2-1-21. COSY spectrum of (-)-duryne F (**2-6**) in $CDCl_3$

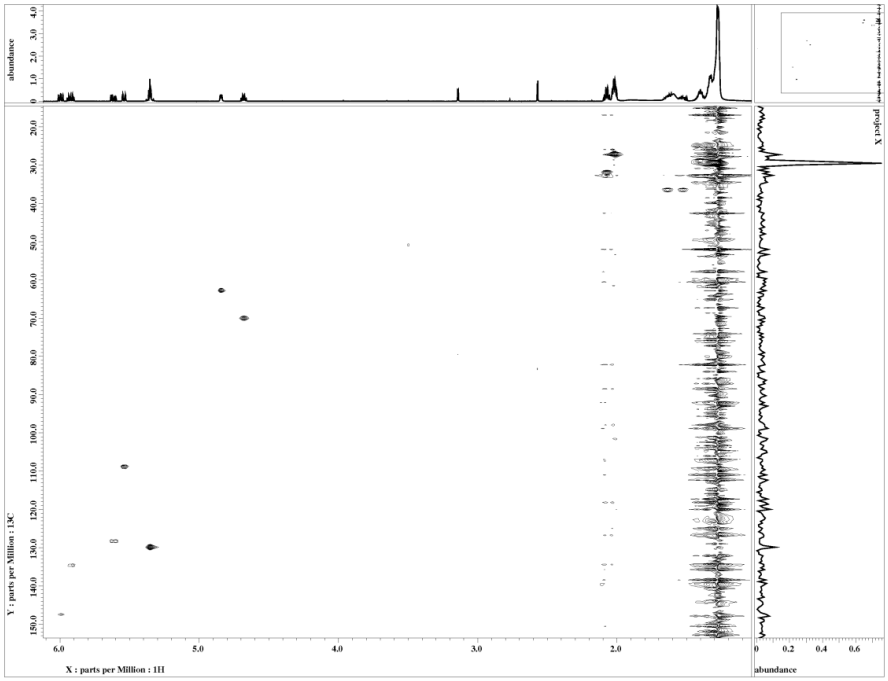

Figure S2-1-22. HSQC spectrum of (-)-duryne F (**2-6**) in $CDCl_3$

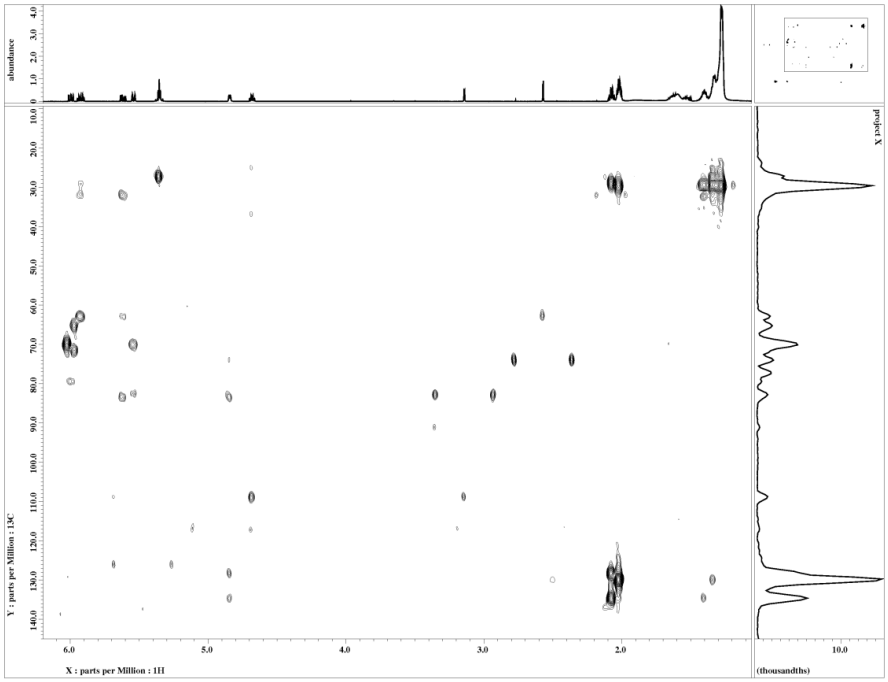

Figure S2-1-23. HMBC spectrum of (-)-duryne F (**2-6**) in $CDCl_3$

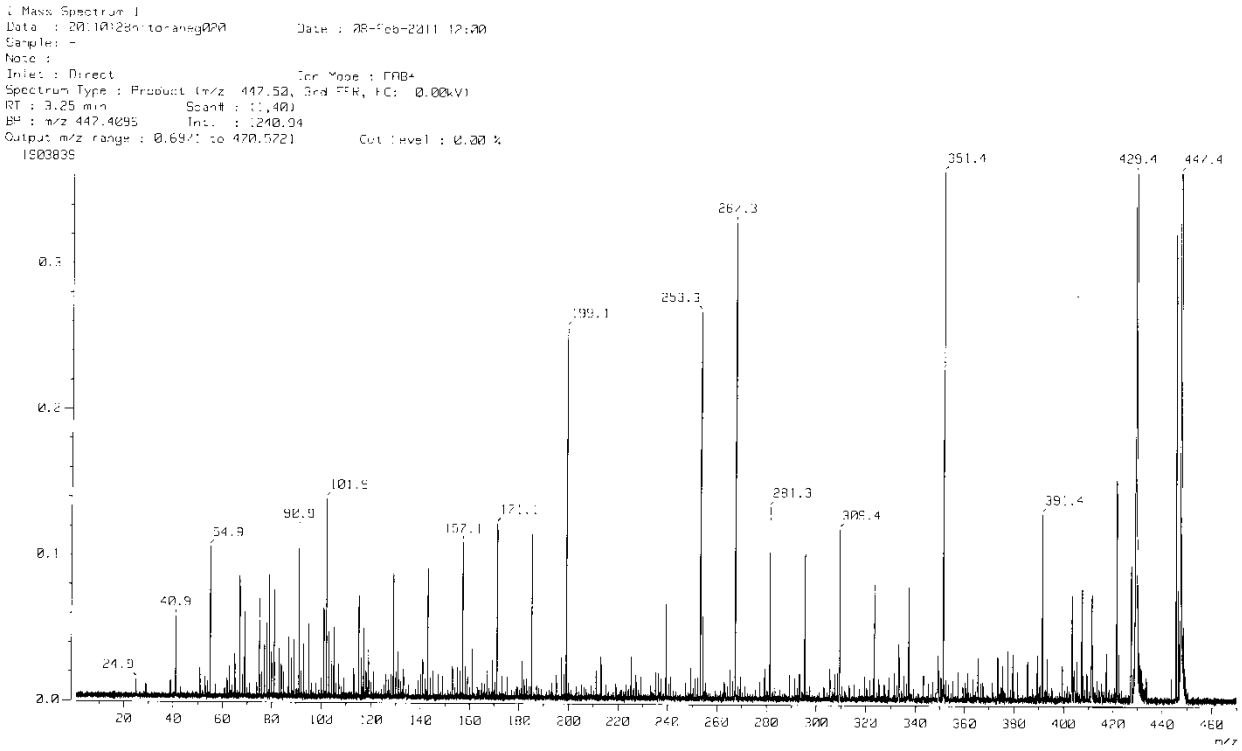

Figure S2-1-24. FABMSMS spectrum of (-)-duryne (**2-1**)

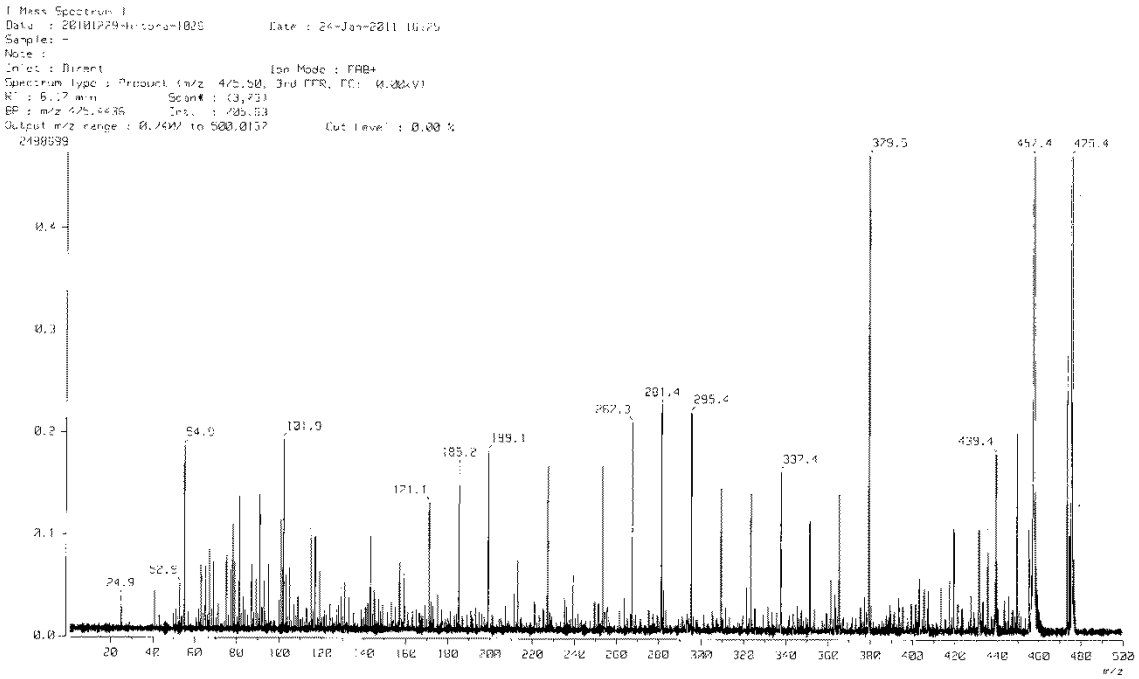

Figure S2-1-25. FABMSMS spectrum of (-)-duryne B (**2-2**)

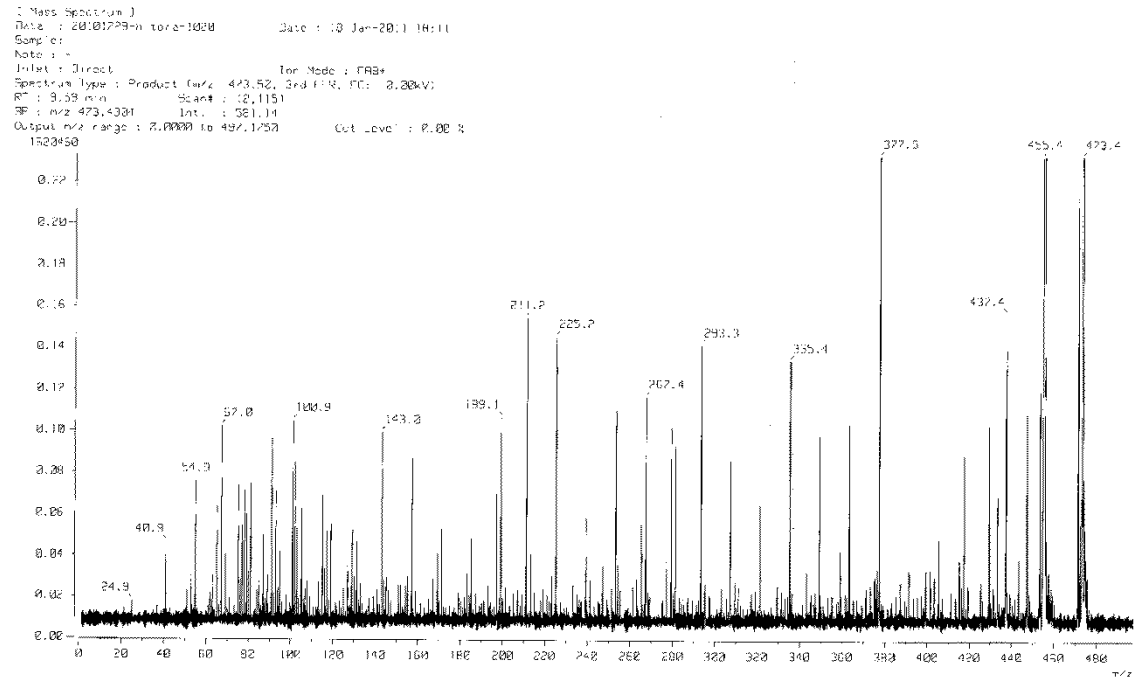

Figure S2-1-26. FABMSMS spectrum of (-)-duryne C (**2-3**)

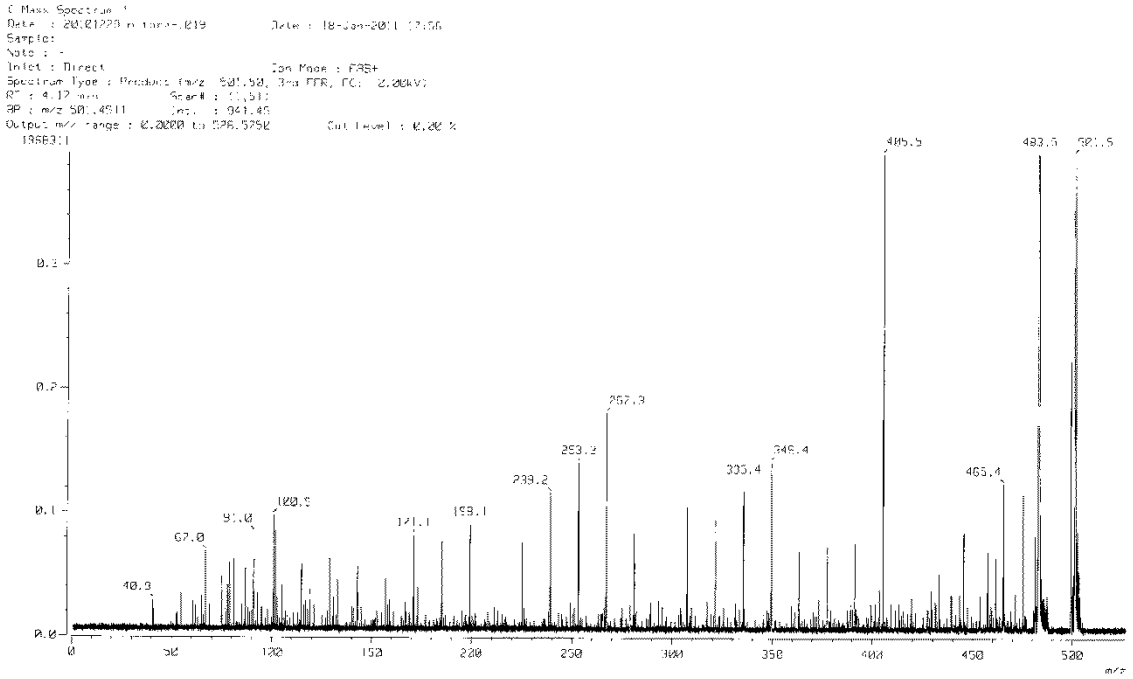

Figure S2-1-27. FABMSMS spectrum of (-)-duryne D (**2-4**)

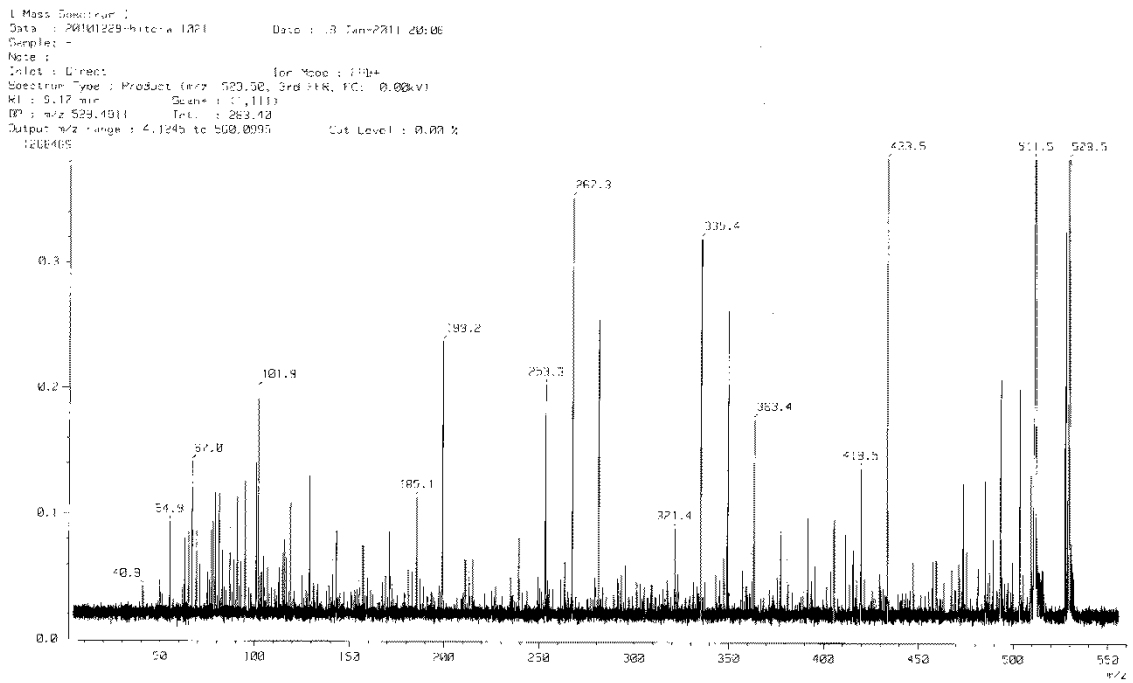

Figure S2-1-28. FABMSMS spectrum of (-)-duryne E (**2-5**)

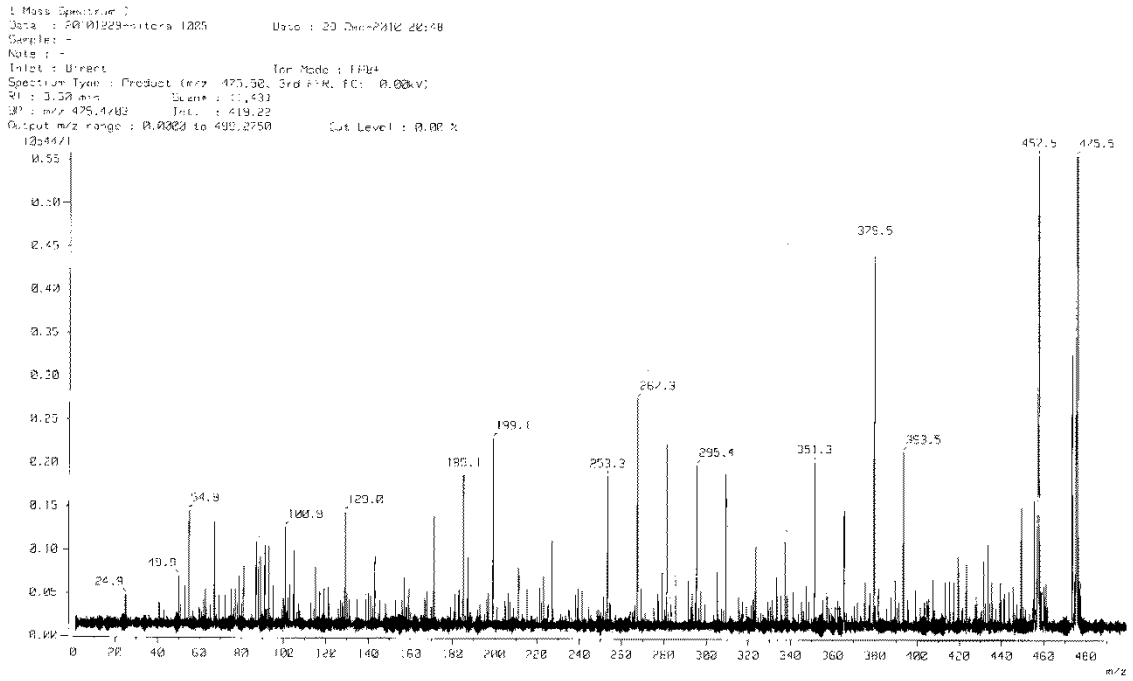

Figure S2-1-29. FABMSMS spectrum of (-)-duryne F (**2-6**)

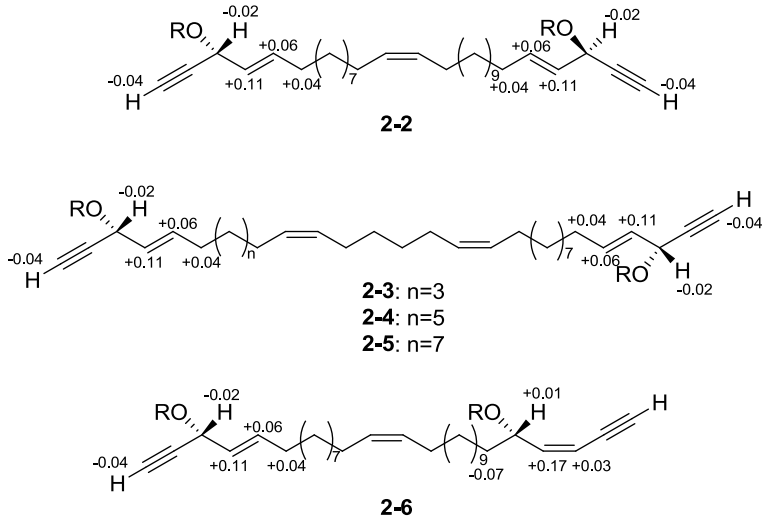

2-2

2-3: n=3
2-4: n=5
2-5: n=7

2-6

R=(*R*)-MTPAor(*S*)-MTPA

Figure S2-1-30. Result of the modified Mosher's method. $\Delta\delta$ (δ_S-δ_R) values for the MTPA esters of **2-2 - 2-6**.

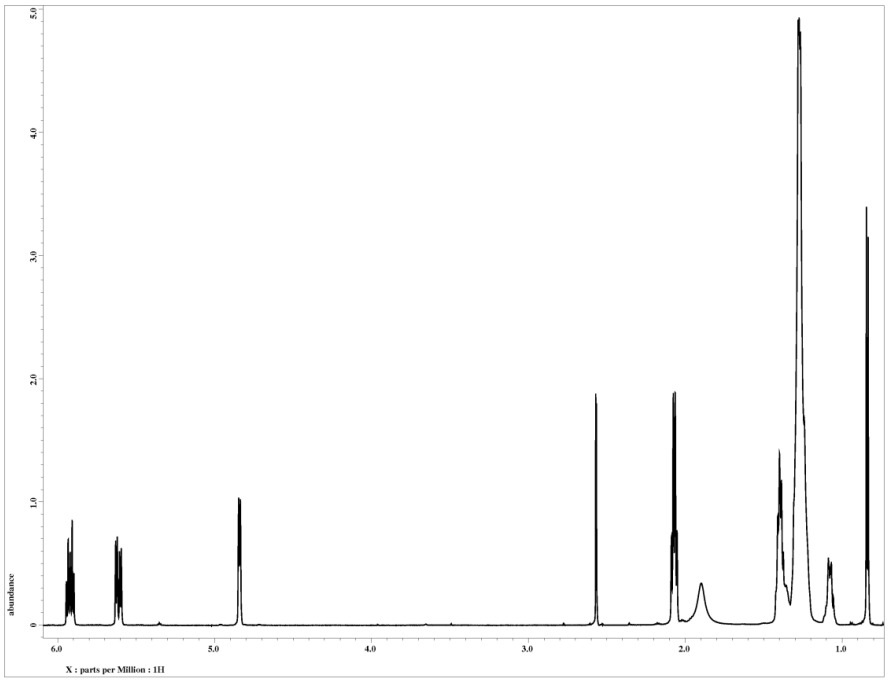

Figure S2-1-31. ^{1}H NMR spectrum of miyakosyne A (**2-7**) in $CDCl_3$

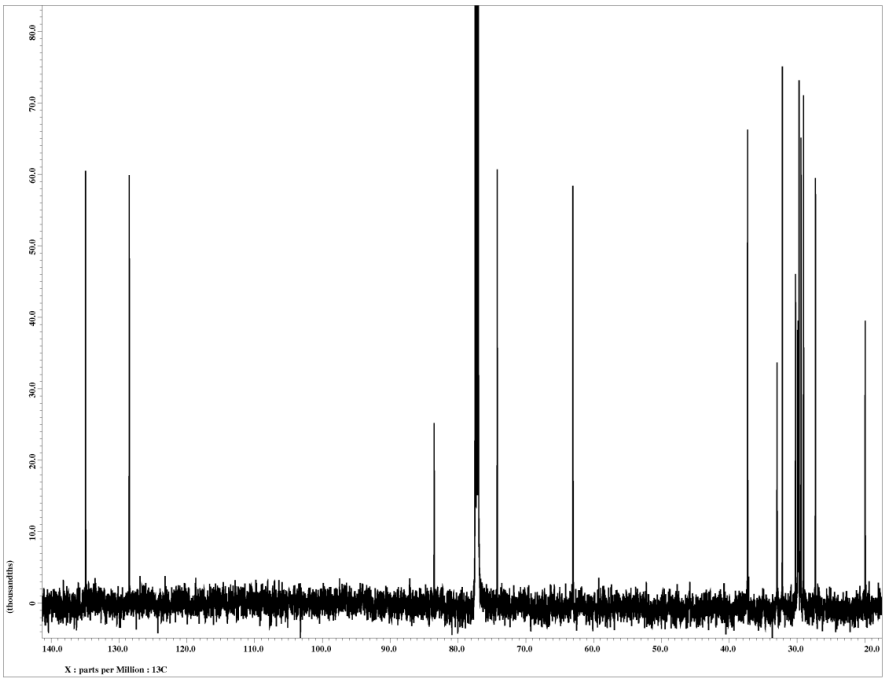

Figure S2-1-32. ^{13}C NMR spectrum of miyakosyne A (**2-7**)

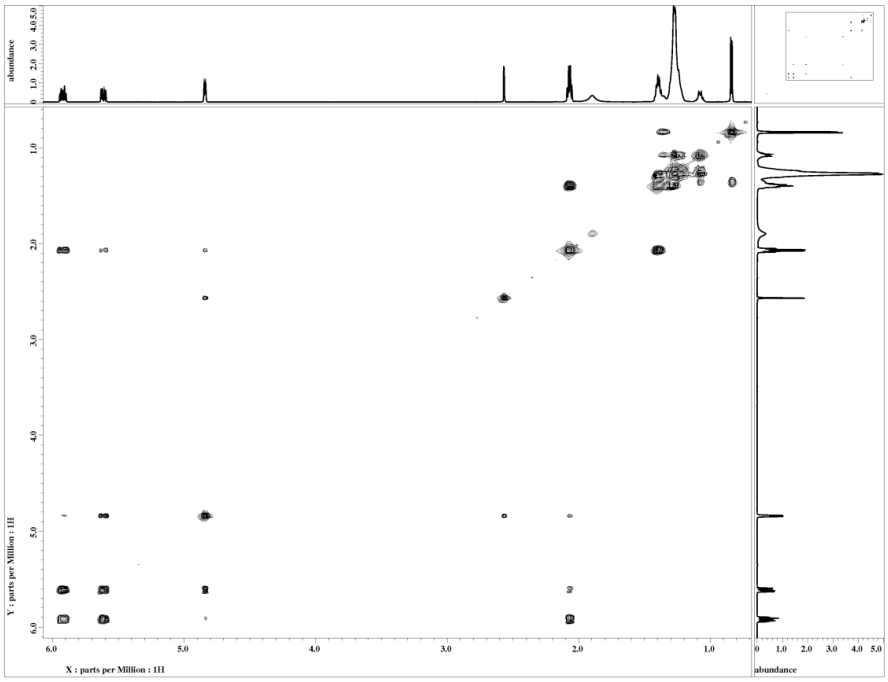

Figure S2-1-33. COSY spectrum of miyakosyne A (**2-7**) in $CDCl_3$

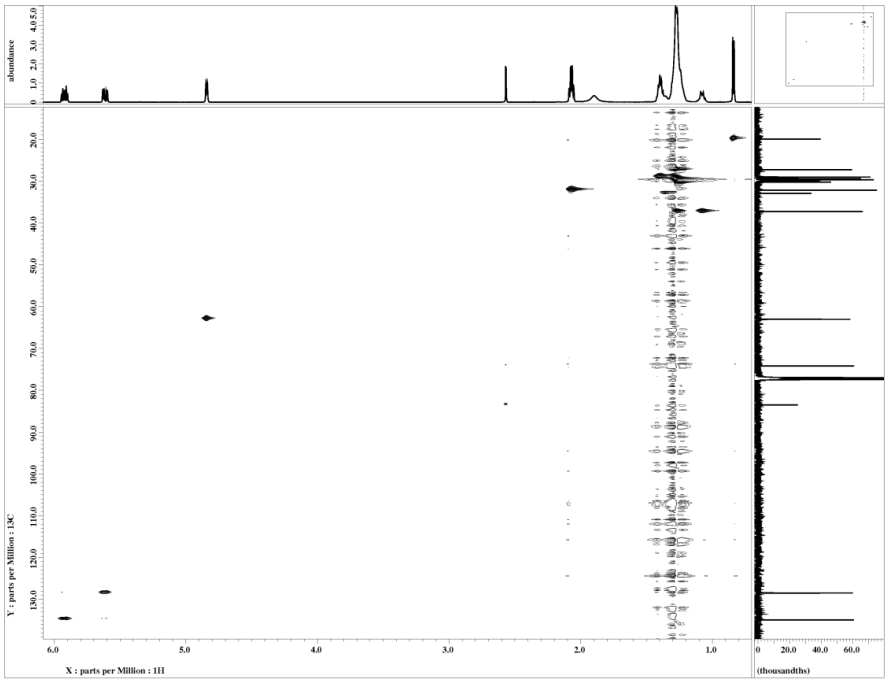

Figure S2-1-34. HSQC spectrum of miyakosyne A (**2-7**) in $CDCl_3$

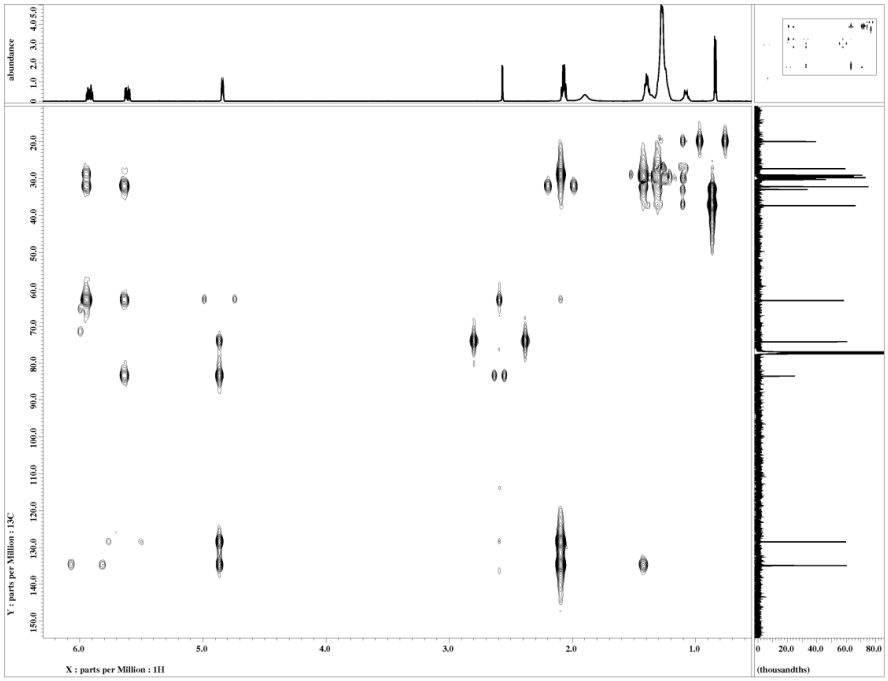

Figure S2-1-35. HMBC spectrum of miyakosyne A (**2-7**) in $CDCl_3$

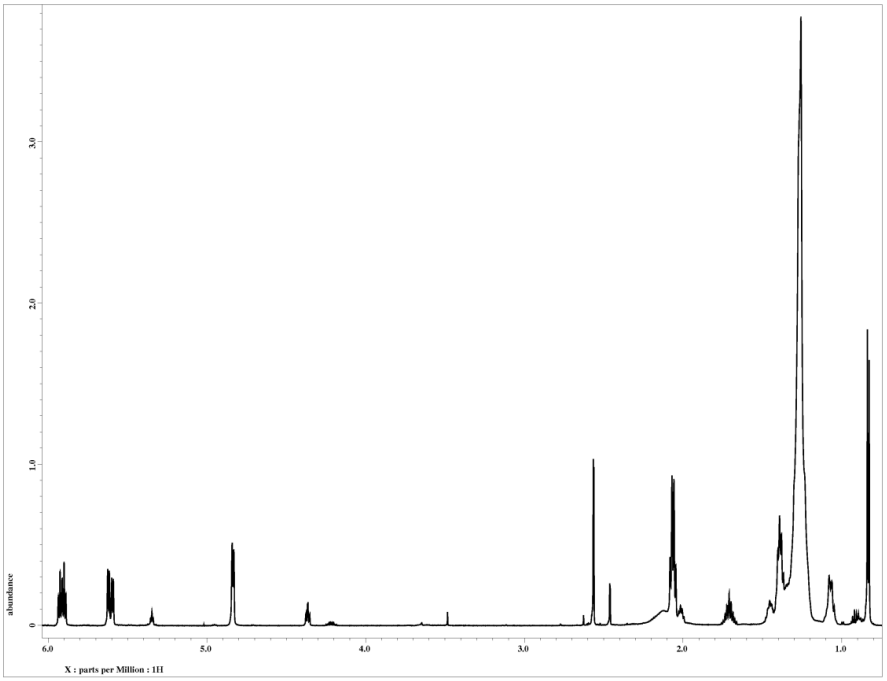

Figure S2-1-36. ^1H NMR spectrum of miyakosyne B (**2-8**) in $CDCl_3$

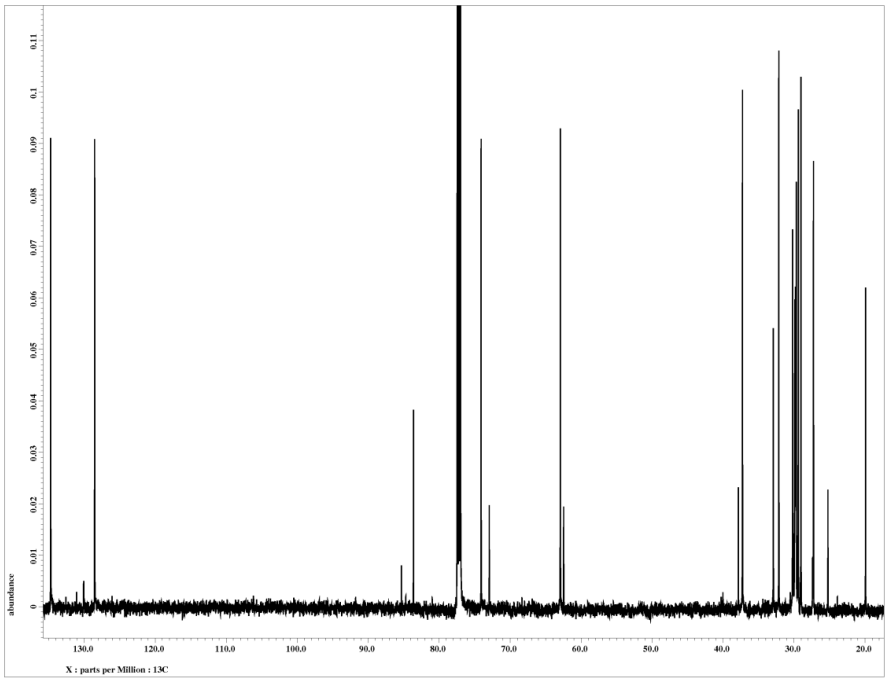

Figure SS2-1-37. ^{13}C NMR spectrum of miyakosyne B (**2-8**) in $CDCl_3$

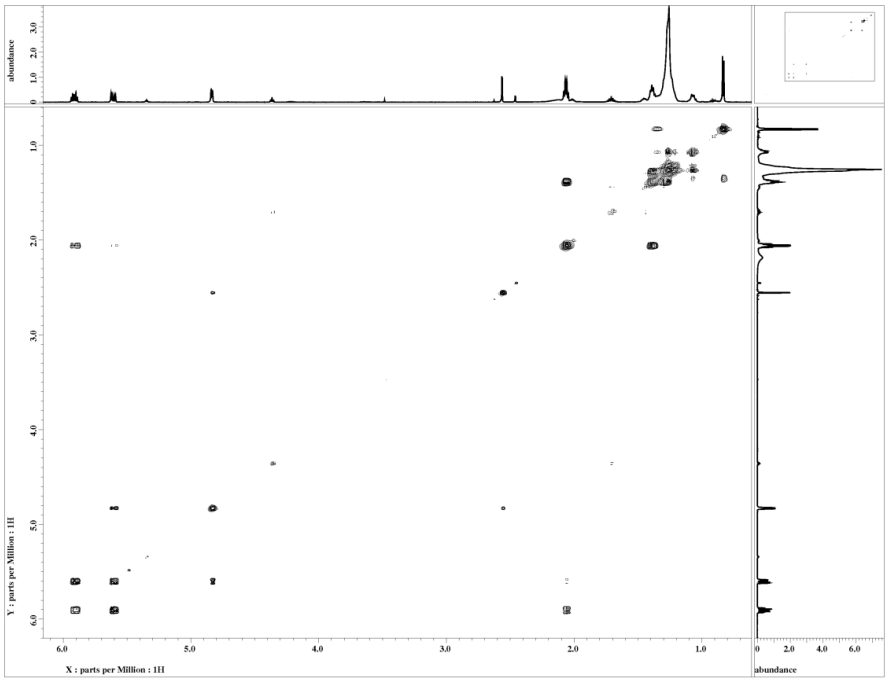

Figure S2-1-38. COSY spectrum of miyakosyne B (**2-8**) in $CDCl_3$

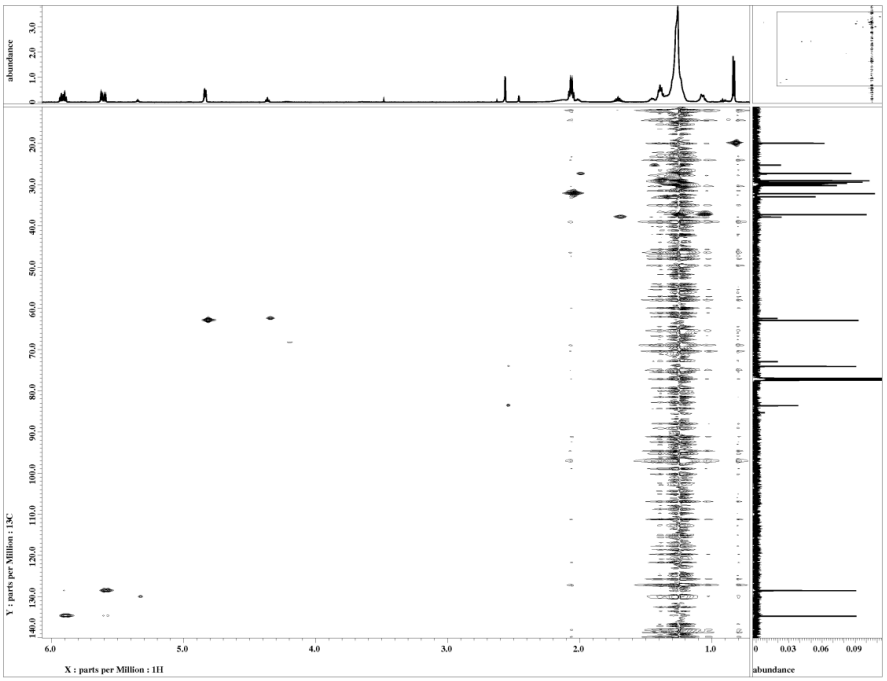

Figure S2-1-39. HSQC spectrum of miyakosyne B (**2-8**) in $CDCl_3$

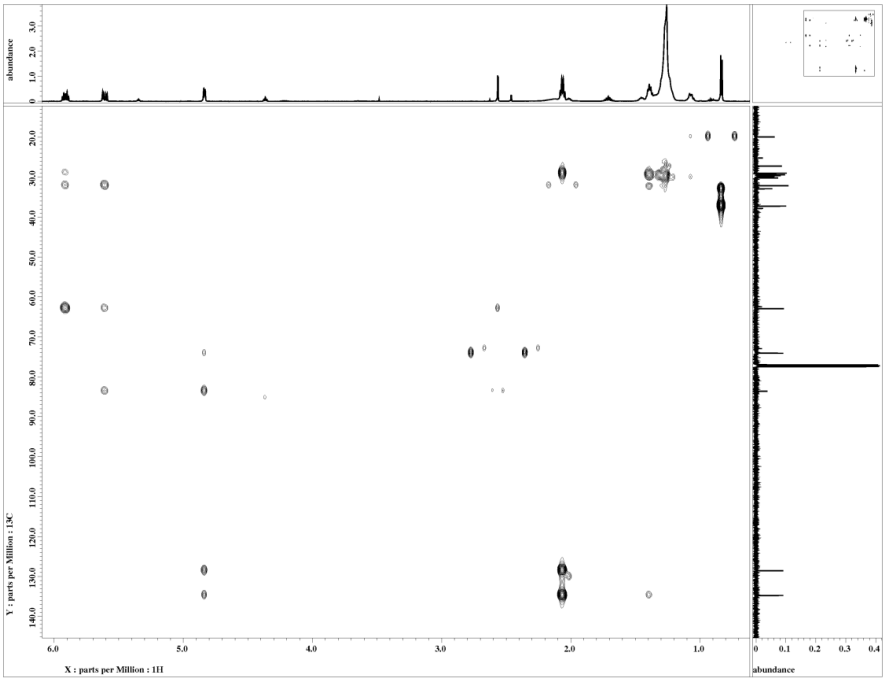

Figure S2-1-40. HMBC spectrum of miyakosyne B (**2-8**) in $CDCl_3$

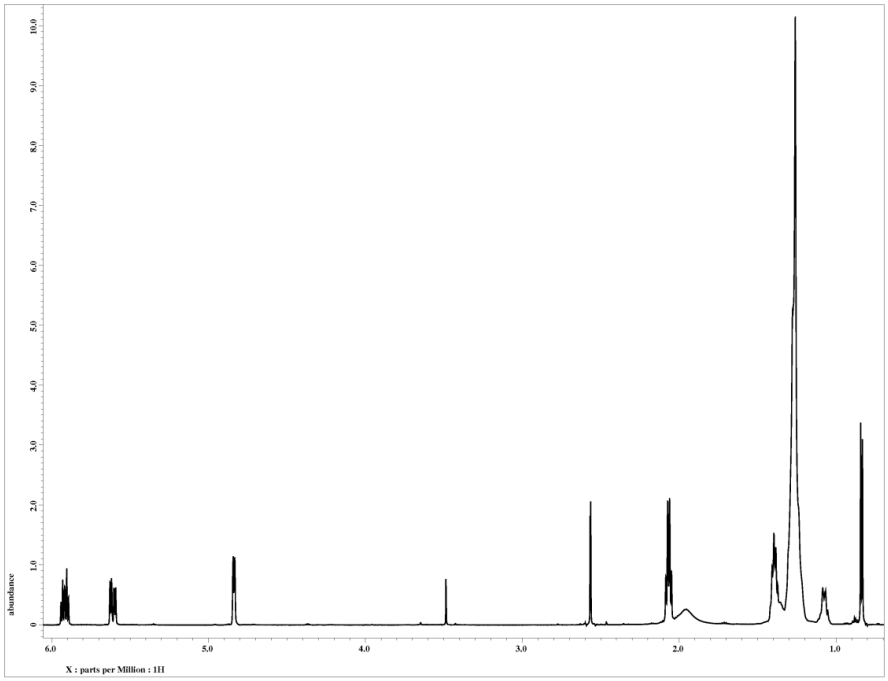

Figure S2-1-41. ^{1}H NMR spectrum of miyakosyne C (**2-9**) in $CDCl_3$

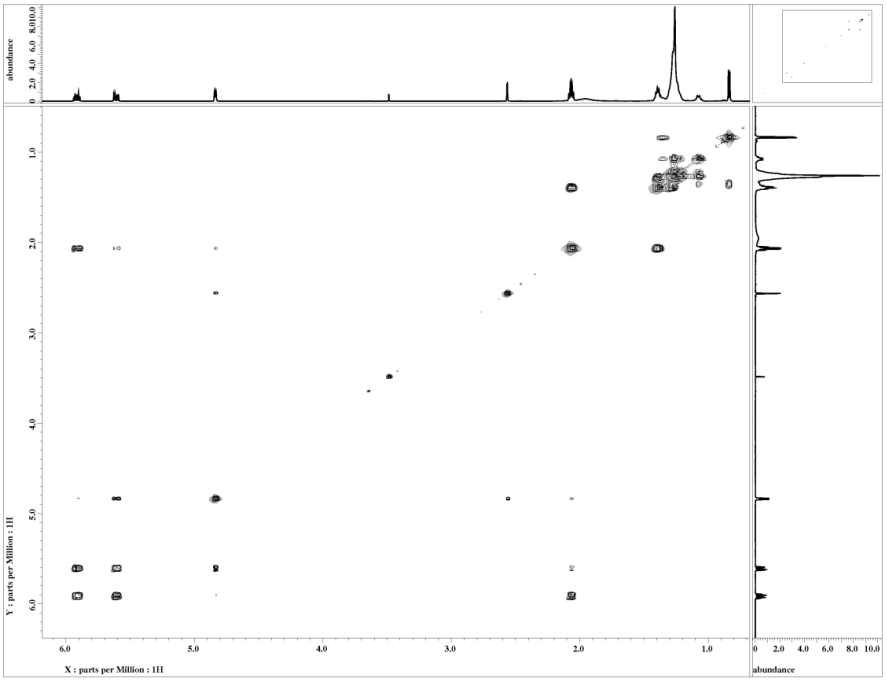

Figure S2-1-42. COSY spectrum of miyakosyne C (**2-9**) in $CDCl_3$

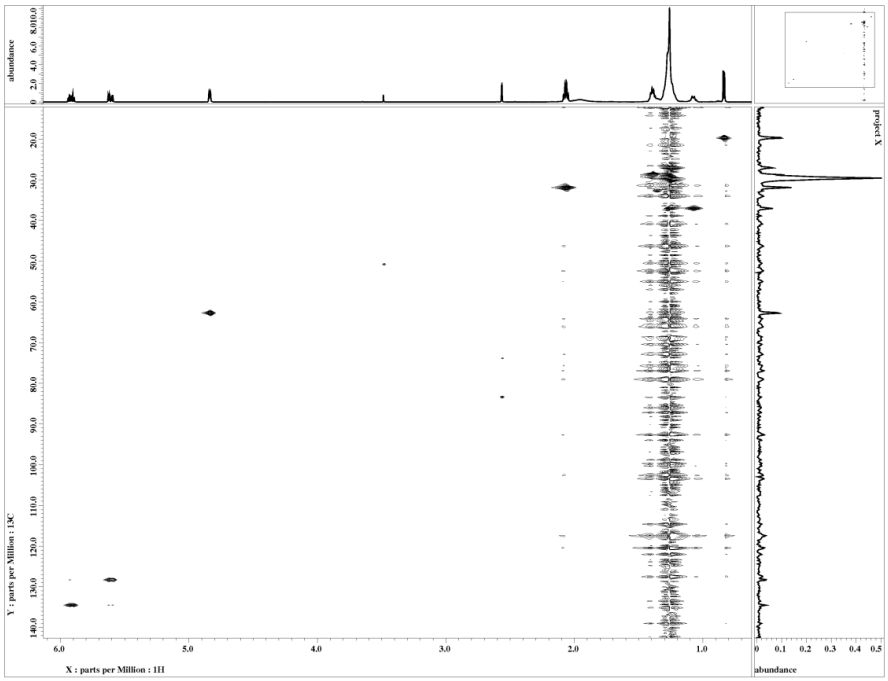

Figure S2-1-43. HSQC spectrum of miyakosyne C (**2-9**) in $CDCl_3$

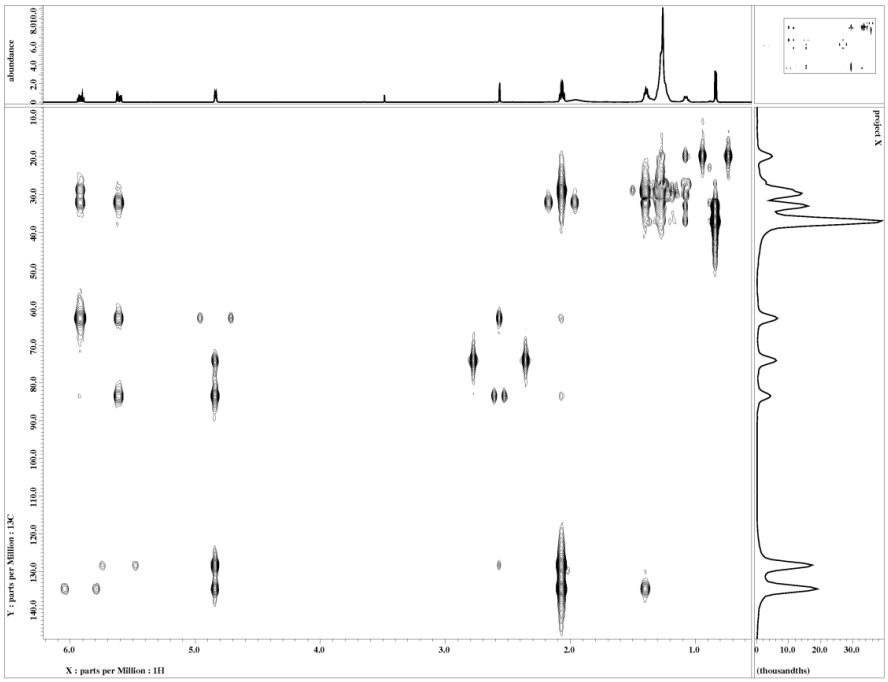

Figure S2-1-44. HMBC spectrum of miyakosyne C (**2-9**) in $CDCl_3$

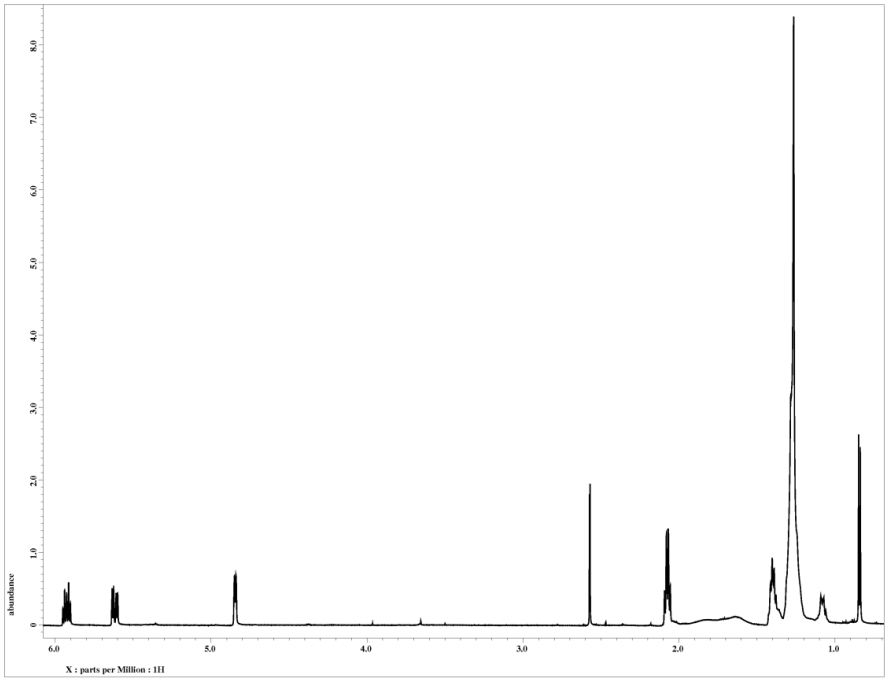

Figure S2-1-45. ^{1}H NMR spectrum of miyakosyne D (**2-10**) in $CDCl_3$

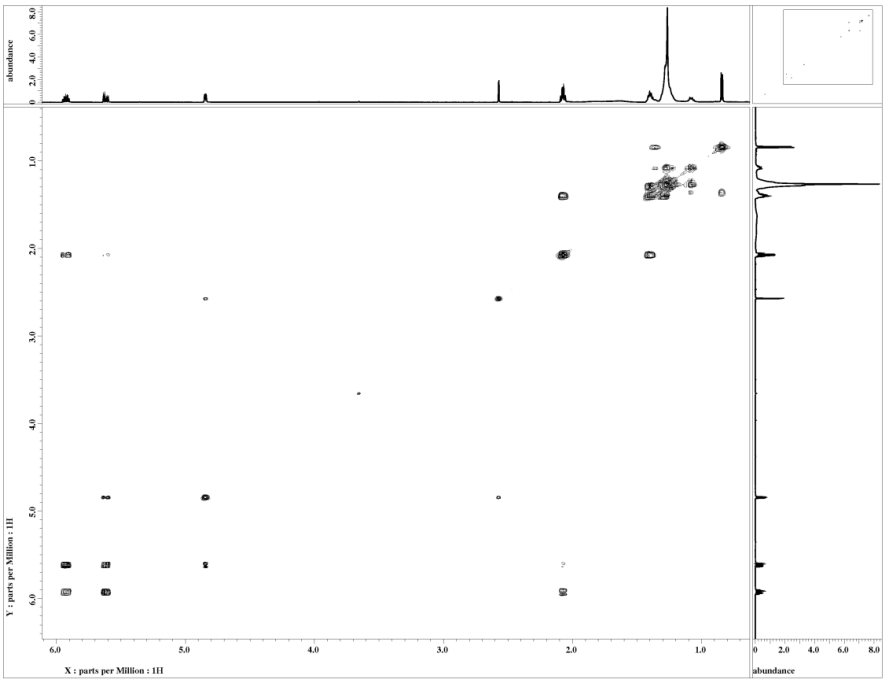

Figure S2-1-46. COSY spectrum of miyakosyne D (**2-10**) in $CDCl_3$

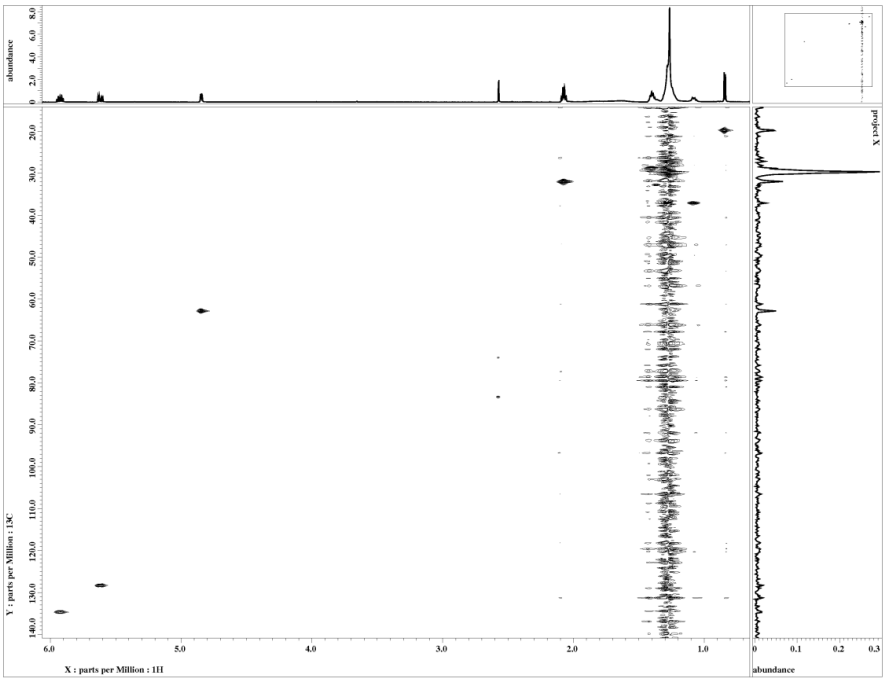

Figure S2-1-47. HSQC spectrum of miyakosyne D (**2-10**) in $CDCl_3$

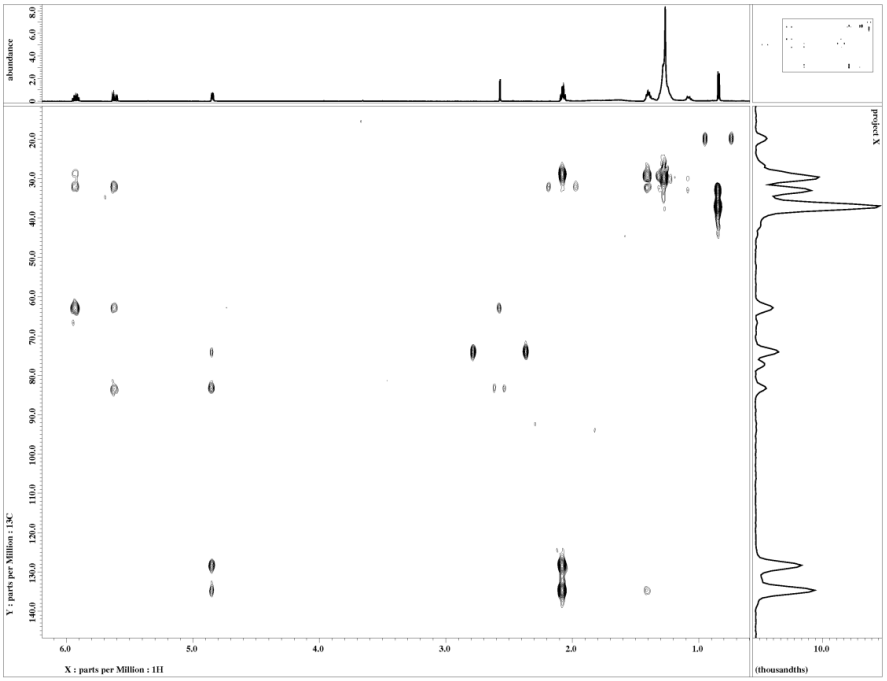

Figure S2-1-48. HMBC spectrum of miyakosyne D (**2-10**) in $CDCl_3$

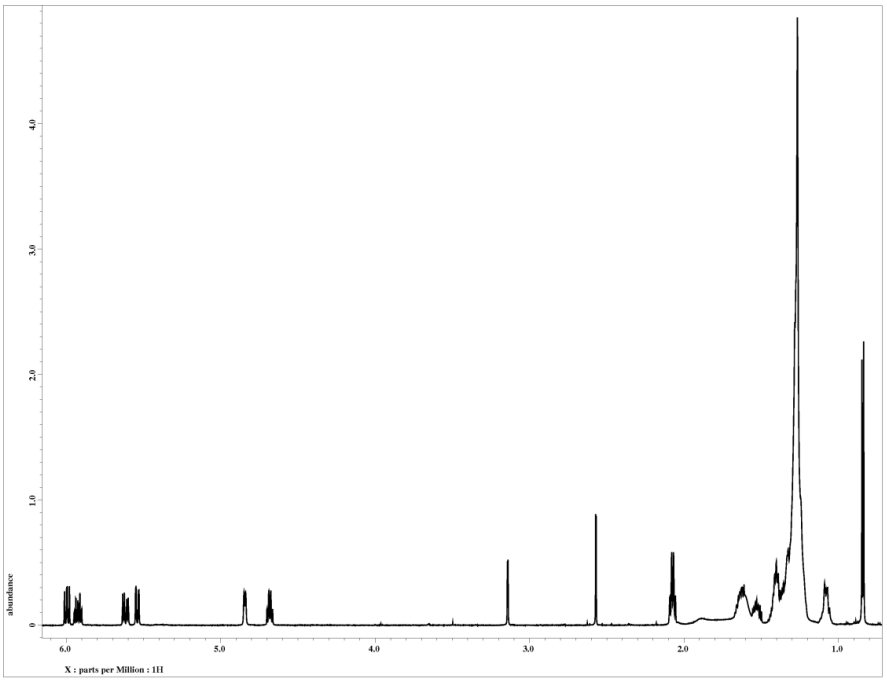

Figure S2-1-49. ^{1}H NMR spectrum of miyakosynes E (**2-11**) and F (**2-12**) in $CDCl_3$

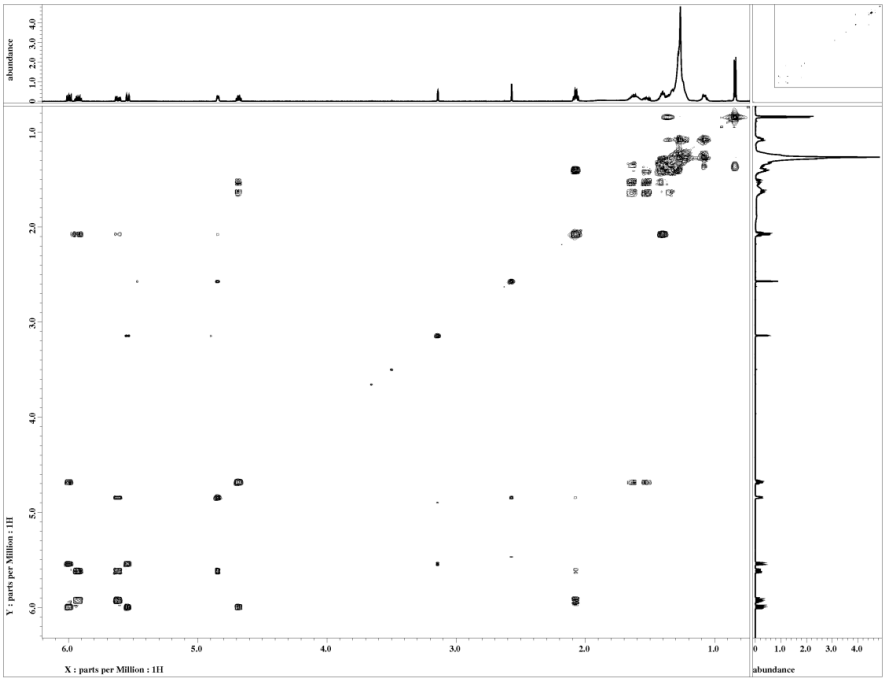

Figure S2-1-50. COSY spectrum of miyakosynes E (**2-11**) and F (**2-12**) in $CDCl_3$

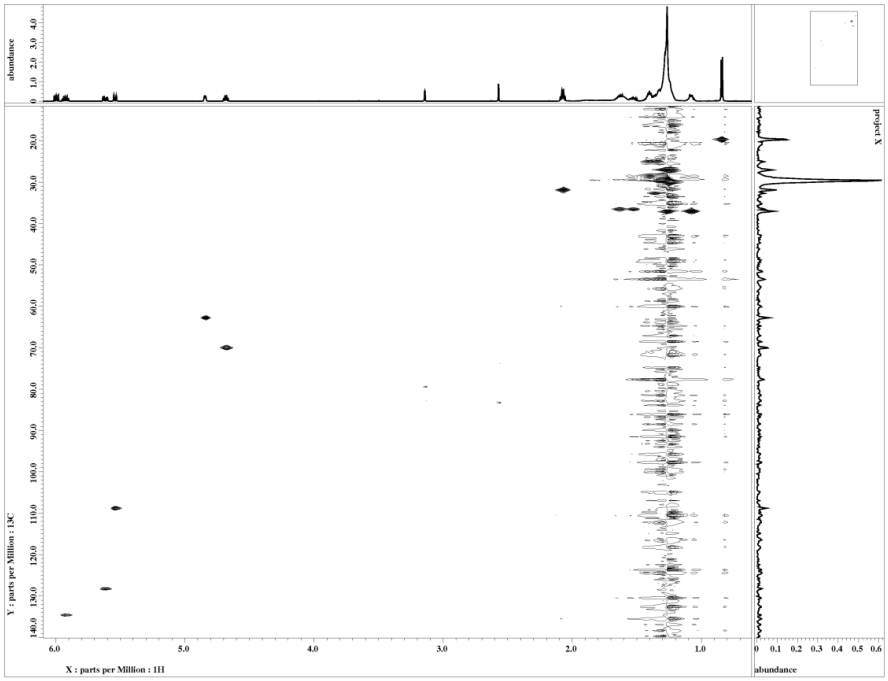

Figure S2-1-51. HSQC spectrum of miyakosynes E (**2-11**) and F (**2-12**) in $CDCl_3$

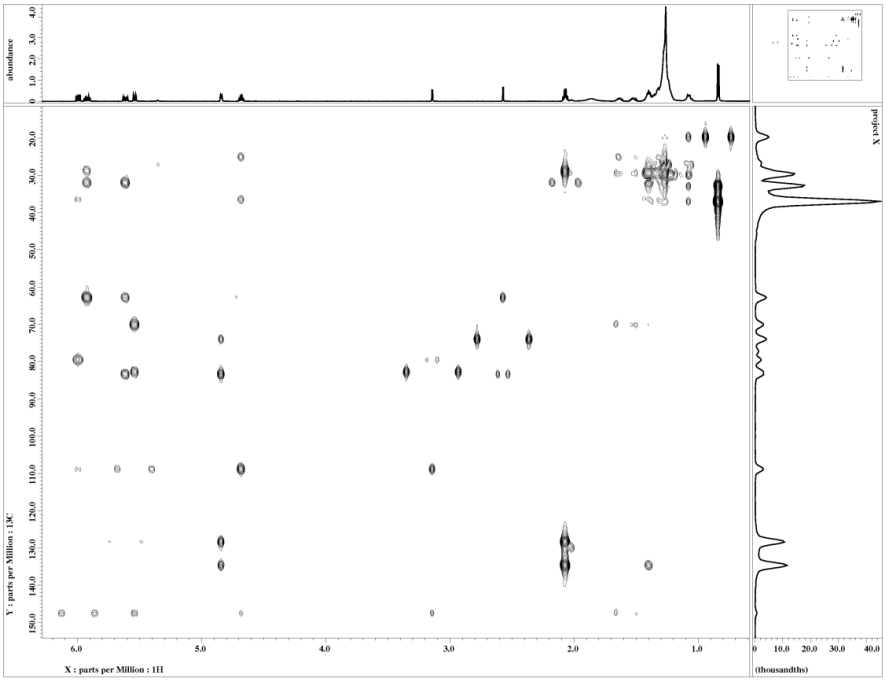

Figure S2-1-52. HMBC spectrum of miyakosynes E (**2-11**) and F (**2-12**) in $CDCl_3$

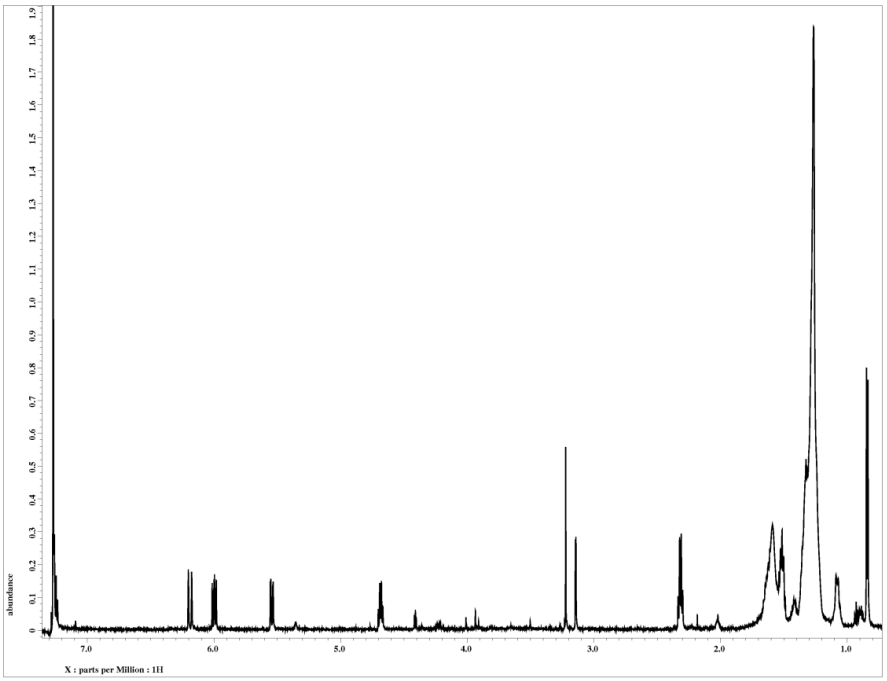

Figure S2-1-53. ^{1}H NMR spectrum of keto-alcohols (**2-13**) and (**2-14**) in $CDCl_3$

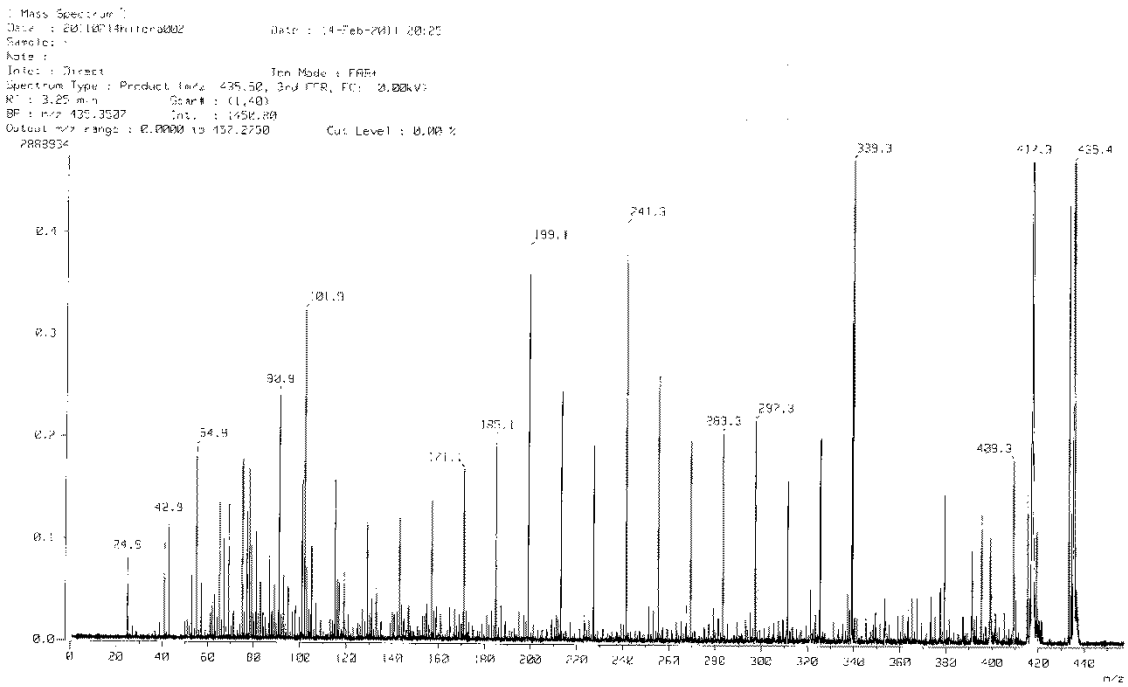

Figure S2-1-54. Tandem FABMS spectrum of miyakosyne A (**2-7**)

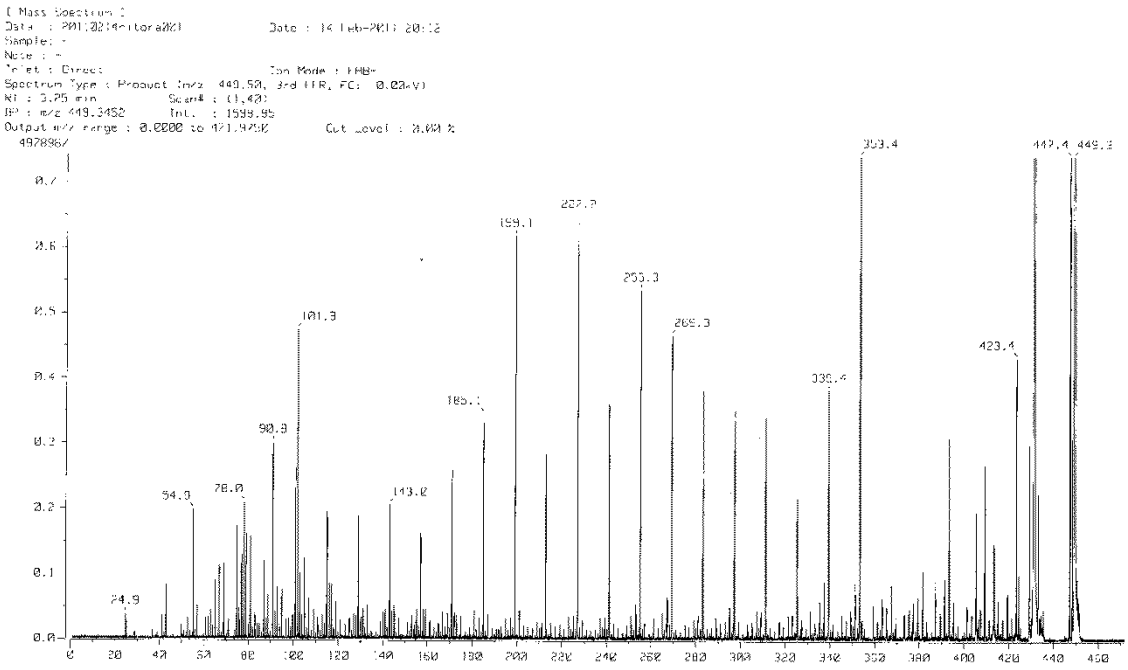

Figure S2-1-55. Tandem FABMS spectrum of miyakosyne B (**2-8**)

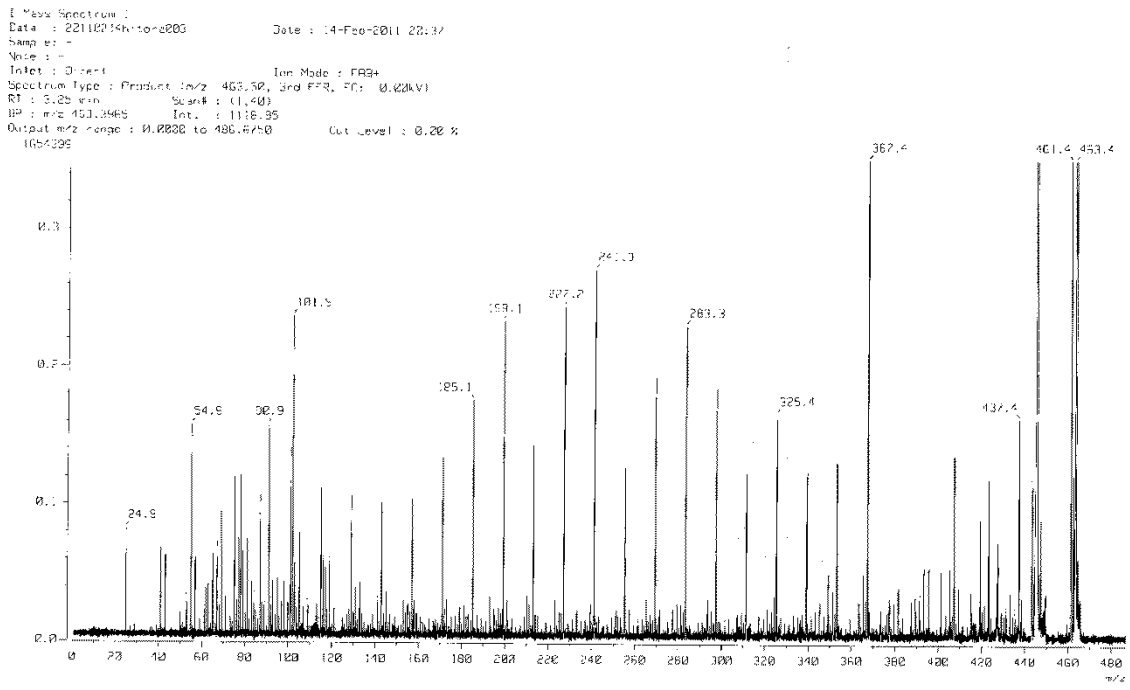

Figure S2-1-56. Tandem FABMS spectrum of miyakosyne C (**2-9**)

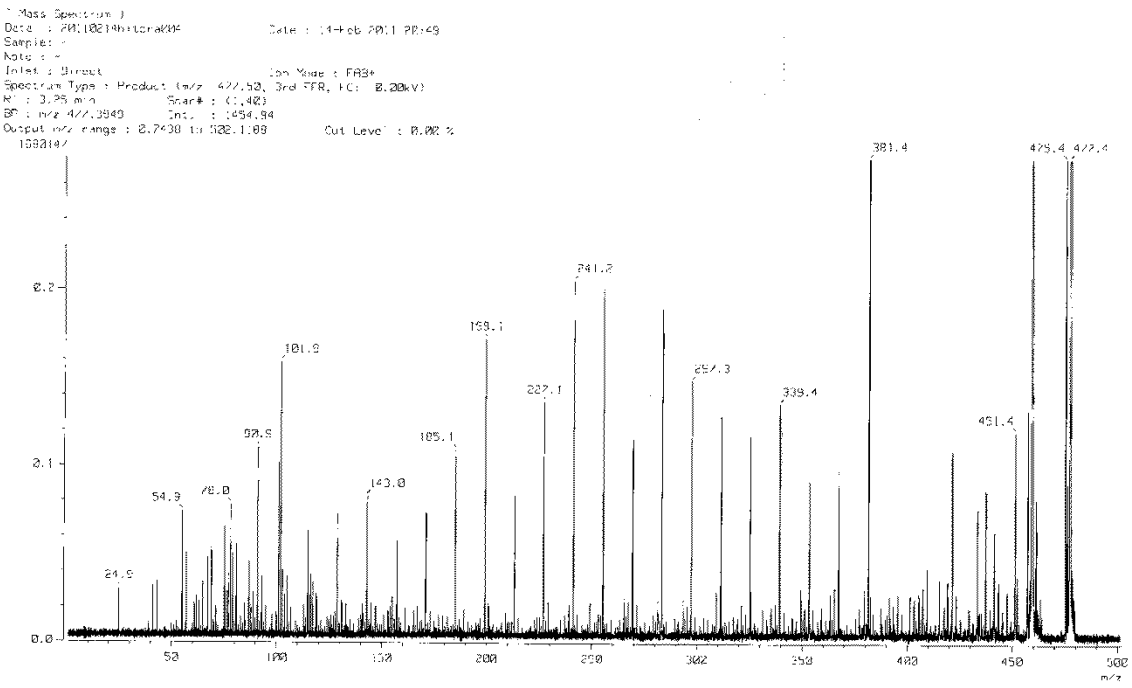

Figure S2-1-57. Tandem FABMS spectrum of miyakosyne D (**2-10**)

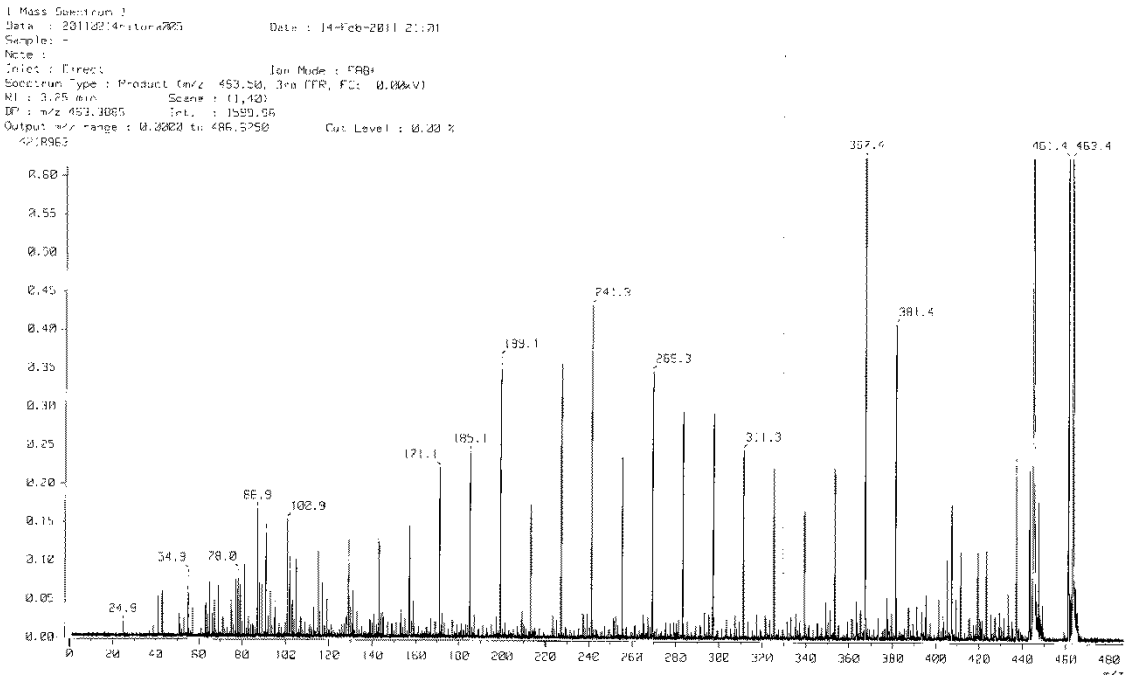

Figure S2-1-58. Tandem FABMS spectrum of miyakosynes E (**2-11**) and F (**2-12**)

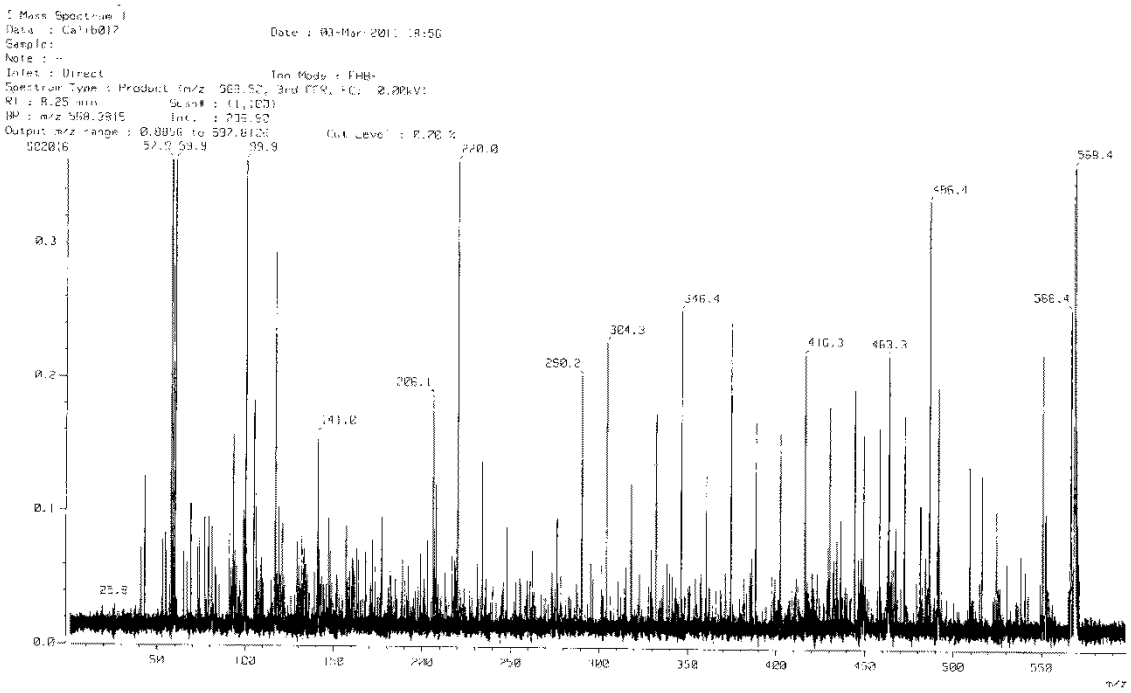

Figure S2-1-59. Tandem FABMS spectrum of Girard's T derivative

Figure S2-1-60. Photograph of the sponge *Petrosia* sp.

2.2. Assignment of the absolute configuration at the isolated methyl branch in miyakosyne A

2.2.1. Introduction

Enantiomer or diastereomers of bioactive compounds often exhibit different biological activity.[25] Therefore, assignment of the absolute configuration of chiral centers in small molecules is the essential part for the structure elucidation of bioactive natural products. Recent improvements of the analytical techniques of NMR, including modified Mosher's method,[5] universal NMR database,[26] and *J*-based configurational analysis,[27] enabled us to analyze complicated configuration of natural products. However, determination of the absolute configuration of chiral centers in the molecules consisting of symmetrical partial structures is problematic, because overlapped NMR signals hamper the assignment of the each signal. Additionally, the chiral discrimination of a branched methyl located at the remote position is also challenging subjects as well.[28, 29]

Miyakosyne A (**2-7**) has the common substructures at both termini, and a

branched methyl in the middle of a long methylene chain, thus assignment of the absolute configuration of the methyl branch was difficult.[30] Innovative X-ray crystallographic analysis using porous complex was applied for the structure elucidation of miyakosyne A, and the absolute configuration of the isolated chiral center was tentatively assigned as 14*S*.[31, 32] In this study, we assigned the absolute configuration of the isolated chiral center of miyakosyne A by chemical degradation and esterification with the Akasaka-Ohrui's reagent (**2-15**, Figure 2-7).[33]

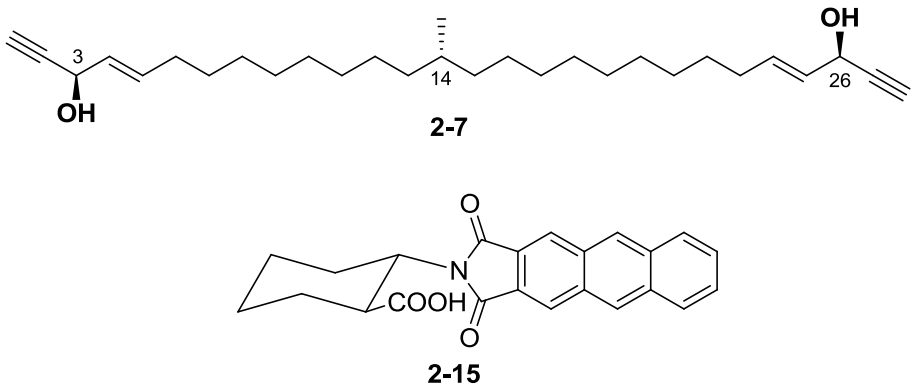

Figure 2-7. Structures of miyakosyne A (**2-7**) and (1*S*,2*S*)-2-(anthracene-2,3-dicarboximido)cyclohexanecarboxylic acid (**2-15**).

2.2.2. Results and Discussion

We first attempted to examine whether miyakosyne A (**2-7**) is a diastereomeric mixture differing in the configuration at C-14 or not. In order to obtain diastereomers of **2-7**, we randomized the configurations of two secondary alcohols by a sequence of oxidation and reduction reactions. Even though the modified Mosher's analysis of the product demonstrated that the two oxygenated methines were racemic, the mixture gave only a single sharp peak in a variety of HPLC conditions.[34]

Then we set out to convert **2-7** into a linear 1,ω-diol. It was reported that a pair of isomers of linear primary alcohols with anteiso-terminus, which are enantiomeric to each other in the absolute configuration of the methyl-substituted methine carbons, could be discernible by ^{1}H NMR spectroscopy by conjugation with the Ohrui's acid (**2-15**) (Ohrui's method).[33] It was also reported that the differences in chemical shifts between the enantiomers were not observed when the branching points were more distant than the 10th carbon atom.[33] With this information in mind, miyakosyne A (**2-7**) was subjected to ozonolysis followed by reduction with $NaBH_4$ to furnish 10-methylicosane-1,20-diol (**2-16**). In compound **2-16** the branched methyl group was placed at 10th and 11th carbon from each terminus, which were too far to apply the Ohrui's method. Therefore, compound **2-16** was dehomologated by means of the Grieco

elimination[35] followed by ozonolysis and reduction with $NaBH_4$ to give 9-methyl-1,18-octadecanediol (**2-18**), in which branched methyl group was placed at 9th and 10th position (Scheme 2-2).

Scheme 2-2. Preparation of 9-methyl-1,18-octadecanediol (**2-18**) from miyakosyne A

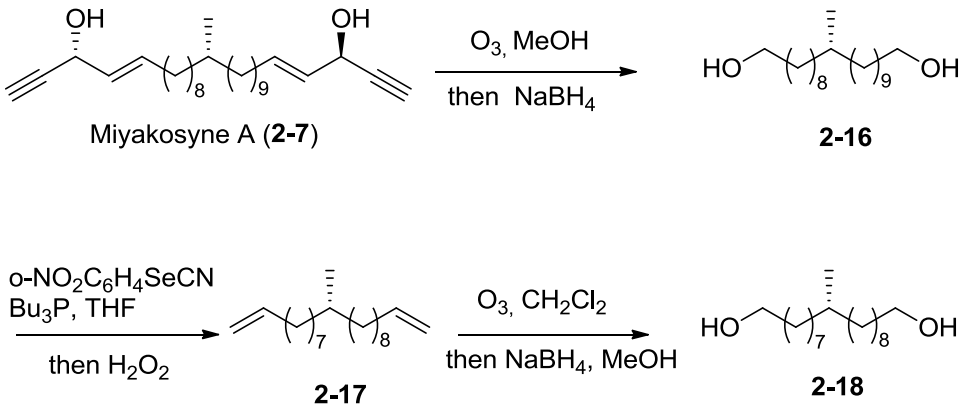

We then prepared both enantiomers of 9-methyl-1,18-octadecanediol.

(*S*)-Citronellal (*S*-**2-19**) was subjected to ozonolysis to afford *S*-**2-20**. *S*-**2-20** was treated with the ylide prepared from phosphonium salt **2-21** to give *S*-**2-22**, which was hydrogenated to give *S*-**2-18** (Scheme 2-3). *R*-**2-18** was synthesized in the same way from *R*-citronellal (*R*-**2-19**).

Scheme 2-3. Synthesis of (*S*)-9-methyl-1,18-octadecanediol (*S*-**2-18**).

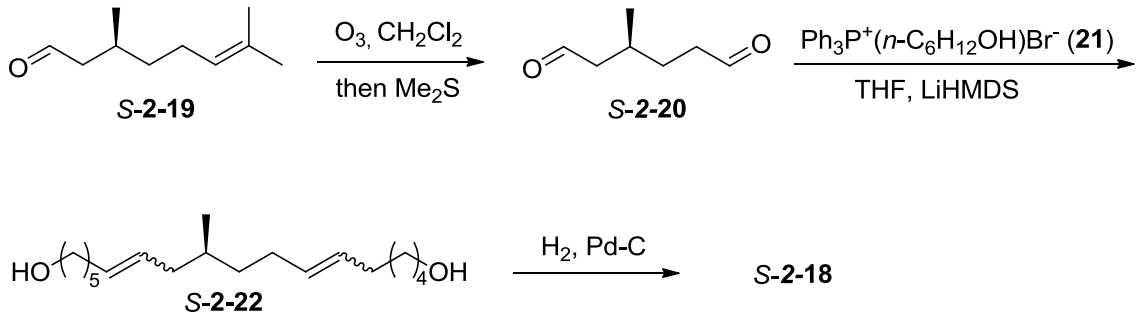

With **2-18** from **2-7** and both enantiomers of **2-18** in hand, we esterified each of them with **2-15**. The ^{1}H NMR spectra of the resulting three diesters appeared identical except for the chemical shift of the branched methyl signal (Figure 2-8). The chemical shift of the methyl signal in the diester of natural **2-18** was identical with that of the diester of *R*-**2-18**, whereas it shifted down-field compared to that of the diester of *S*-**2-18**. From this result we considered that miyakosyne A has 14*R*-configuration.

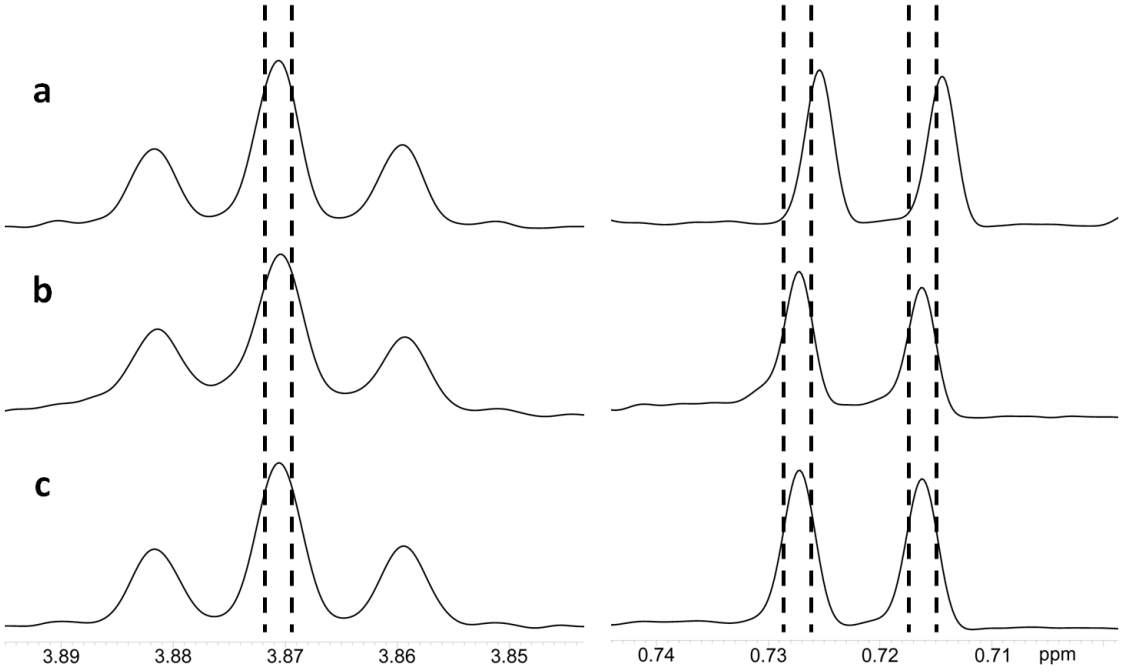

Figure 2-8. Expanded plots of the ^{1}H NMR spectrum of the terminal oxygenated methylene protons (Left) and the branched methyl (Right) signals of the diesters. (a) *S*-**2-18**, (b) *R*-**2-18**, and (c) **2-18** prepared from miyakosyne A (**2-7**).

2.2.3. Conclusion

The absolute configuration of the methyl branch in miyakosyne A (**2-7**) has been determined to be 14*R* by comparing the ^{1}H NMR data of a degradation product with those of synthetic standards after derivatization with the Ohrui's acid. This study demonstrates the efficiency of derivatization with the Ohrui's acid to assign the absolute configuration of remote stereogenic centers once reference compounds are available.[28]

The differentiation of a methyl branch 9 and 10 carbons away from the terminal hydroxyl groups was fulfilled by ^{1}H NMR, permitting us to conclude that the natural miyakosyne A has the 3*R*, 14*R*, 26*R*-configuration.

2.2.4. Experimental Section

2.2.4.1. General Experimental Procedures

^{1}H and ^{13}C NMR spectra were recorded on a JEOL alpha 600 NMR spectrometer. Chemical shifts were referenced to solvent peaks: δ_H 7.24 and δ_C 77.0 for $CDCl_3$. High resolution mass spectra were obtained on a JEOL JMS-700T mass spectrometer. Optical rotations were measured on a JASCO DIP-1000 digital polarimeter.

2.2.4.2. 10-Methyl-1,20-icosanediol (2-16)

O_3 was bubbled through a solution of miyakosyne A (**2-7**, 3.5 mg) in MeOH (2.5 mL) at -78 °C until the color of the solution changed to blue. After excess O_3 was purged with N_2, $NaBH_4$ was added and stirred for 1 h. To the reaction mixture water was added and the solution was extracted with EtOAc to afford 10-methyl-1,20-icosanediol (**2-16**, 2.3 mg) as a colorless oil: ^{1}H-NMR (600 MHz, $CDCl_3$) δ 0.81 (d, *J* = 6.9 Hz, 3H), 1.06 (m, 2H), 1.19–1.33 (m, 28H), 1.52–1.57 (m, 5H), 3.62 (t, *J* = 6.9 Hz, 4H); HRFABMS calcd for $C_{21}H_{45}O_2$ [M+H^+] 329.3414, found: 329.3412.

2.2.4.3. 10-Methyl-1,19-icosadiene (2-17)

To a solution of **2-16** (1.5 mg) in THF (0.3 mL) *o*-NO_2PhSeCN (5 mg) and Bu_3P (6 μL) was added. After stirring for 4 h, the reaction mixture was cooled to 0 °C, and H_2O_2 (0.2 mL) in THF (3 mL) was added. The reaction mixture was stirred at 0 °C for 30 min, and allowed to warm to room temperature and stirred overnight. The reaction mixture was quenched by addition of saturated aqueous $NaHCO_3$, and the mixture was extracted with EtOAc. The organic layer was concentrated, and the residue was subjected to silica gel column chromatography (*n*-hexane) to afford 10-methyl-1,19-icosadiene (**2-17**, 1.5 mg) as a pale yellow solid: ^{1}H-NMR (600 MHz, $CDCl_3$) δ 0.81 (d, *J* = 6.9 Hz, 3H), 1.06 (m, 2H), 1.19–1.35 (m, 24H), 1.56 (m, 1H), 2.01 (m, 4H), 4.91 (brd, *J* = 9.6 Hz, 2H), 4.97 (brd, *J* = 17.1 Hz, 2H), 5.80 (m, 2H).

2.2.4.4. 9-Methyl-1,18-octadecanediol (2-18)

17 (1.5 mg) was dissolved in CH_2Cl_2 and O_3 was bubbled through the solution until the color turned blue. After the excess O_3 was purged with N_2, MeOH and $NaBH_4$ were added and stirred for 1 h at room temperature. The reaction mixture was concentrated and partitioned between water and EtOAc. Concentration of the organic layer afforded 9-methyl-1,18-octadecanediol (**2-18**, 1.0 mg) as a colorless oil: ^{1}H-NMR (600 MHz, $CDCl_3$) δ 0.81 (d, *J* = 6.9, 3H), 1.05 (m, 2H), 1.23–1.33 (m, 24H), 1.52–1.66 (m, 5H),

3.62 (t, *J* = 6.9, 4H); HRFABMS calcd for $C_{19}H_{41}O_2$ [M+H$^+$] 301.3101, found: 301.3100.

2.2.4.5. (*S*)-3-Methyl-1,6-hexanedial (*S*-2-20)

A solution of (*S*)-(-)-citronellal (*S*-**2-19**) (170 mg, 1.1 mmol) in CH_2Cl_2 (7 mL) was kept at -78 °C and bubbled with ozone until the color of the solution turned blue. Me_2S (180 μL) was added to the reaction mixture and gradually warmed to room temperature. The reaction mixture was stirred for overnight, and the solvent was removed by evaporation. The residue was purified by silica gel column chromatography (*n*-hexane/ ethyl acetate 1:1) to afford a fraction enriched with (*S*)-3-methyl-1,6-hexanedial (*S*-**2-20** 110 mg) as a colorless oil which was used in the next step: $[\alpha]^{23}_D$ -12 (*c* 0.75, $CHCl_3$); ^{1}H-NMR (600 MHz, $CDCl_3$) δ 0.95 (m, 3H), 1.47–1.56 (m, 1H), 1.69 (m, 1H), 1.95 (m, 1H), 2.16 (m, 1H), 2.30–2.44 (m, 3H), 9.71 (brs, 1H), 9.73 (brs, 1H); ^{13}C-NMR (200 MHz, $CDCl_3$) δ 19.0, 26.8, 28.0, 40.7, 50.0, 202.0, 202.1; HRFABMS calcd for $C_7H_{11}O_2$ [M-H$^-$], 127.0765, found: 127.0771.

A fraction enriched with (*R*)-3-Methyl-1,6-hexanedial (*R*-**2-20**) was prepared in the same way from (*R*)-(+)-citronellal (*R*-**2-19**). The product was used in the next step without further purification: $[\alpha]^{23}_D$ +8.4 (*c* 1.8, $CHCl_3$); ^{1}H-NMR (600 MHz, $CDCl_3$) δ

0.95 (m, 3H), 1.47–1.56 (m, 1H), 1.69 (m, 1H), 1.95 (m, 1H), 2.16 (m, 1H), 2.30–2.44 (m, 3H), 9.71 (brs, 1H), 9.73 (brs, 1H); ^{13}C-NMR (200 MHz, $CDCl_3$) δ 19.0, 27.1, 28.0, 41.0, 50.2, 202.1, 202.2; HRFABMS calcd for $C_7H_{11}O_2$ [M-H$^-$], 127.0765, found: 127.0771.

2.2.4.6. (6-Hydroxyhexyl)-triphenylphosphonium bromide (2-21)

6-Bromo-1-hexanol (500 mg) and triphenylphosphine (800 mg) in MeCN (4 mL) were refluxed at 90 °C overnight. The reaction mixture was cooled to room temperature and concentrated. The resulting residue was dissolved in acetone and diluted with dry diethyl ether to precipitate the phosphonium salt. After stirring for 1 h, the precipitate was obtained by decantation and dried *in vacuo* to afford the desired phosphonium salt (**2-21**, 1.1 g) as white solids: $[\alpha]^{24}_D$ -0.65 (*c* 0.97, $CHCl_3$); ^{1}H-NMR (600 MHz, $CDCl_3$) δ 1.43–1.77 (m, 8H), 2.03 (brs, 1H), 3.54–3.70 (m, 4H), 7.65–7.79 (m, 15H); ^{13}C-NMR (200 MHz, $CDCl_3$) δ 22.0 (d, *J* = 4.3 Hz), 22.2 (d, *J* = 49.9 Hz), 24.5, 29.3 (d, *J* = 15.9 Hz), 31.7, 61.0, 118.0 (d, *J* = 86.0 Hz), 130.3 (d, *J* = 12.3 Hz), 133.3 (d, *J* = 10.1 Hz), 134.8 (d, *J* = 2.2 Hz); HRFABMS calcd for $C_{24}H_{29}OP$ [M$^+$-Br] 363.1872, found: 363.1869.

2.2.4.7. (*S*)-9-Methyl-6,12-octadecadiene-1,18-diol (*S*-2-22)

To a suspension of **2-21** (250 mg) in dry THF (4 mL) was added LiHMDS (1.0 M in THF, 1.4 mL). The solution was stirred for 1h under nitrogen atmosphere, and then a solution of *S*-**2-20** (15 mg) was added. The reaction mixture was stirred for 4 h, and NH_4Cl saturated water was added and extracted with EtOAc. The organic layer was concentrated and purified by silica gel column chromatography (*n*-hexane/EtOAc 1:3) to give (*S*)-9-methyl-6,12-octadecadiene-1,18-diol (*S*-**2-22**, 11 mg) as a pale yellow oil: $[\alpha]^{23}_{D}$ +3.5 (*c* 0.48, $CHCl_3$); ^{1}H-NMR (600 MHz, $CDCl_3$) δ 0.85 (d, *J* = 6.9, 3H), 1.12–1.54 (m, 23H), 3.60 (t, *J* = 6.9, 4H), 5.31 – 5.38 (m, 4H); ^{13}C-NMR (200 MHz, $CDCl_3$) δ 19.5, 25.37, 25.39, 27.2, 27.3, 29.3, 29.4, 29.5, 32.56, 32.60, 33.0, 34.3, 36.6, 62.8, 128.4, 129.5, 130.1, 130.4; HRFABMS calcd for $C_{19}H_{37}O_2$ [M+H$^+$] 297.2788, found: 297.2788.

(*R*)-9-Methyl-6,12-octadecadiene-1,18-diol (*R*-**2-22**) was prepared in the same way from *R*-**2-20**: $[\alpha]^{22}_{D}$ -4.3 (*c* 0.34, $CHCl_3$); ^{1}H-NMR (600 MHz, $CDCl_3$) δ 0.85 (d, *J* = 6.9, 3H), 1.12–1.58 (m, 23H), 3.62 (t, *J* = 6.9, 4H), 5.32–5.38 (m, 4H); ^{13}C-NMR (200 MHz, $CDCl_3$) δ 19.5, 25.3, 25.4, 27.0, 27.1, 29.2, 29.4, 29.5, 32.5, 32.9, 34.3, 36.6, 62.7, 128.4, 129.5, 130.1, 130.4; HRFABMS calcd for $C_{19}H_{37}O_2$ [M+H$^+$] 297.2788, found: 297.2794.

2.2.4.8. (*S*)-9-Methyl-1,18-octadecanediol (*S*-2-18)

S-**2-22** (10 mg) was dissolved in methanol, and Pd/C (3 mg) was added to the solution. The suspension was stirred vigorously overnight under H_2. The resultant mixture was filtered, and concentration of the filtrate afforded the diol (*S*-**2-18**, 7.0 mg) as colorless oil: $[\alpha]^{22}_D$ -0.52 (*c* 0.21, $CHCl_3$); ^{1}H-NMR (600 MHz, $CDCl_3$) δ 0.81 (d, *J* = 6.9, 3H), 1.24–1.33 (m, 20H), 1.54–1.65 (m, 11H), 3.62 (t, *J* = 6.9, 4H); ^{13}C-NMR (200 MHz, $CDCl_3$) δ 19.7, 25.70, 25.71, 25.72, 27.0, 29.38, 29.42, 29.50, 29.54, 29.59, 29.61, 29.90, 29.94, 32.7, 32.8, 37.0, 63.0; HRFABMS calcd for 301.3101. found: 301.3122.

R-**2-18** was prepared in the same way using *R*-**2-22**: (*R*)-9-Methyl-1,18-octadecanediol (*R*-**2-18**); $[\alpha]^{23}_D$ +0.64 (*c* 0.14, $CHCl_3$); ^{1}H-NMR (600 MHz, $CDCl_3$) δ 0.81 (d, *J* = 6.9, 3H), 1.24–1.33 (m, 20H), 1.54–1.65 (m, 11H), 3.62 (t, *J* = 6.9, 4H); ^{13}C-NMR (200 MHz, $CDCl_3$) δ 19.7, 25.70, 25.71, 27.0, 29.38, 29.40, 29.51, 29.55, 29.56, 29.60, 29.88, 29.93, 32.8, 37.0, 63.0; HRFABMS calcd for $C_{19}H_{41}O_2$ [M+H$^+$] 301.3101, found: 301.3106.

2.2.4.9. (1*S*, 2*S*)-15-diester of 2-18 derived from natural miyakosyne A

To a solution of a 9-methyl-1,18-diol (**2-18**, 1 mg) in CH_2Cl_2, (1*S*,2*S*)-**2-15** (1.2 mg),

1-ethyl-3-(3-dimethylaminopropyl)carbodiimide, hydrochloride (1 mg), and *N*,*N*-dimethyl-4-aminopyridine (0.2 mg) were added and stirred for 4 h. The solution was concentrated and the residue was purified by HPLC (COSMOSIL 5SL-II) to afford (1*S*, 2*S*)-**2-15**-diester (0.2 mg) of **2-18**, and a mixture of monoesters (0.2 mg).

^{1}H-NMR (600 MHz, $CDCl_3$) of the (1*S*, 2*S*)-diester of **2-18** derived from miyakosyne A: δ 0.722 (d, *J* = 6.9 Hz, 3H), 0.85-1.60 (m, 37H), 1.82-1.89 (m, 6H), 2.12-2.15 (m, 2H), 2.25 (dd, *J* = 3.6, 12.6 Hz, 2H), 3.50 (dt, *J* = 3.5, 11.8 Hz, 2H), 3.87 (dt, *J* = 1.4, 6.7 Hz, 4H), 4.43 (dt, *J* = 4.0, 11.8 Hz, 2H), 7.58 (dd, *J* = 3.2, 6.4 Hz, 4H), 8.04 (dd, *J* = 3.3, 6.5 Hz, 4H), 8.45 (s, 4H), 8.59 (s, 4H); HRFABMS calcd for $C_{65}H_{75}N_2O_8$ [M+H$^+$] 1011.5523, found: 1011.5532.

2.2.4.10. (1*S*, 2*S*)- 2-15-diester of *S*-2-18

(1*S*, 2*S*)-**2-15**-diester of *S*-**2-18** was prepared in the same way using *S*-**2-18**: ^{1}H NMR spectrum was almost superimposable on that of (1*S*, 2*S*)-**2-15**-diester of **2-18** except for the branched methyl (δ 0.720); HRFABMS calcd for $C_{65}H_{75}N_2O_8$ [M+H$^+$] 1011.5523, found: 1011.5512.

2.2.4.11. (1*S*, 2*S*)-2-15-diester of *R*-2-18

(1*S*, 2*S*)- **2-15**-diester of *R*-**2-18**was prepared in the same way using *R*-**2-18**: (1*S*, 2*S*)-**2-15**-diester of *R*-**2-18**: ^{1}H NMR was almost superimposable on that of (1*S*, 2*S*)-**2-15**-diester of **2-18** (chemical shift of the branched methyl δ 0.722); HRFABMS calcd for $C_{65}H_{75}N_2O_8$ [M+H$^+$] 1011.5523, found: 1011.5573.

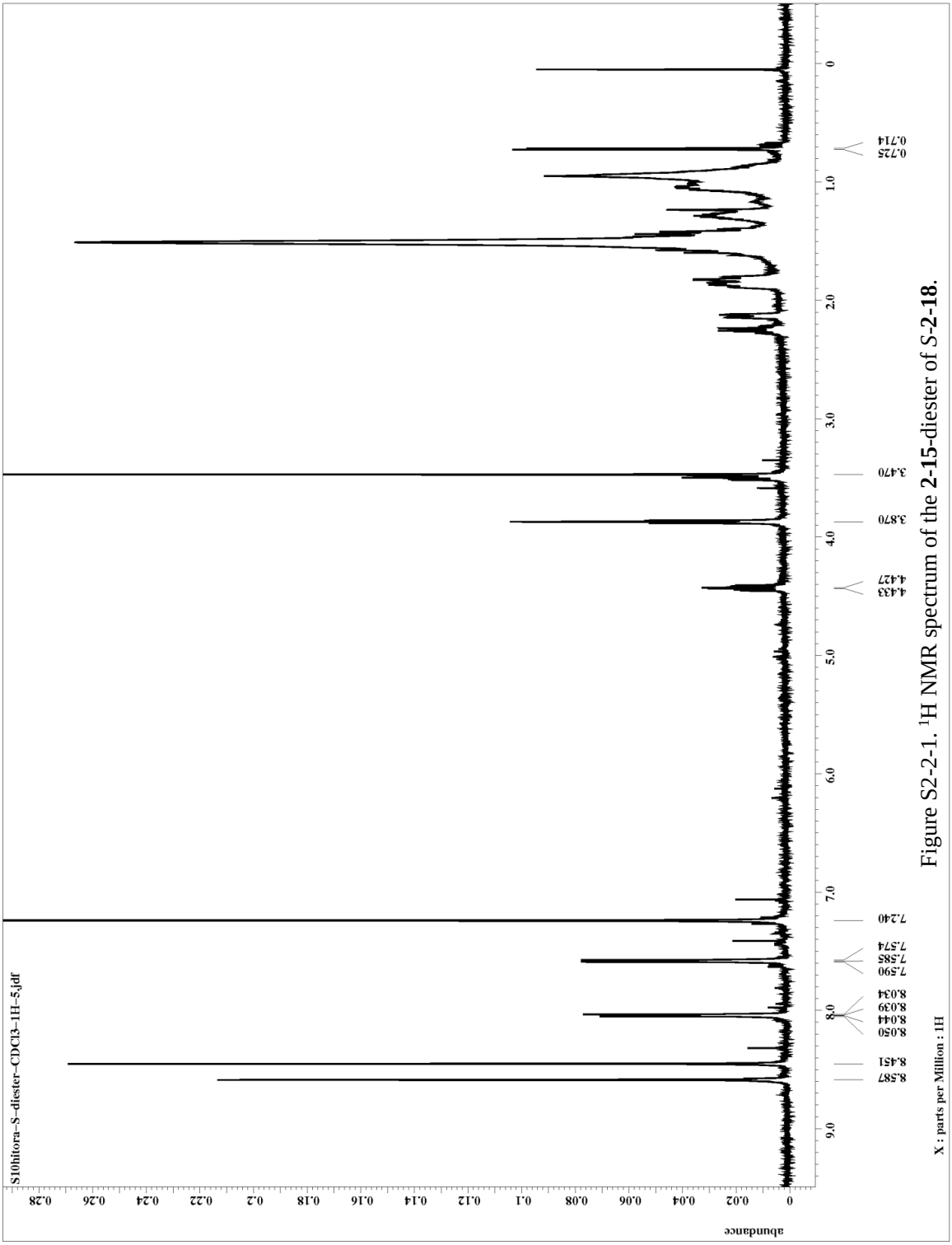

Figure S2-2-1. ^{1}H NMR spectrum of the **2-15**-diester of *S*-**2-18**.

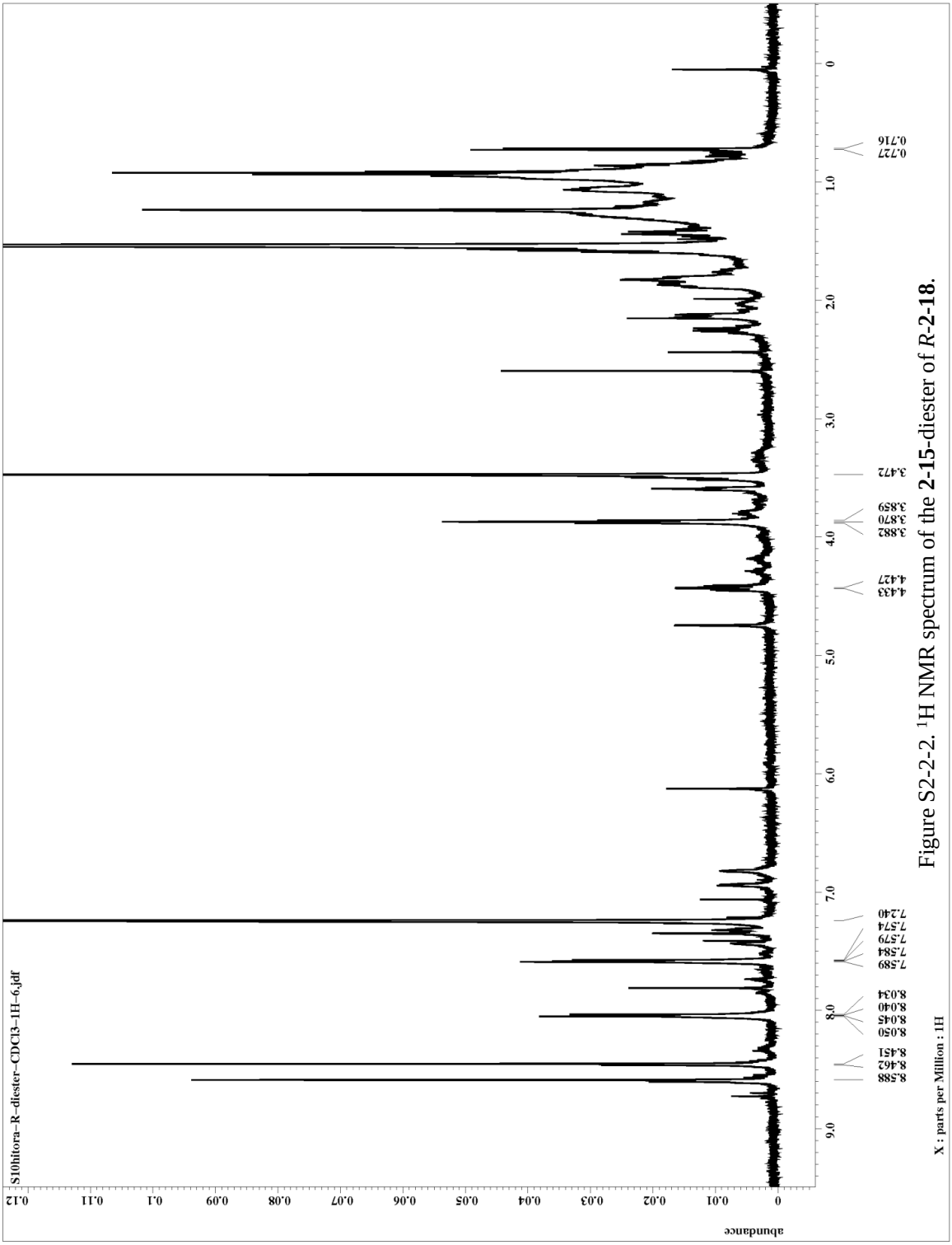

Figure S2-2-2. ^{1}H NMR spectrum of the **2-15**-diester of *R*-**2-18**.

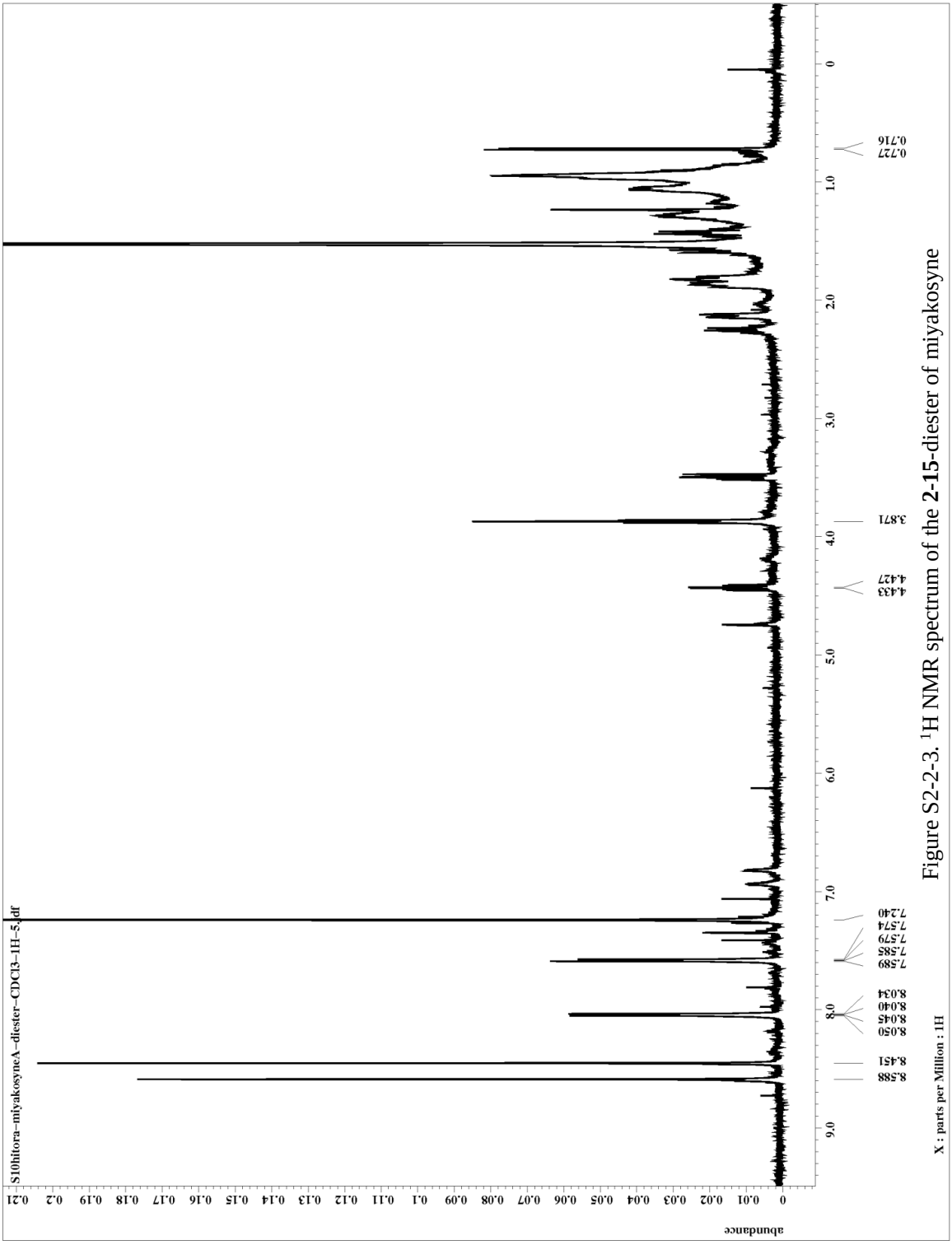

Figure S2-2-3. ^{1}H NMR spectrum of the **2-15**-diester of miyakosyne A-derived **2-18**.

Chapter 3.

Poecillastrin C and its analogue, potent cytotoxic macrolide lactams, from a deep-sea marine sponge.

3. 1. Introduction

Deep-sea sponges and microorganisms are intriguing target for the discovery of new bioactive compounds. The environment of the deep-sea is very different from that of shallow water in terms of sun light, temperature, and water pressure. Therefore, deep-sea inhabitants are thought to inherit distinct genome and produce unique secondary metabolites. Recent advances of collecting deep-sea organisms enabled us to investigate the bioactive compounds from deep-sea sponges or bacteria. A number of deep-sea derived marine natural products were isolated.[1, 2] Chondropsin/poecillastrin type of macrolide lactams are one of the typical deep-sea sponge derived metabolites.[3-9] These macrolide lactams exhibited potent antitumor activity and inhibited vacuolar type (H^+)-ATPase.[10]

During the course of our screening for cytotoxicity of sponge metabolites, an

unidentified deep-sea sponge S09-1060-01 exhibited potent cytotoxicity against HeLa cells. Bioactivity-guided fractionation of the extract resulted in the isolation of new poecillastrin analogue termed poecillastrin E (**3-1**) together with the known poecillastrin C (**3-2**).

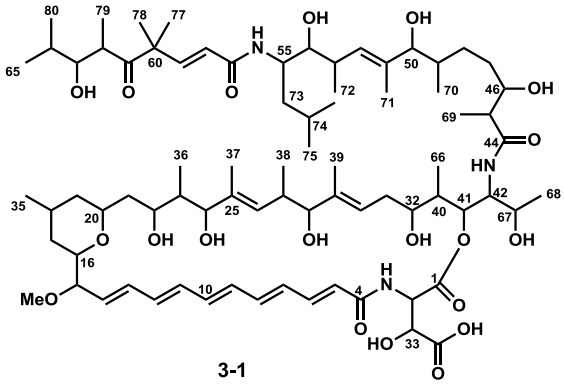

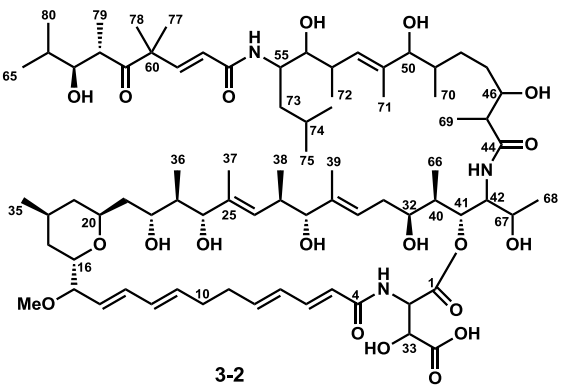

3. 2. Results and Discussion

The extract of an unidentified marine sponge S09-1060-01 was partitioned between $H_2O/CHCl_3$, and aqueous layer was concentrated and partitioned between H_2O/*n*-BuOH. The organic layer was concentrated and partitioned between 90 % MeOH/*n*-hexane, respectively. The *n*-BuOH and 90 % MeOH fractions were combined and subjected to ODS column chromatography. Bioactive fraction was purified by reversed phase HPLC to afford compounds **3-1** and **3-2**.

The molecular formula of **3-1** was determined to be $C_{78}H_{127}N_3O_{20}$ by

HRESIMS (1448.8923 $[M+Na]^+$, calcd for $C_{78}H_{127}N_3O_{20}Na$, 1448.8911). ^1H NMR and HSQC spectra of **1** resembled those of poecillastrin C. With this structural similarity in mind, 1D and 2D NMR spectra of **3-1** were analyzed. Detailed analysis of COSY and TOCSY spectra together with HMBC spectra revealed that **3-1** had the identical carbon skeleton with that of poecillastrin C, with the exception of the presence of pentaen moiety (Figure 3-1, Table 3-1). UV absorption at λ 356 nm validated the assignment of the pentaen structure.

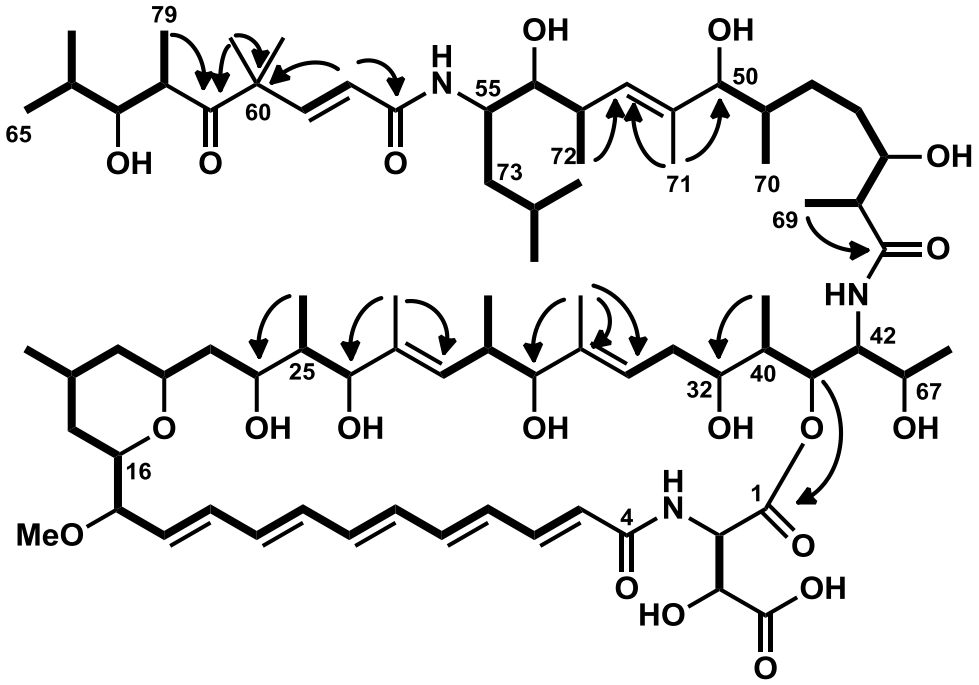

Figure 3-1. COSY and TOCSY correlations (bold lines) and key HMBC correlations (arrows) of poecillastrin E (**3-1**).

Table 3-1. ^{1}H and ^{13}C NMR data of Poecillastrin E (**3-1**) in CD_3OD.

Poecillastrin E (**3-1**)					
No.	δ_H, mult.	δ_C	No.	δ_H, mult.	δ_C
1		174.2	41	5.18, d (10.7)	78.2
2	4.92	57.4	42	4.14, d (5.0)	54.7
3			43		
4		168.2	44		178.6
5	6.19, d (15.0)	124.9	45	2.56	48.3
6	7.24, dd (11.3, 15.0)	142.3	46	3.56	74.2
7	6.47, dd (9.8, 14.8)	131.4	47a	1.48	33.0
8	6.74 dd (11.1, 14.8)	141.3	47b	1.57	
9	6.45, dd (11.1, 14.9)	133.4	48a	1.22	29.7
10	6.65, dd (10.8, 14.9)	138	48b	1.35	
11	6.46, dd (10.8, 14.5)	133.9	49	1.64	36.5
12	6.55, dd (10.6, 14.5)	136.2	50	3.66, brd (8.3)	83.9
13	6.49, dd (10.6, 14.6)	135.7	51		137.6
14	5.68 dd (9.6, 14.6)	135.4	52	5.37, d (9.9)	131.1
15	3.99, t (9.6)	81.7	53	2.62	36.1
16	3.63	75.8	54	3.37	78.7
17a	1.21	34.6	55	4.05	51.3
17b	1.88		56		
18	1.86	27.2	57		167.0
19a	0.90	41.4	58	6.10, d (15.7)	124.0
19b	1.49		59	6.94, d (15.7)	148.3
20	3.54	69.4	60		51.6
21a	1.12	43.3	61		216.7
21b	1.39		62	3.14, dd (6.6, 9.7)	45.6
22	4.01, q (7.0)	66.0	63	3.56	77.9
23	1.30	42.4	64	1.78	30.0
24	3.48, d (9.9)	80.7	65	0.96	20.4
25		137.0*	66	0.94	22.7
26	4.89	135.1	67	3.74	69.7
27	2.50	35.8	68	1.17, d (6.2)	21.4
28	3.44	84.1	69	1.18	15.6
29		137.1	70	0.97	15.9
30	5.22, brt (5.4)	128.7	71	1.55	11.9
31a	1.91	34.6	72	1.01, d (7.0)	17.7
31b	2.29		73	1.49	40.2
32	3.44	69.5	74	1.59	25.8
33	4.88	72.8	75	0.93	21.9
34		175.3	76	0.93	24.3
35	0.93	22.7	77	1.28	23.9
36	0.50, d (7.0)	8.6	78	1.31	23.9
37	1.54	10.4	79	0.88	15.7
38	0.54, d (7.0)	17.5	80	0.85, d (6.6)	14.2
39	1.58	11.2	15-OMe	3.26	56.4
40	1.78	40.6			

^{1}H NMR apectrum was measured at 600 MHz, δ_C was assigned by HSQC data.

The geometries of its pentaene portion were determined to be all *E* by large $^{3}J_{HH}$ coupling constants between H5/H6, H7/H8. H9/H10, H11/H12 and H13/H14, which was confirmed by a series of NOE correlations between H6/H8, H8/H10, H10/H12, and H12/H14. NOE correlations between H24/H26, H28/H30, and H50/H52 established the *E* configuration of olefins at $\Delta^{25, 26}$, $\Delta^{29, 30}$, and$\Delta^{51, 52}$. $^{3}J_{H58H59}$ of 15.6 Hz confirmed the *E*-geometry at $\Delta^{58, 59}$. Finally, the planar structure of **3-1** was confirmed to be the hybrid type of poecillastrin C and mirabalin, and **3-1** was named as poecillastrin E. Polyene macrolactam structure was reported to be unstable under the light, and **3-1** decomposed under the ambient light condition.[9] The molecular weight, NMR spectra, specific rotation, and retention time in HPLC of compound **3-2** were identical with those of poecillastrin C. Therefore, **3-2** was identified as poecillastrin C (Table S3-1).[7, 8]

Neither the relative configuration nor the absolute configuration of chondropsin/poecillastrin class of compounds have been completed because of the complexity of the molecule and limited amount of the sample. In this study, the relative configurations of the partial structures of **3-2** were investigated based on the interpretation of NOESY and DQF-COSY data. First, the configuration of tetrahydropyrane ring was examined by NOESY data. H15 exhibited NOE correlations to H18 and H20, pointing out the axial orientation of the alkyl substituent at C16.

Another NOE correlation between H18 and H20 supported the 1,3-diaxial relationship. Analysis of coupling constants and NOESY spectra revealed the relative configurations of C20/C21, and C21/C22. A large coupling constant between H20 and H21a (8.4 Hz) indicated their *anti* relationship, and NOESY correlations between H19 and H21b, and H20 and H22 assigned the relative configuration of C20/C21 (Figure 3-2a). The relative configuration of C21/C22 was assigned by a $^{3}J_{H21bH22}$ value of 10.5 Hz and NOE correlations between H21ab and Me36 (Figure 3-2b). The *anti* configuration of Me36 and hydroxyl group at C24 was apparent from a large $^{3}J_{H21bH22}$ value of 10.8 Hz and NOE correlation from Me36 to Me37 and H26 (Figure 3-2c). Generally, the relative configuration of 2-methyl-1,3-diol spin system (C22/C23/C24) could be determined by comparison of the ^{13}C NMR chemical shift of the methyl carbon with Kishi's universal NMR database, in which 7.1 ppm represents for *syn*/*syn* configuration, 10.7 ppm for *syn*/*anti* or *anti*/*syn* configuration, and 11.6 ppm for *anti*/*anti* configuration.[11] However, an intermediate chemical shift at δ_C 8.6 ppm of Me36 was not appropriate for the assignment of the relative configuration in this molecule. The relative configuration between C27 and C28 was also assigned by the large coupling constant between H27 and H28, and NOE correlation between Me38 and Me39 (Figure 3-2d). NOE correlations observed from H32 to H40 and H41, and from H31 to H40 and Me66

assigned the relative configuration at C32/C40 (Figure 3-2e). The relative configuration at C40/C41 was established from a large coupling constant between H40 and H41 together with NOE correlation between Me66 and H42 (Figure 3-2f). The relative configuration at C41/C42 was determined by the small $^{3}J_{H41H42}$ of 1.4 Hz and NOE correlations between H41/H67 and Me66/H42 (Figure 3-2g). Me79 and hydroxyl group at C63 was assigned to be *anti* from a large $^{3}J_{H62H63}$ and NOE correlation between Me79 and H64 (Figure 3-2h). The modified Mosher's method was attempted to determine the absolute configuration of the chiral center substituted to the secondary alcohol, however we ended up with the dehydration of the compound.[12]

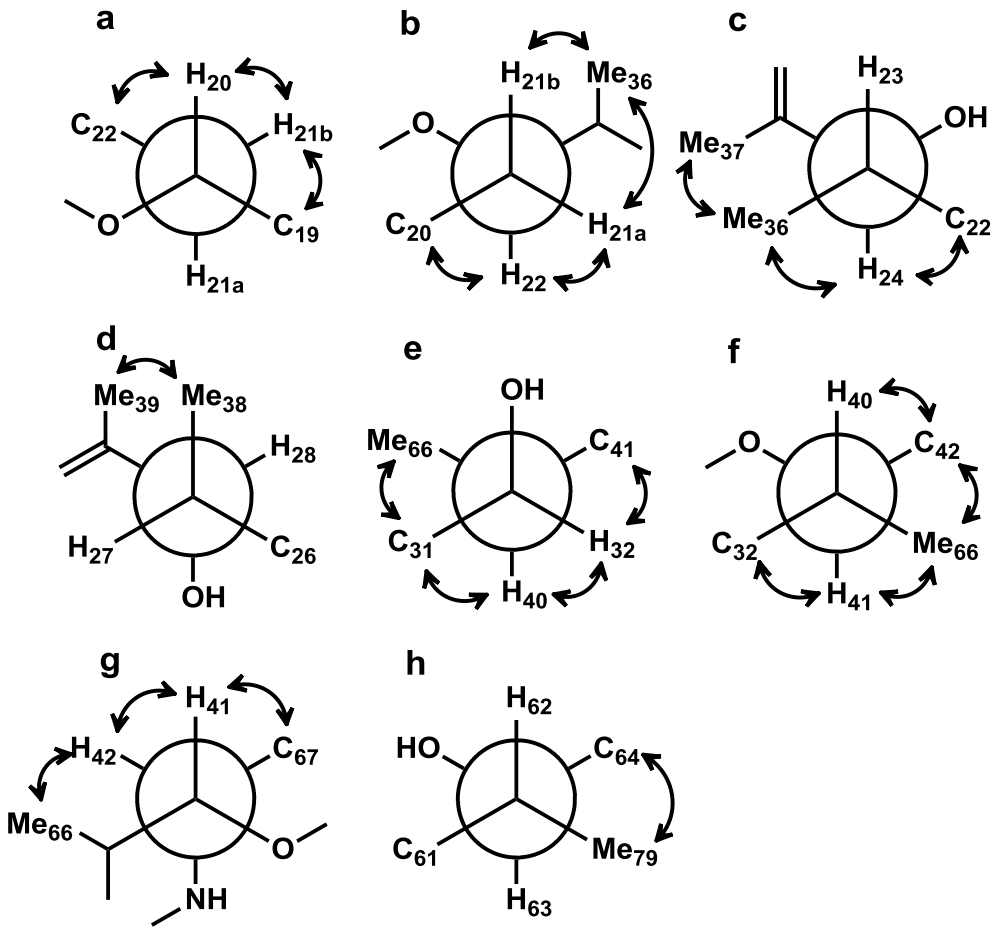

Figure 3-2. Conformational analysis of poecillastrin C for assignment of the relative configuration of (a) C20/C21, (b) C21/C22, (c) C23/C24, (d) C27/C28, (e) C32/C40, (f) C40/C41, (g) C41/C42, (h) C62/C63. NOESY correlations were illustrated as arrows.

Chondropsin/poecillastrin type of macrolide lactams are reported to inhibit vacuolar-type $(H)^+$-ATPase and show potent cytotoxicity against various type of cancer cells.[3-10] HeLa cells treated with poecillastrins C or E at concentrations ranging from 4 ng/mL to 100 ng/mL did not show cell growth and died in 2 days. Poecillastrins E (**3-1**) exhibited potent cytotoxicity against HeLa cells with an IC_{50} value of 1.8 ng/mL, of the IC50 value of poecillastrin C (**3-2**) was 0.99 ng/mL.

3.3. Experimental Section

3.3.1. General Experimental Procedures.

Optical rotations were measured on a JASCO DIP-1000 digital polarimeter in MeOH. NMR spectra were recorded on a JEOL alpha 600 NMR spectrometer at 300 K. Chemical shifts were referenced to solvent peaks: δ_H3.30 and δ_c49.0 for $CDCl_3$. ESI mass spectra were measured on a JEOL JMS-T100LC.

3.3.2. Animal Material.

An unidentified marine sponge S09-1060-01 was collected at Miyako sea-knoll, southwestern Japan by using the Remotely Operated Vehicle ‘Hyper-Dolphin’ in October 2009during a cruise of R/V Natsushima,

3.3.3. Extraction and Isolation.

The frozen marine sponge (600 g) was extracted with 1.8 L of 50 % MeOH, and EtOH. The crude extracts were combined and partitioned between H_2O and $CHCl_3$. The aqueous layer was extracted with *n*-BuOH. The organic layer was concentrated *in vacuo* and partitioned with 90 % MeOH and *n*-hexane. *n*-BuOH and 90 % MeOH layers were combined, concentrated and fractionated by ODS column chromatography eluted with

50 % MeOH, 70 % MeOH, 90 % MeOH, MeOH, and a mixture of $CHCl_3$, MeOH and H_2O (6:4:1). 70 % MeOH fraction was concentrated and purified by reversed phase HPLC with a linear gradient from MeCN/H_2O (11:9) containing 1 % AcOH to MeCN/H_2O (7:3) containing 1 % AcOH to afford 2.5 mg of **3-1** and 2.8 mg of **3-2**.

3.3.1. Poecillastrin E (**3-1**): pale yellow solid; $[\alpha]^{18}_{D}$ +28 (c = 0.15, MeOH); UV (MeOH) λmax 373 (17,000), 356 (20,000), 205 (18,000);^{1}H and ^{13}C NMR data, see table 1; HRESIMS *m/z* 1448.8923 $[M+Na]^+$, calcd for $C_{78}H_{127}N_3O_{20}Na$, 1448.8911.

3.3.4. Cytotoxicity Evaluation.

The cytotoxicities of **3-1** and **3-2** against HeLa cells were evaluated by an MTT assay. HeLa human cervical cancer cells were cultured in Dulbecco's modified Eagle's medium containing 10% fetal bovine serum, penicillin and streptomycin at 37°C under an atmosphere of 5% CO_2. After overnight preincubation, sample was added to each well of a 96-well microplate containing 200 μL of tumor cell suspension (1 x 10^4 cells/mL), and further incubated for 72 h. MTT saline solution was added to each well, and the plate was incubated for 3 h. The supernatant was discarded and formazan dye was dissolved in 150 μL of DMSO. The absorbance was measured to determine IC_{50} values.

Table S3-1. ^{1}H and ^{13}C NMR chemical shifts of poecillastrin C (**3-2**).

Poecillastrin C (**3-2**)					
No.	δ_H	δ_C	No.	δ_H	δ_C
1		174.6	41	5.16	78.1
2	4.87	57.5	42	4.14	54.6
3			43		
4		168.4	44		178.6
5	6.11	123.9	45	2.54	48.3
6	7.14	142.2	46	3.55	74.1
7	6.32	129.8	47a	1.46	32.9
8	6.22	143.1	47b	1.56	32.9
9	2.34	35.0	48a	1.20	29.6
10	2.23	33.5	48b	1.46	29.6
11	5.87	135.9	49	1.63	36.5
12	6.32	131.6	50	3.65	83.9
13	6.33	135.8	51		137.4
14	5.56	131.9	52	5.36	131
15	3.93	81.7	53	2.61	36.0
16	3.63	75.7	54	3.36	78.6
17a	1.21	34.5	55	4.04	51.2
17b	1.88	34.5	56		
18	1.86	26.7	57		167.2
19a	0.89	41.3	58	6.07	123.9
19b	1.52	41.3	59	6.93	148.3
20	3.52	68.8	60		51.9
21a	1.15	42.9	61		216.8
21b	1.44	42.9	62	3.13	45.5
22	4.21	65.9	63	3.55	78.4
23	1.39	41.7	64	1.77	29.9
24	3.74	81.2	65	0.86	14.1
25		136.9	66	0.93	
26	5.00	135.3	67	3.73	69.8
27	2.51	35.9	68	1.16	21.1
28	3.48	84.4	69	1.18	15.4
29		137.2	70	0.97	15.8
30	5.24	128.6	71	1.55	11.8
31a	1.91	34.4	72	1.00	17.6
31b	2.28	34.4	73	1.49	40.2
32	3.46	69.7	74	1.56	25.7
33	4.85	72.9	75	0.92	21.8
34		175.9	76	0.92	24.2
35	0.93	22.6	77	1.27	23.7
36	0.55	8.6	78	1.30	23.8
37	1.57	10.4	79	0.89	15.5
38	0.60	17.4	80	0.95	20.4
39	1.58	10.6	15-OMe	3.23	56.1
40	1.79	40.4			

^{1}H NMR spectrum was measured at 600 MHz,
δ_C was assigned by HSQC data.

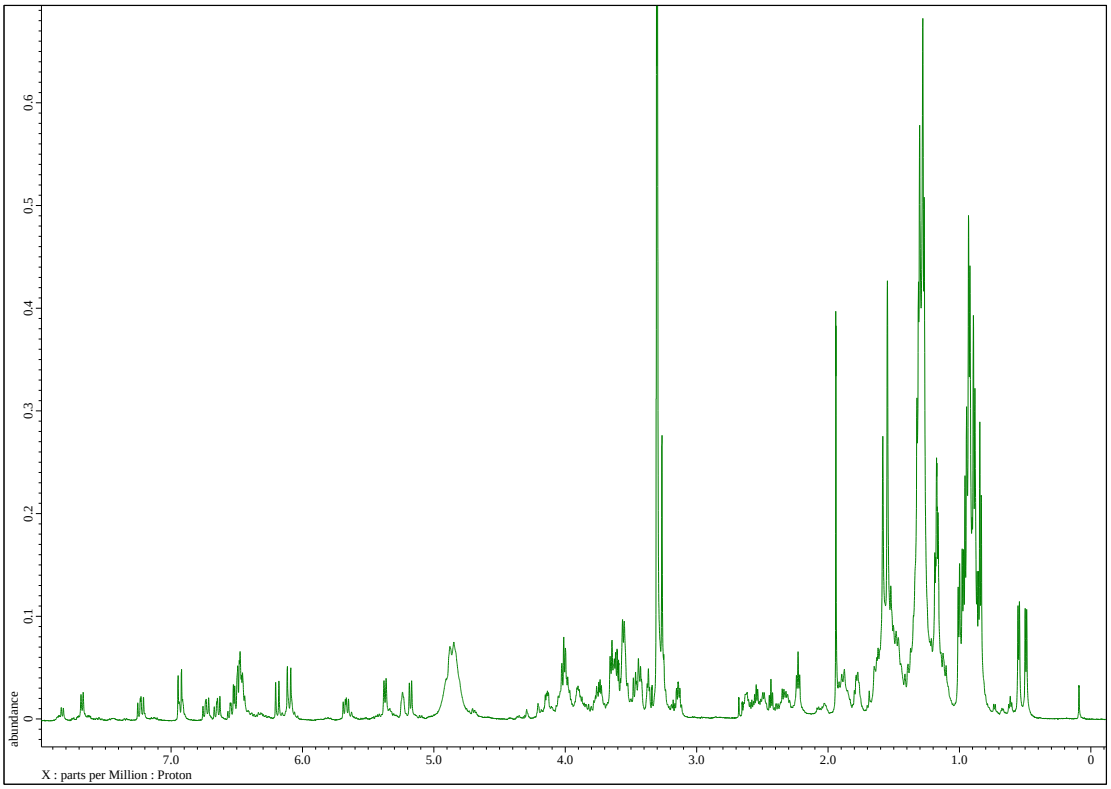

Figure S3-1. ^{1}H NMR spectrum of **3-1**

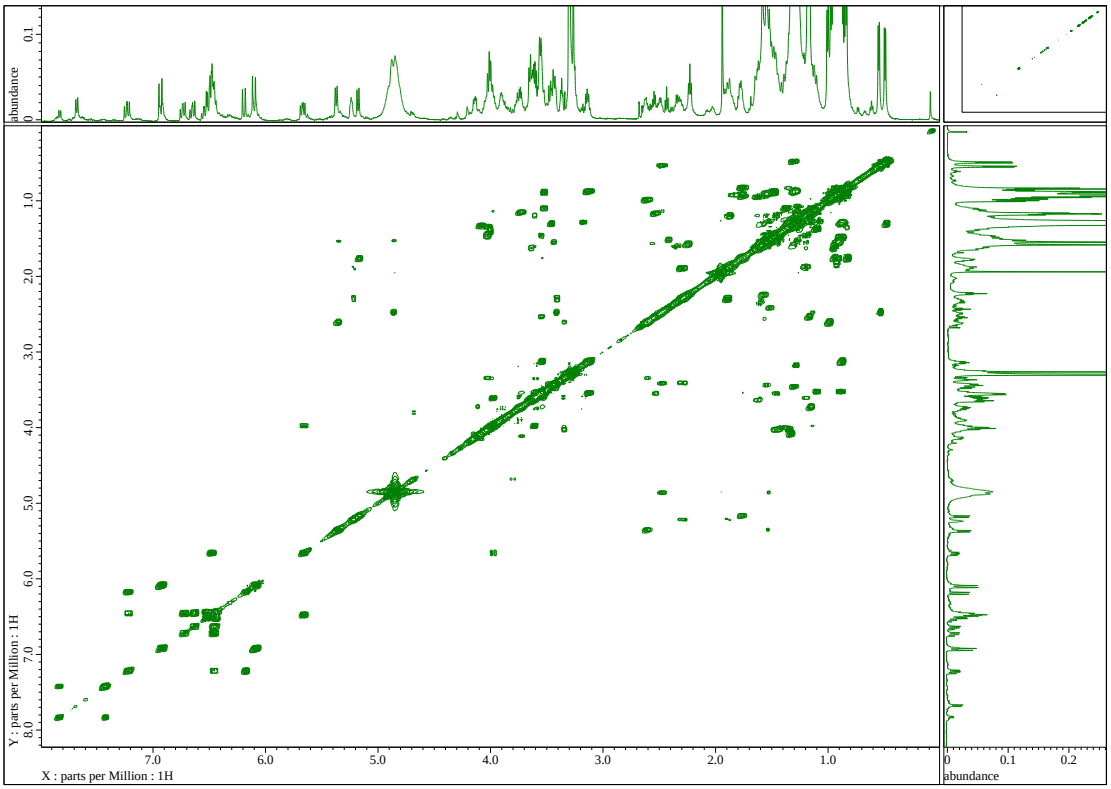

Figure S3-2. COSY spectrum of **3-1**.

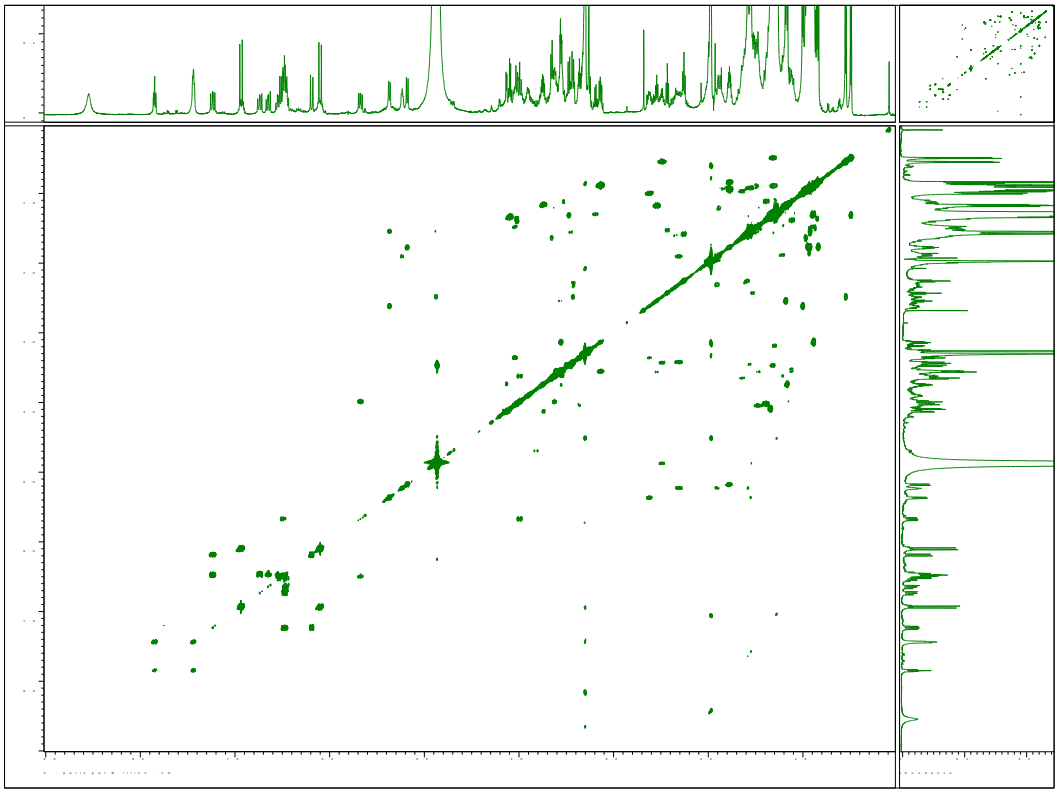

Figure S3-3. DQF-COSY spectrum of **3-1**.

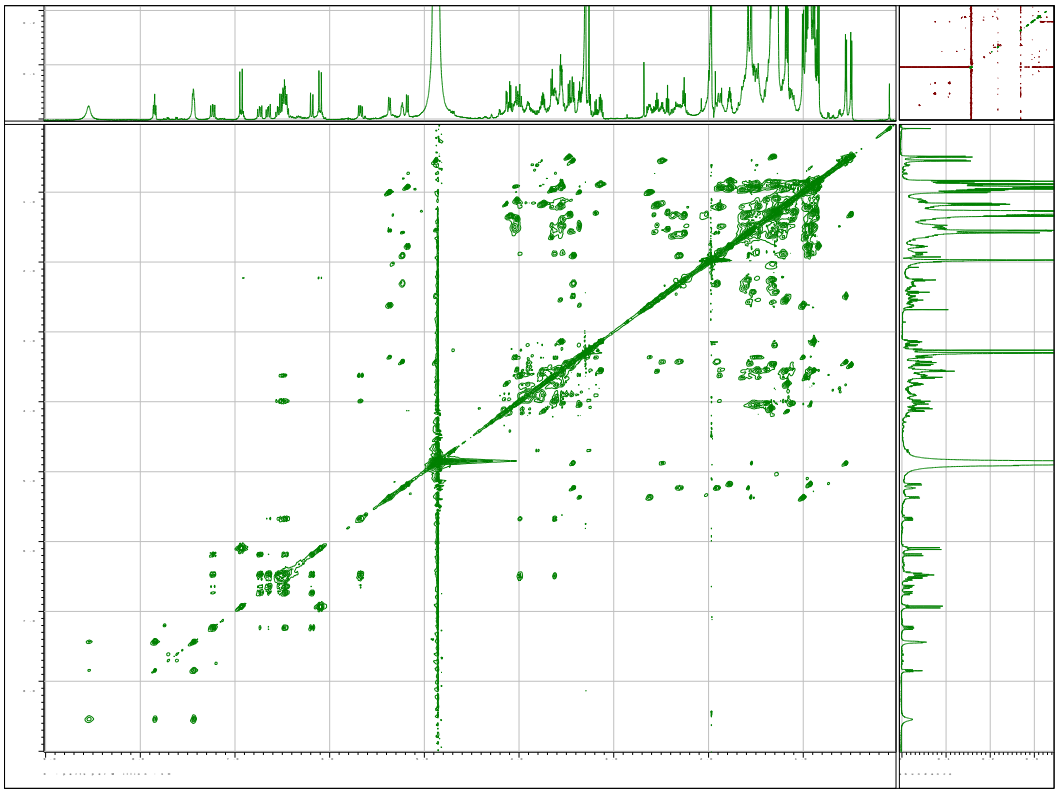

Figure S3-4. TOCSY spectrum of **3-1**.

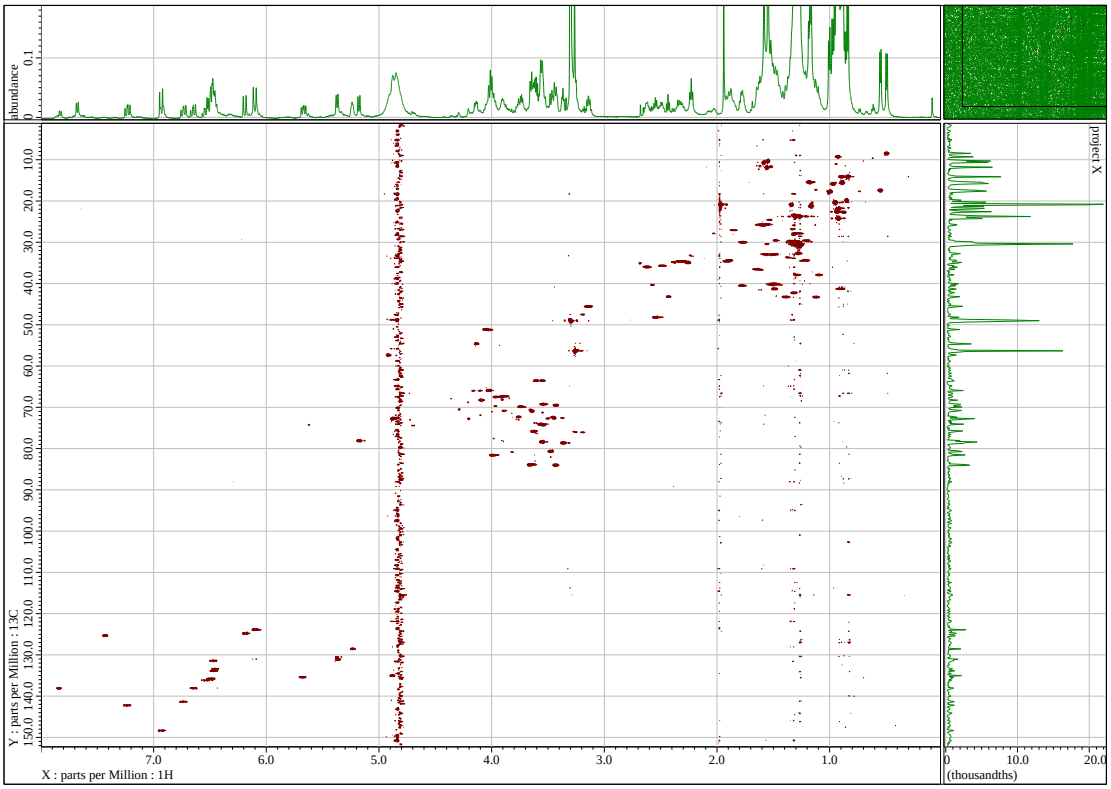

Figure S3-5. HSQC spectrum of **3-1**.

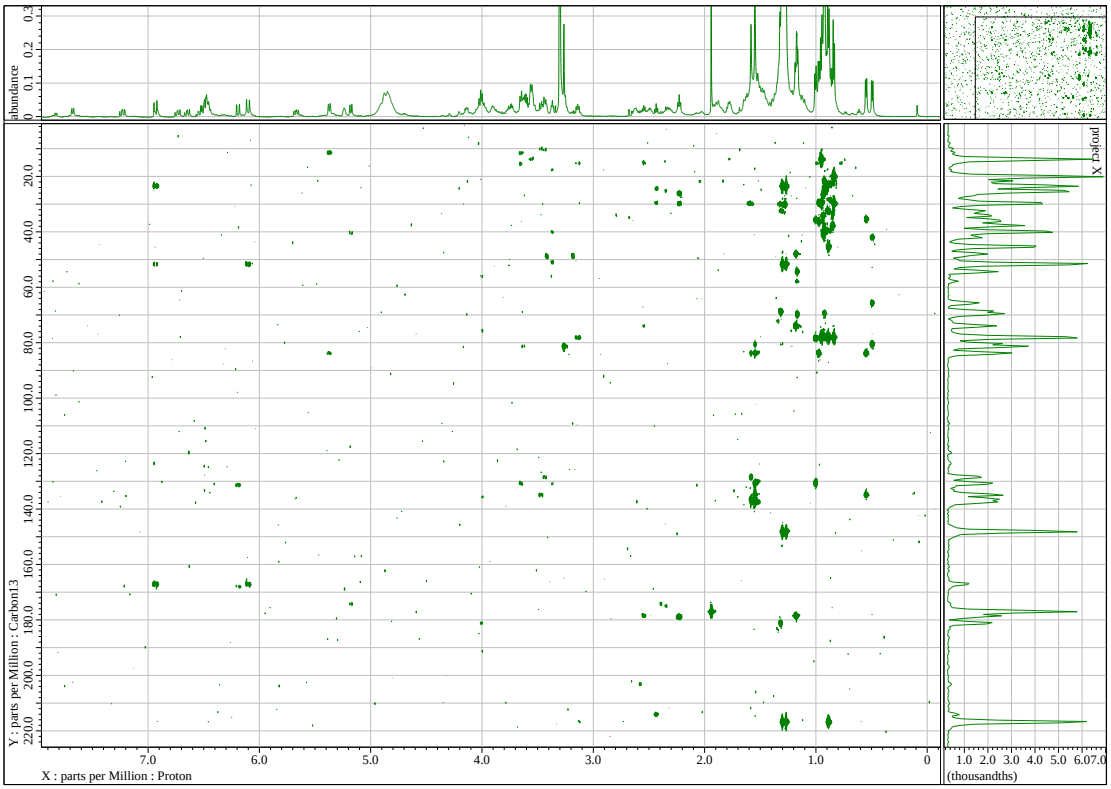

Figure S3-6. HMBC spectrum of **3-1**.

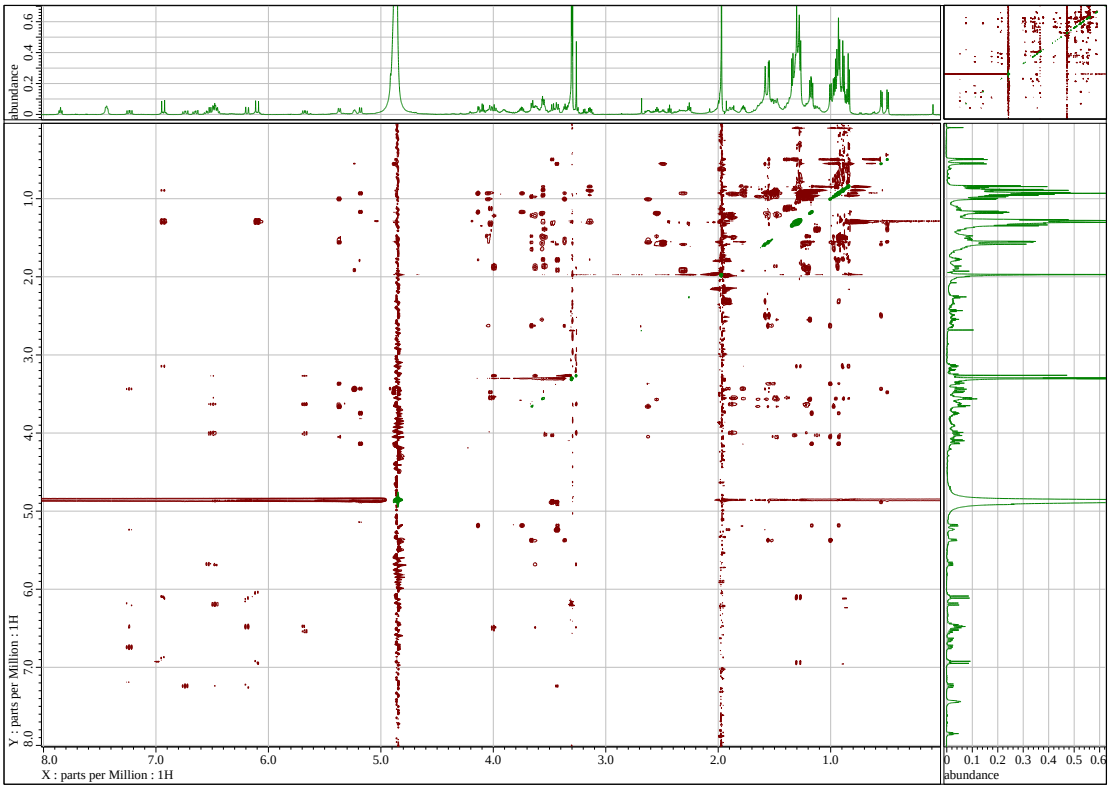

Figure S3-7. NOESY spectrum of **3-1**.

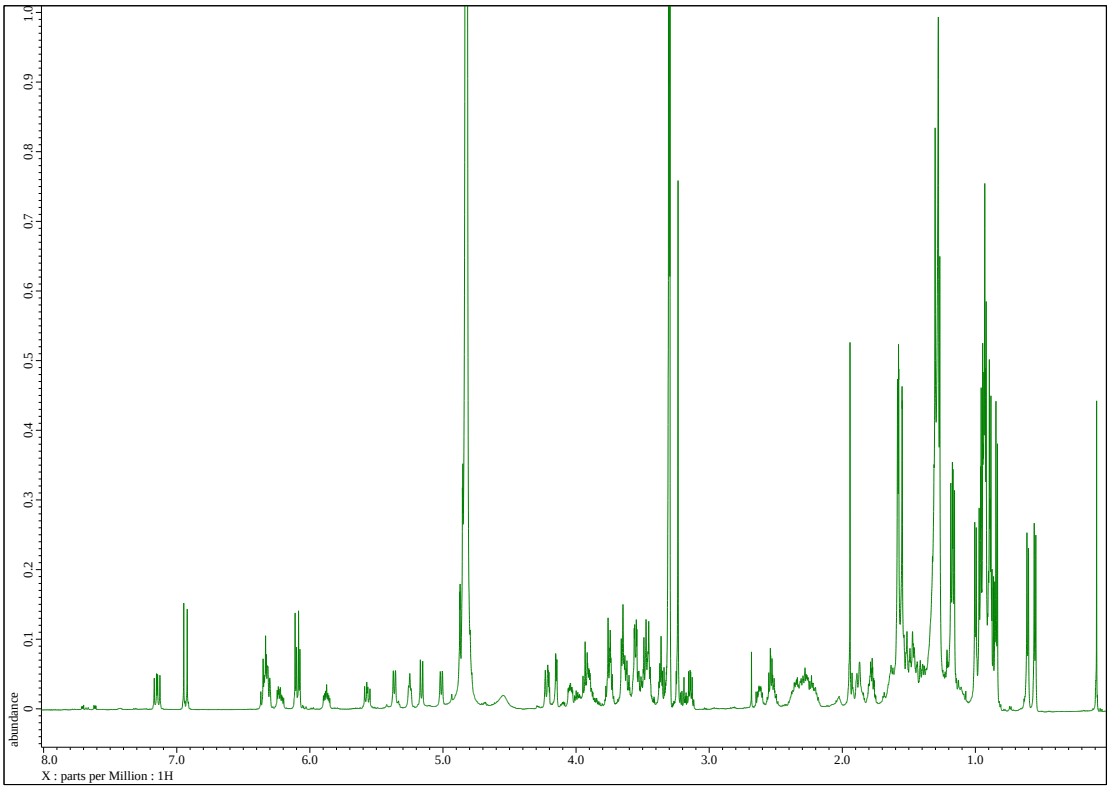

Figure S3-8 ^{1}H NMR spectrum of **3-2**.

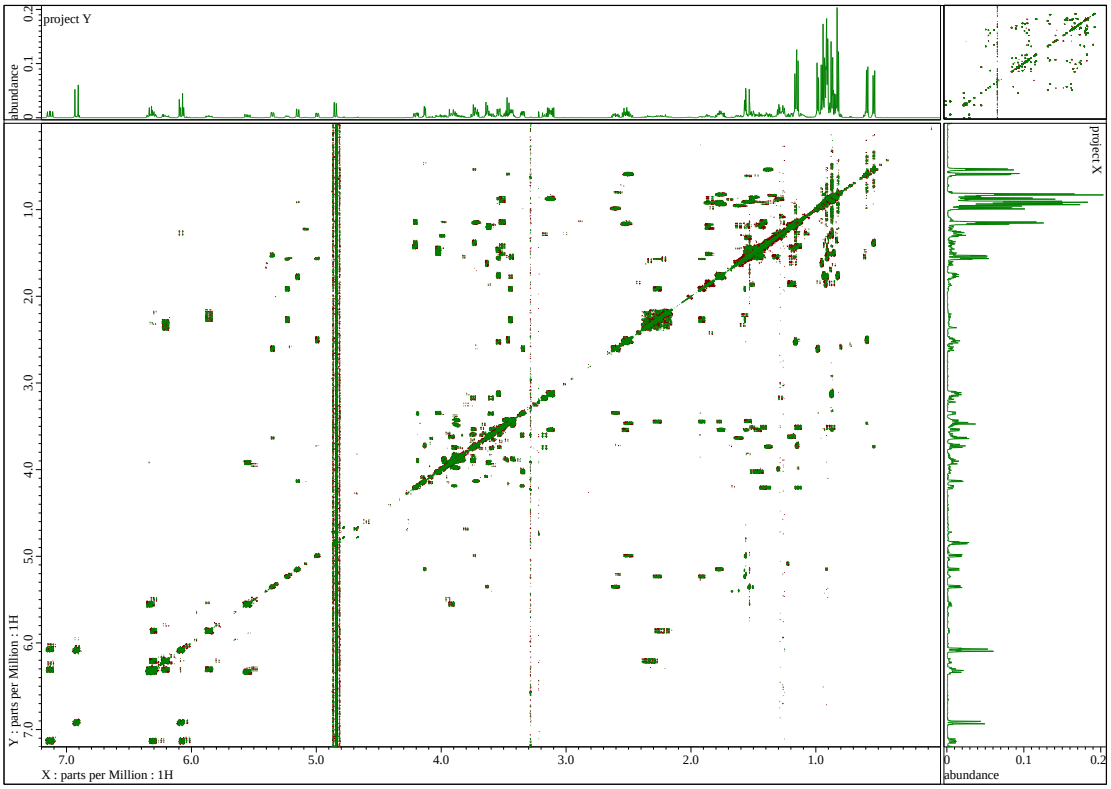

Figure S3-9. DQF-COSY spectrum of **3-2**.

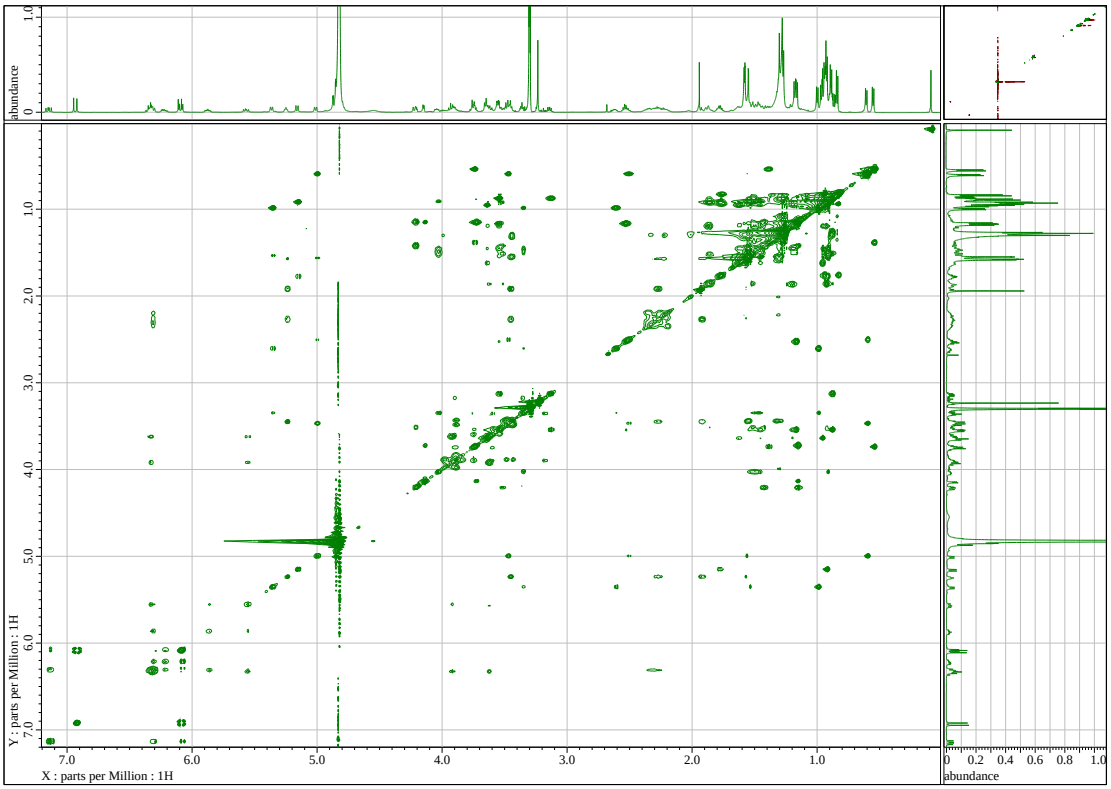

Figure S3-10. TOCSY spectrum of **3-2**.

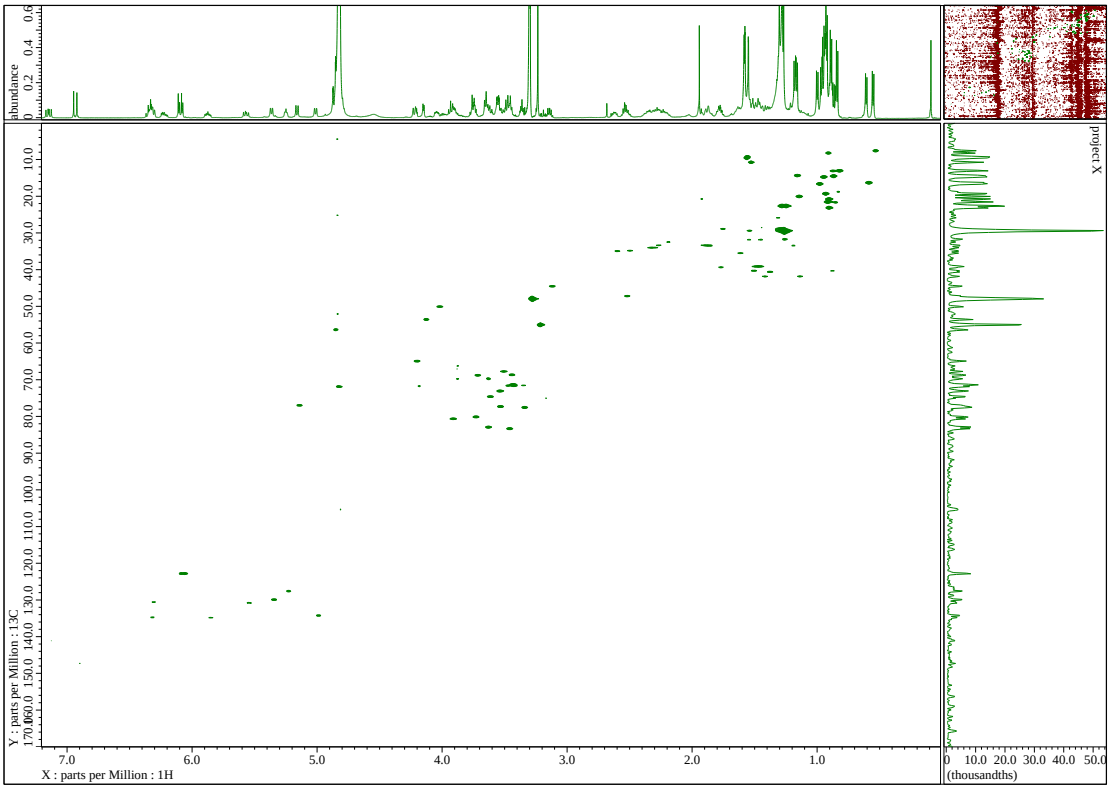

Figure S3-11. HSQC spectrum of **3-2**.

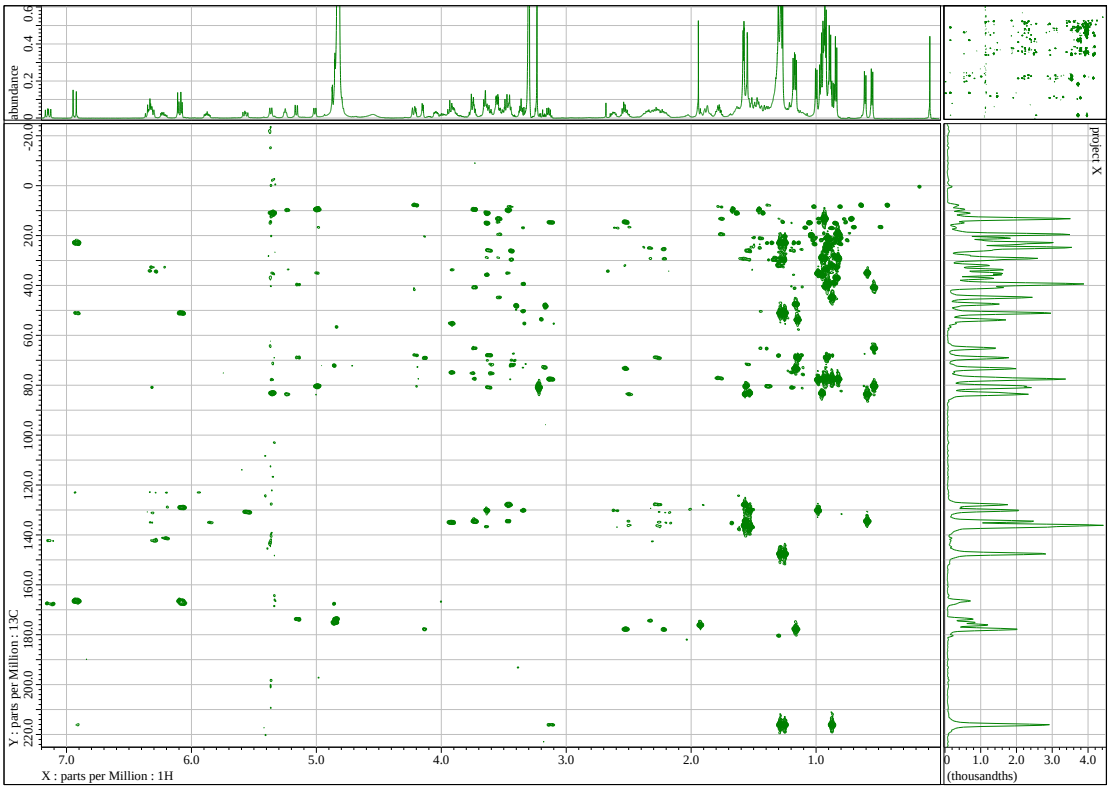

Figure S3-12. HMBC spectrum of **3-2**.

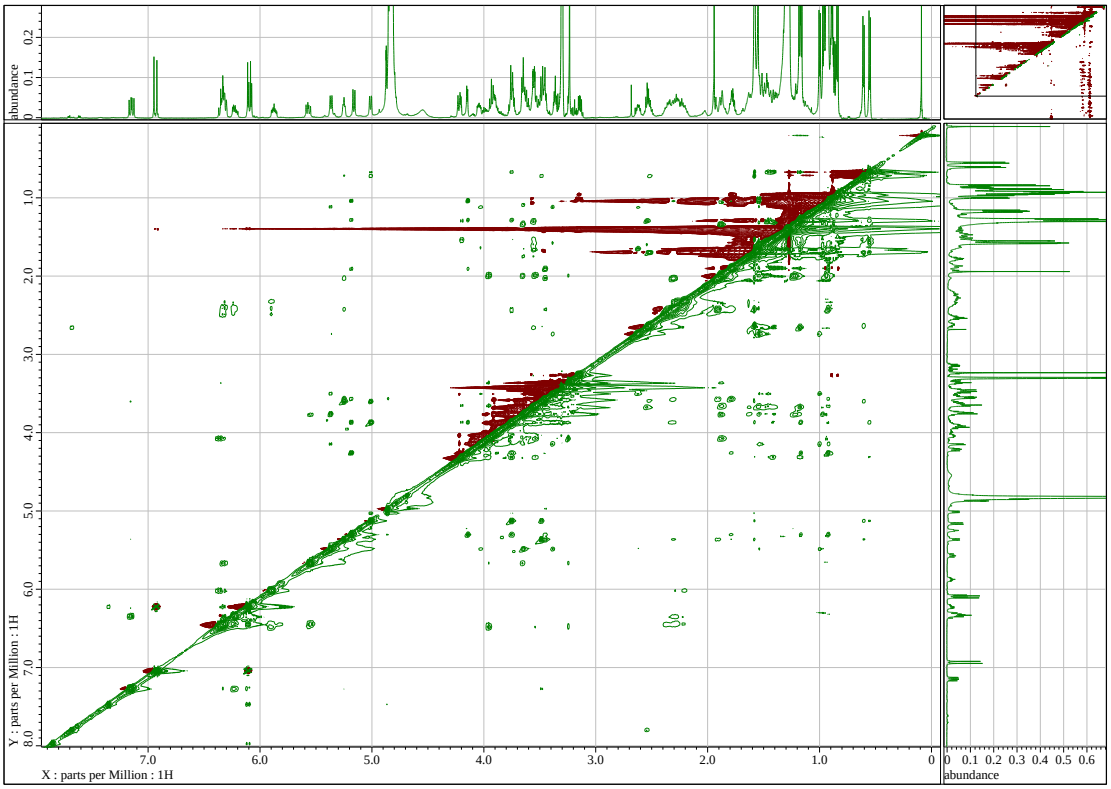

Figure S3-13. NOESY spectrum of **3-2**.

Figure S3-14. Photograph of an unidentified marine sponge S09-1060-01.

Chapter 4.

Introduction of fluorescent time-lapse imaging of HeLa/Fucci2 cells for the identification of cell cycle arrest inducers

4.1. Screening of cell cycle arrest inducers.

4.1.1. Introduction

A wide variety of anticancer agents induce cell death by affecting replication of DNA or microtubule dynamics, which play key roles in the cell cycle progression.[1] The perturbation of the control of cell division results in the induction of cell cycle arrest and apoptosis. Therefore, metabolites that induce cell cycle arrest can be candidates for leads compounds for anticancer agents. The conventional way to analyze the cell cycle progression requires measurement of cellular DNA content by flow cytometory.[2] Because, this method is low throughput, it is not suitable for the screening of a large number of extracts.

Fucci (Fluorescent Ubiquitination-based Cell Cycle Indicator) developed by RIKEN is the dual-color fluorescent probe which enables the real-time imaging of the

cell cycle progression.[3] Fucci2, a second generation of Fucci probe, was developed by fusing a red fluorescent protein (mCherry) and green fluorescent protein (mVenus) to the ubiquitination domain of human Cdt1 and Geminin, respectively.[4] Cdt1 is DNA replication factor, and is accumulated inside the nuclei at G1 phase and degraded at S phase.[5] On the other hand, Geminin, DNA replication inhibitor, accumulates inside the nuclei through S to M phases and degraded during mitosis.[5] As a result, red fluorescent protein accumulates inside the nuclei of cells at G1 phase, and green fluorescent protein accumulates through S/G2/M phase in Fucci2 transfected cells (Figure 4-1). Hence, the time-dependent change of cell cycle progression can be visualized at the single cell level. In this study, I applied time-lapse imaging of Fucci2 transfected HeLa cells (HeLa/Fucci2) and examined the effects of a library of marine natural products crude extracts of marine organisms.

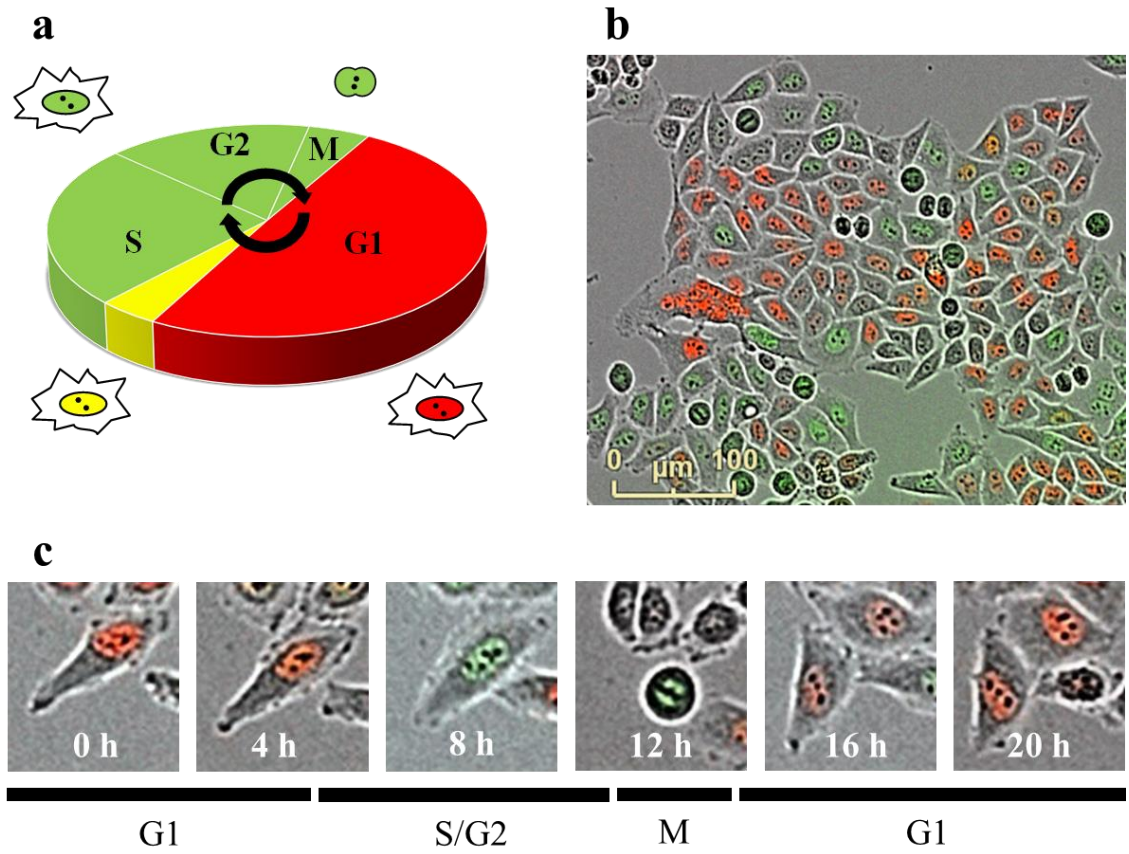

Figure 4-1. (a) Scheme of the cell cycle progression of HeLa/Fucci2 cells. (b) Fluorescence image of HeLa/Fucci2 cells. (c) Time-dependent change of cell cycle progression of HeLa/Fucci2 cells.

4.1.2. Results and Discussion

First, 27 pure marine natural products were evaluated in the HeLa/Fucci2 assay. The compounds tested in this study are as follows:13-deoxytedanolide,[6] purpuramine,[7] theonellamide A,[8] curcuphenol,[9] tetrapyrrol,[10] dibromophakellin,[11] mycalolide A,[12] onnnamide B,[13] misakinolide A,[14] rubroside F,[15] halistanolsulfate,[16] bistellettadine A,[17]

koshikamide A,[18] dogger bank itch,[19] penarolide sulfate A_1,[20] penarolide sulfate A_2,[20] discodermine A,[21] polytheonamide A,[22] aurantoside A,[23] stellettadine A,[24] corticatic acid,[25] aerothionine,[26] stelliferin E,[27] toxadocial A,[28] petrosynol,[29] oroidin,[30] and cylindramide[31] (Table 4-1). Several compounds exhibited acute cytotoxicity at higher concentrations and induced cell death within a few hours. Notably, HeLa/Fucci2 cells treated with onnamide B at lower concentrations showed time-dependent characteristic phenotypical change (Figure 4-2). From several hours after treatment of the compound, green fluorescence gradually increased inside the nuclei, and resulted in cell death. Onnamide B, a member of pederin family, is known to inhibit the protein synthesis by targeting the ribosomal E-site.[13] Inhibition of ribosomal protein synthesis by onnamide B induces activation of stress-activated protein kinases.[32] These molecular mechanism resulted in the induction of cell cycle arrest at S/G2 phase and cell death.

Table 4-1. List of the pure marine natural products assayed by the time-lapse imaging of HeLa/Fucci2 cells.

13-Deoxytedanolide	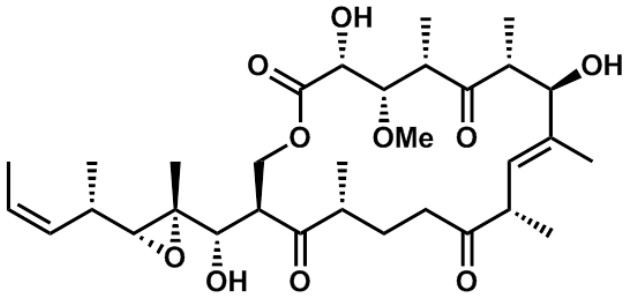	Cytotoxicity
Purpuramine	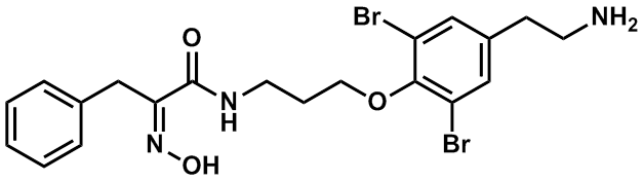	-
Theonellamide A	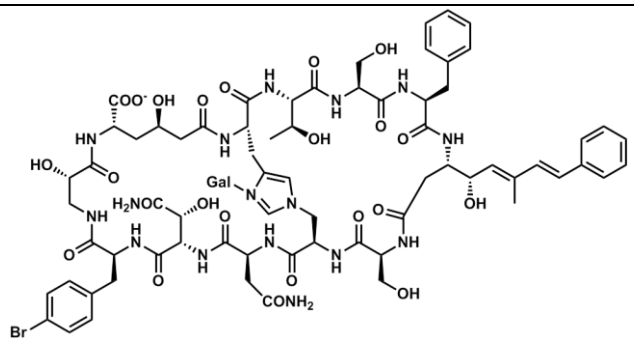	Vacuole formation
Curcuphenol	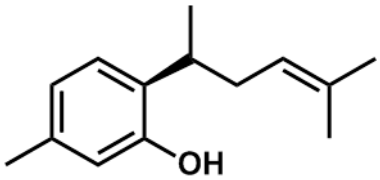	-
Tetrapyrrol	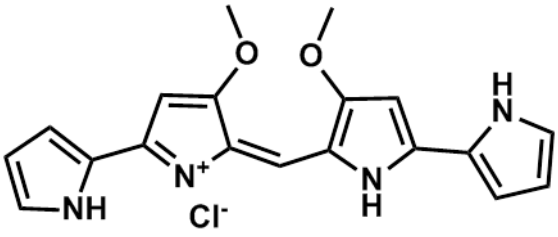	Cytotoxicity

Dibromophakellin	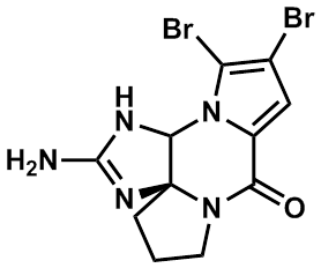	Cytotoxicity
Mycalolide A	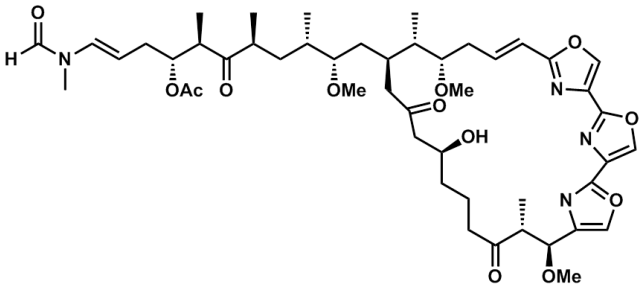	Morphological change (Figure 4-1-3)
Onnamide B	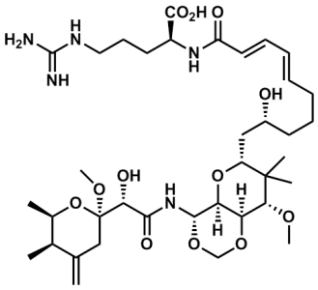	Mitotic arrest (Figure 4-1-2)
Misakinolide A	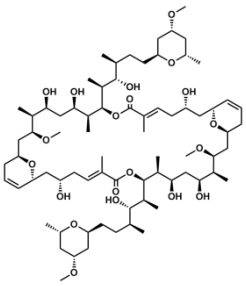	Morphological change (Figure 4-1-3)
Rubroside F	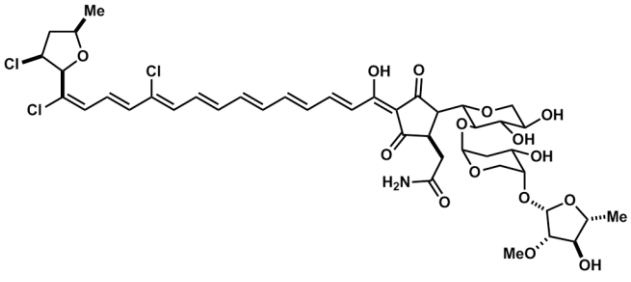	Cytotoxicity

Halistanol sulfate	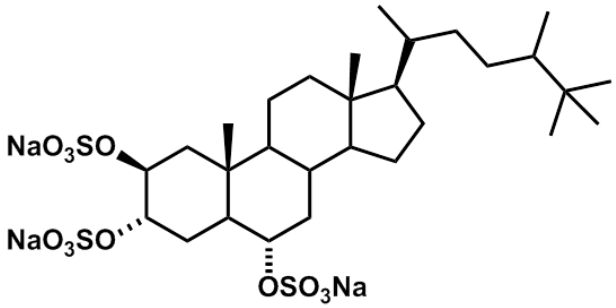	-
Bistellettadine A	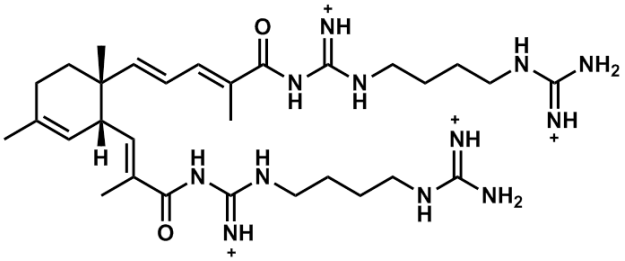	-
Koshikamide A	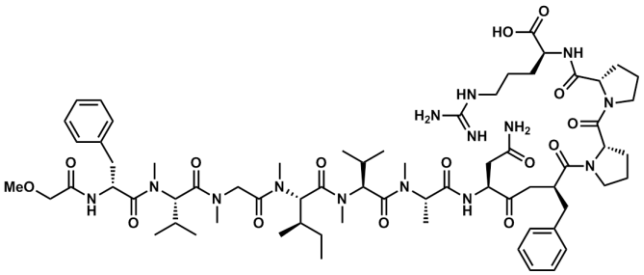	Cytotoxicity
Dogger bank itch	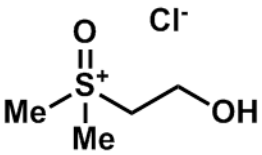	Mitotic arrest
Penarolide sulfate A_1	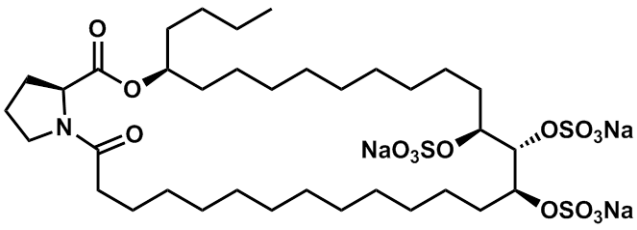	Cytotoxicity

Penarolide sulfate A_2	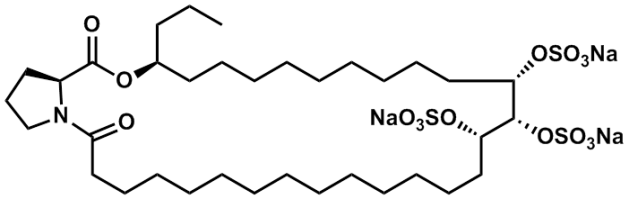	Cytotoxicity
Discodermine A	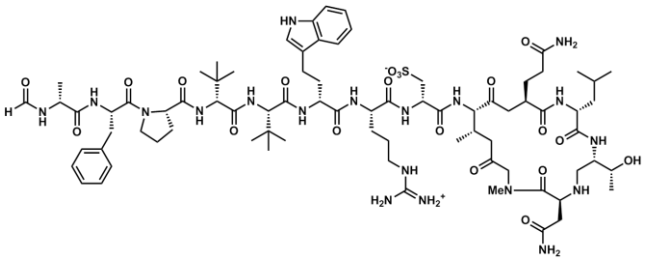	Cytotoxicity
Polytheonamide A	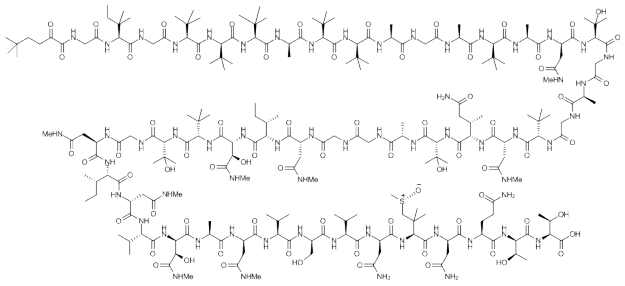	Cytotoxicity
Aurantoside A	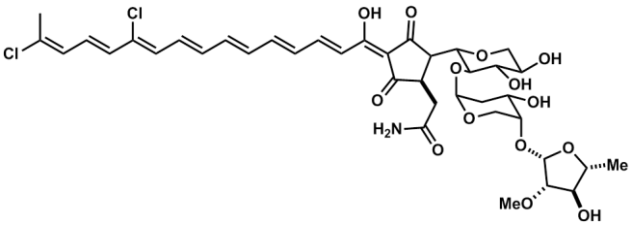	Cytotoxicity
Stellettadine A	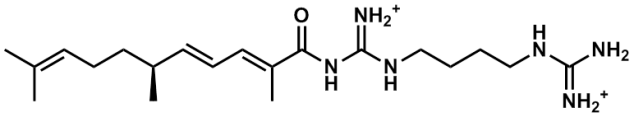	-

Corticaic acid	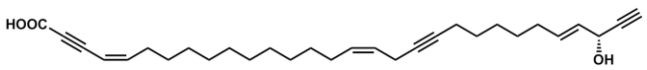	-
Aerothionine	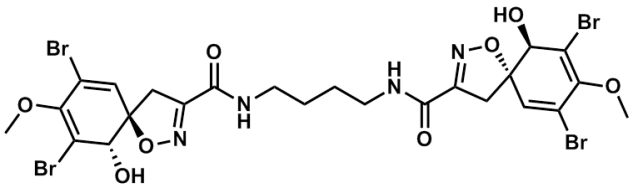	-
Stelliferin E	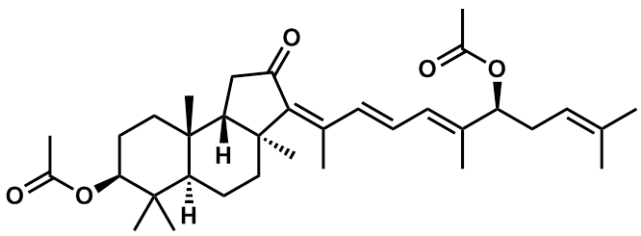	Cytotoxicity
Toxadocial A	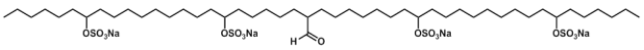	Cytotoxicity
Petrosynol	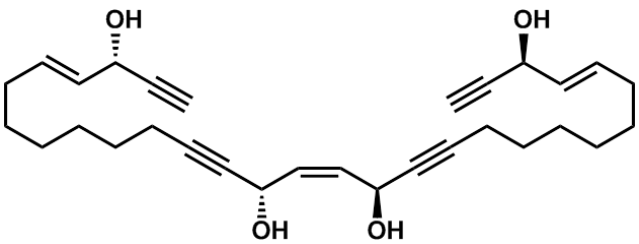	-

Oroidin	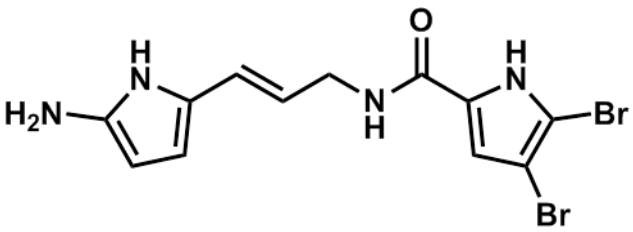	-
Cylindramide	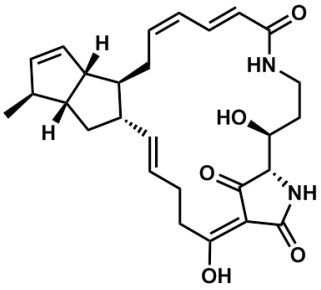	Vacuole formation

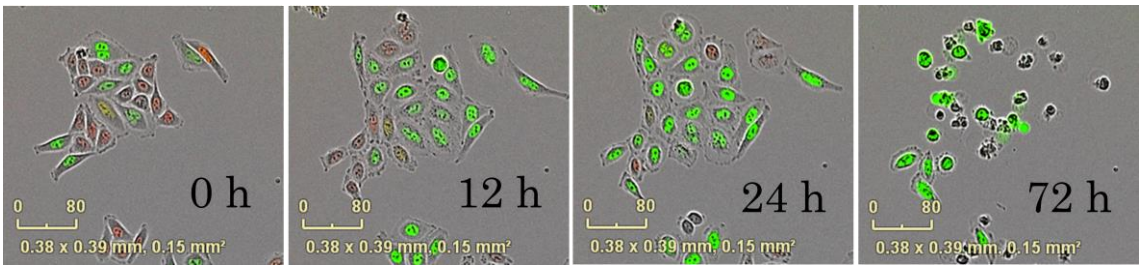

Figure 4-2. Typical fluorescent images of HeLa/Fucci2 cells treated with 0.3 μg/mL of onnamide B.

Mycalolide A and misakinolide A, whose molecular target is actin, induced characteristic morphological changes of HeLa/Fucci2 cells. Mycalolide A is a trisoxazole macrolide isolated from a marine sponge *Mycale* sp.[12] Mycalolide A binds to G-actin and severs and depolymerizes F-actin.[33] HeLa/Fucci2 cells treated with

mycalolide A were inhibited in cytokinesis and led to endoreplication and polyploid formation (Figure 4-3). Misakinolide A also depolymerized actin cytoskeleton and induced polyploidal giant cells (Figure 4-3).[14]

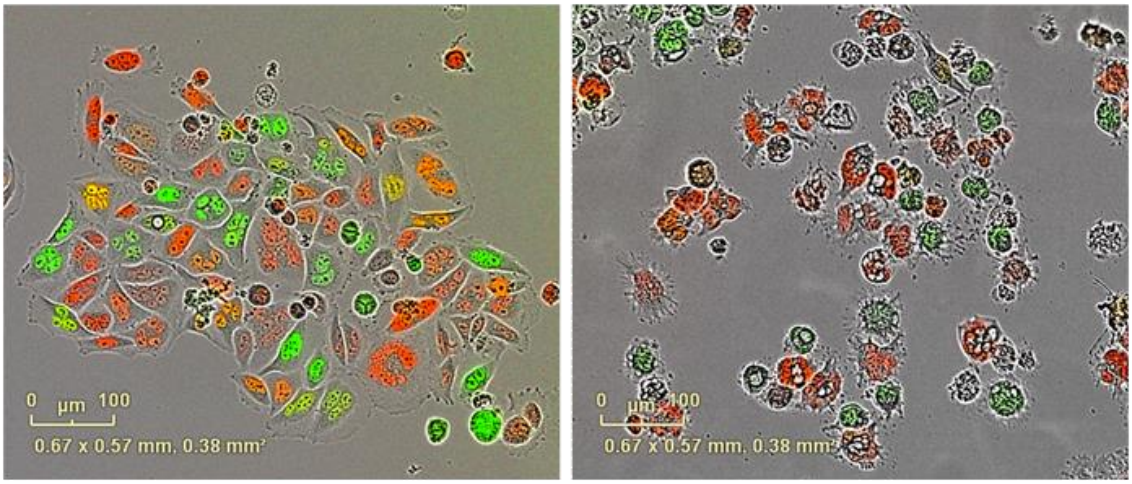

Figure 4-3. Fluorescent microscopic images of HeLa/Fucci2 cells treated with 8 ng/mL of mycalolide A (Left), and 12 ng/mL of misakinolide A (Right).

Then, biological activity of the crude extract library of marine invertebrates was evaluated by the time-lapse imaging assay of HeLa/Fucci2 cells. Approximately 800 crude extracts of marine invertebrates collected between 1997 and 2013 were tested. 20 samples potently induced cell cycle arrest at S/G2 phase. The crude extracts of unidentified marine sponges S01-162 and S09-1060-15 induced inhibitory activity of mitosis. Bioactivity-guided fractionation of the marine sponge S01-162 afforded a potent cell cycle arrest inducing compound. The bioactive compound was identified as

meridine, an antifungal pyridoacridine compound, by comparing the NMR spectroscopic data with those in the literature (Figure 4-4A).[34] Another marine sponge S09-1060-15 also contained meridine and its congeners. HeLa/Fucci2 cells treated with meridine were at S/G2phase within 12 hours and entered endorepliction cycle (Figure 4-4B). This phenotypical change was similar to that treated with antitumor agents, doxorubicin and etoposide (Figure 4-4A), whose modes of action are DNA intercalation and inhibition of DNA topoisomerase II, respectively.[35] The DNA-directed activity and topoisomerase II inhibitory activity of pyridoacridines were reported. Therefore, it is well expected that meridine induces cell cycle arrest at S/G2 phase.[36]

4.1.3. Conclusion

Fluorescent time-lapse imaging of HeLa/Fucci2 cells enabled the identification of the inhibitor of cell cycle progression, as well as bioactive compounds that change the morphology of the cells. This cell-based assay gives much more information on the bioactivity than the conventional cell viability assays. Therefore, this assay will be an efficient method that detects metabolites affecting one or more points in the cell cycle progression.

A

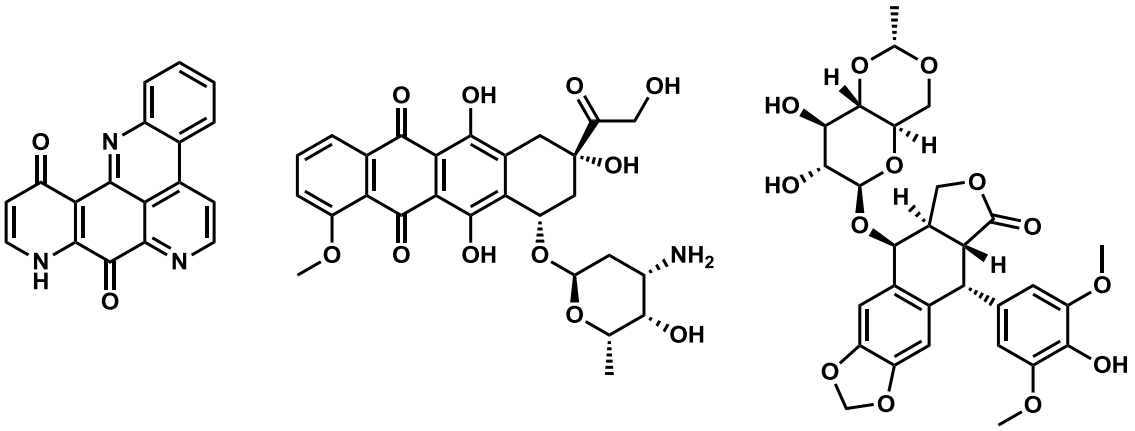

Meridine Doxorubicin Etoposide

B

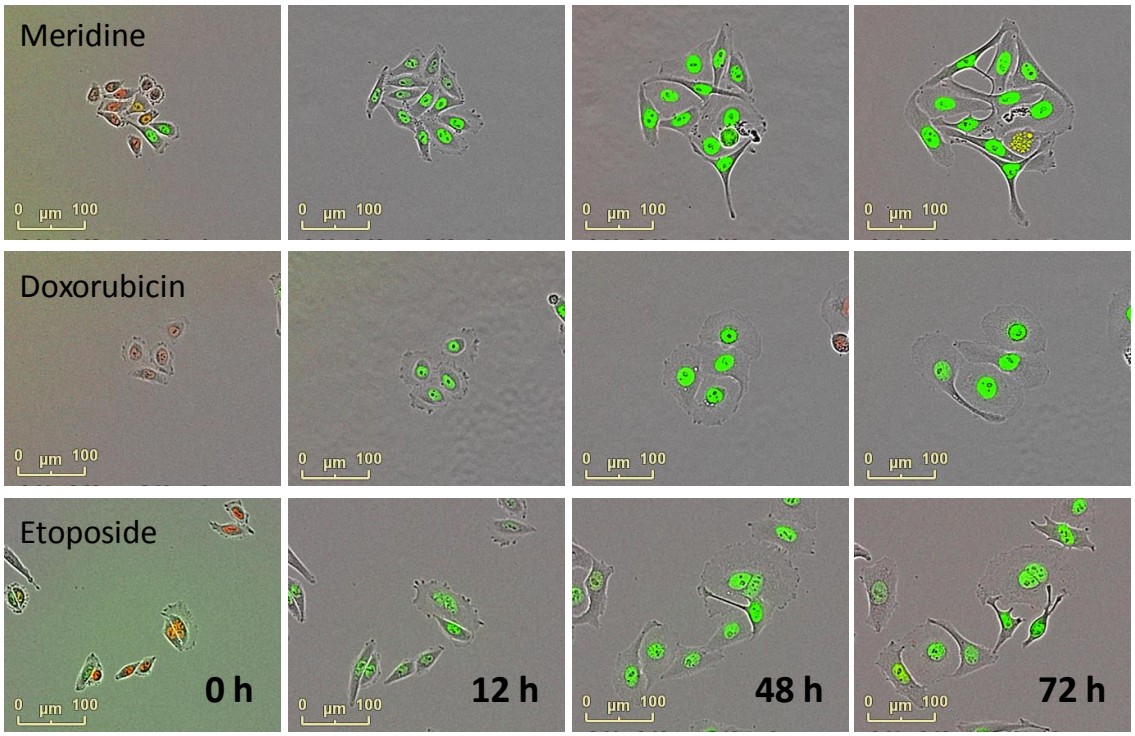

Figure 4-4. Investigation of mitosis inhibitor from marine sponges. (A) Chemical structures of meridine, doxorubicin, and etoposide. (B) Fluorescent time-lapse images of HeLa/Fucci2 cells treated with 2 μg/mL of meridine, 0.7 ng/mL of doxorubicin, and 2 μg/mL of etoposide.

4.1.4. Experimental section

4.1.4.1. General Experimental Procedures.

NMR spectra were recorded on a JEOL alpha 600 NMR spectrometer. ESI mass spectra were measured on a Bruker AmaZon SL. Time-lapse imaging of cells was conducted on the Essen bioscience IncuCyte Zoom.

4.1.4.2. Cell Culture and time-lapse imaging assay.

HeLa/Fucci2 cells were purchased from RIKEN Bio Resource Center CELL BANK and grown in FluoroBrite DMEM media (life technologies) supplemented with 10 % fetal bovine serum, 4 mM L-glutamine, 100 units/mL penicillin and 0.1 mg/mL streptomycin. Cells were seeded into 96 multi well plates (1.0×10^5 cells in 200 μLof medium). After overnight preincubation, cells were treated with 2 μL of MeOH solution of tested sample and incubated for 3 days. Fluorescent microscopic images were taken every two hours.

4.1.4.3. Extraction and Isolation of meridine.

The frozen marine sponge (120 g) was extracted with EtOH and mixture of MeOH /$CHCl_3$ (1:1). The crude extract was concentrated and partitioned between H_2O and

$CHCl_3$. The organic layer was further partitioned between 90 % MeOH and n-hexane. The 90 % MeOH layer was concentrated and fractionated by ODS column chromatography eluting with 70 % MeOH, 90 % MeOH, MeOH, and mixture of $CHCl_3$/MeOH/H_2O (14:6:1). 70 % MeOH fraction was concentrated and purified by ODS HPLC (COSMOSIL AR-II; 10 x 250 mm) with linear gradient from 20 % MeCN to 50 % MeCN to afford meridine (0.9 mg).

4.2. Isolation and structure elucidation of novel terpene quinones as cell cycle arrest inducers.

4.2.1. Introduction

Mitosis and cytokinesis are the primordial cellular mechanisms to distribute the identical genome to two daughter cells. The cell cycle consists of four stages, G1, S, G2 and M phases, and their progression was elaborately regulated by the intricate checkpoint systems governed by Cdks (cyclin-dependent kinases), p53, and ATM.[37] However, cancer cells lacks these checkpoint functionalities and undergo unrestricted cell proliferation. Numbers of clinically used antitumor drugs directly inhibit the cell cycle progression of cancer cells by disturbing spindle assembly, DNA replication, and cytokinesis.[38] Therefore, investigation of marine natural products which induce cell cycle arrest may lead to the discovery of leads compounds for developing new antitumor drugs. Fucci (Fluorescent Ubiquitination-based Cell Cycle Indicator) enables the fluorescent visualization of cell cycle progression in living cells.[3,4] In this study, we investigated the marine natural products that induce cell cycle arrest by using the time-lapse assay of HeLa/Fucci2 cells.

In the course of searching for marine sponge metabolites that inhibit cell cycle

progression against HeLa/Fucci2 cells, the crude extract of an unidentified marine sponge S09-1061-2 induced mitotic arrest. Bioassay-guided fractionation of the extract afforded two novel terpene quinones termed metachromins X and Y (**4-1**, **4-2**) together with the known metachromins C (**4-3**), J (**4-4**) and T (**4-5**).[39-41] Further investigation of bioactive compounds that inhibit mitosis from other sponges resulted in the isolation of another terpene quinone analogue 5-*epi*-isospongiaquinone (**4-6**) from an unidentified sponge S13-013. Evaluation of the biological activities of these compounds revealed that all of them exhibited moderate cytotoxicity against HeLa/Fucci2 cells, and metachromin X (**4-1**), metachromin C (**4-3**), and 5-*epi*-isospongiaquinone (**4-6**) induced mitotic arrest.

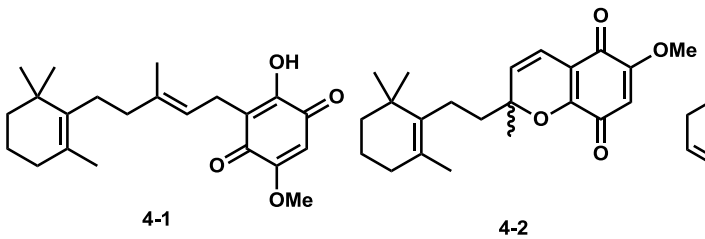

4-1

4-2

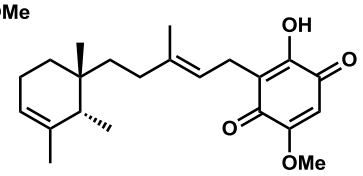

4-3

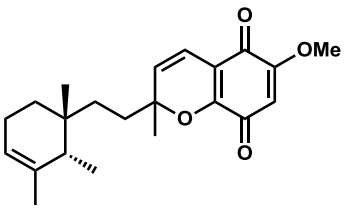

4-4

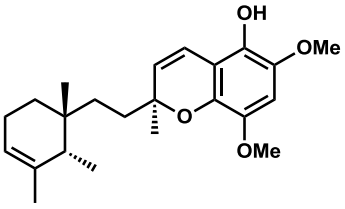

4-5

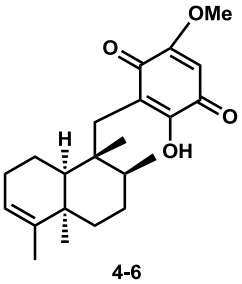

4-6

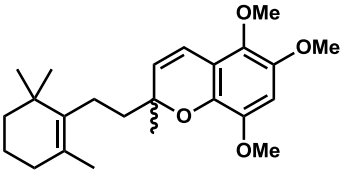

4-7

4.2.2. Results and Discussion

The MeOH extract of the marine sponge S09-1061-02 was partitioned between $CHCl_3$ and H_2O. The organic layer was concentrated and partitioned between 90% MeOH and *n*-hexane. The 90% MeOH fraction was subjected to ODS flash column chromatography, and the bioactive fraction was purified by RP-HPLC to afford compounds **4-1** and **4-2** together with known terpene quinones, metachromins C (**4-3**), J (**4-4**), and T (**4-5**).[39-41]

The molecular formula of **4-1** was determined to be $C_{22}H_{30}O_4$ by HRESIMS [*m/z* 381.2051, $(M+Na)^+$, Δ0.9 mmu]. Interpretation of the ^1H NMR spectrum in conjunction with the HSQC spectrum revealed the presence of two aliphatic methyls, two vinylic methyls, one methoxy group, six methylenes, two olefinic protons, and one hydroxyl proton. ^{13}C NMR spectrum showed two quinone signals at δ181.1 and 182.6, two oxygenated aromatic signals at δ150.8 and 160.6, and four olefinic carbon signals between δ 126.4-138.1. The presence of trisubstituted1,4-benzoquinone moiety was confirmed by the HMBC correlations from H19 (δ 5.82) to C17 (δ 150.8), C20 (δ 160.6), and C21 (δ 181.1), from phenolic proton (δ 7.22) to C17, and C18 (δ 182.6), and from methoxy protons (δ 3.84) to C20 (Figure 4-5). Three spin systems, H2-H4, H7-H8, and H10-H11, inferred by COSY correlations were connected with each other based on

the HMBC correlations, and the monocyclic sesquiterpene moiety was assigned. HMBC correlations from H11 to C16 (δ 138.1) and C21 (δ 181.5) established the linkage between sesquiterpene moiety and the benzoquinone ring system via C11-C16 bond. The *E* geometry of the double bond at C9 was determined by the NOESY correlation between H8 and H10 (Figure 4-5).

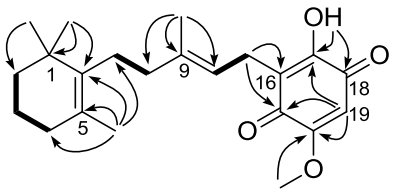

Figure 4-5. COSY (bold lines) and key HMBC correlations (arrows) in **4-1**.

Compound **2** had a molecular formula of $C_{20}H_{28}O_4$ as assigned by HRESIMS. The ^{1}H NMR, HSQC, COSY, and HMBC spectra of **4-2** confirmed that **4-1** and **4-2** shared the common cyclohexene ring system. The mutually coupled *Z*-olefin protons of H10 and H11 at δ 5.53 and 6.48 ($^3J_{HH}$= 10.3 Hz) were connected to the benzoquinone ring via the C11-C16 bond, which was inferred from the HMBC correlations between H10 and C16 and between H11 and both C17 and C21. Furthermore, HMBC correlations from the olefinic protons to a quaternary carbon C9 (δ 83.4) revealed the pyrane fused to the benzoquinone via an ether bond between C9 and C21. A singlet

methyl proton showed HMBC correlations to C8 and C9, permitting us to complete the assignment of the planer structure of compound **4-2** (Figure 4-6).

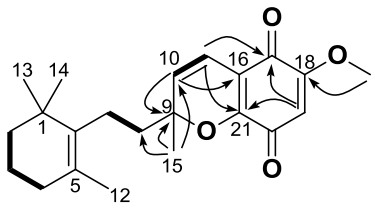

Figure 4-6. COSY (bold lines) and key HMBC correlations (arrows) in **4-2**.

Table 4-2. ^{1}H NMR and ^{13}C NMR chemical shifts of **4-1** and **4-2**

	metachromin X (**1**)		metachromin Y (**2**)	
position	δ_H	δ_C	δ_H	δ_C
1		34.9		127.7
2	1.38 (m)	39.8	1.85 (t, 6.6)	32.7
3	1.53 (m)	19.5	1.51(m)	19.7*
4	1.87 (t, 6.9)	32.7	1.36 (m)	39.7
5		126.9		35.0
6		136.9		135.8
7	1.99 (m)	27.6	2.07	22.3
8	1.97 (m)	40.1	1.70 (m)	41.6
			1.86 (m)	
9		138.2		84.0
10	5.13 (t, 6.3)	118.7	5.53 (d, 10.3)	127.7
11	3.14 (d, 7.6)	21.7	6.48 (d, 10.3)	115.2
12	0.95 (s)	28.6	1.52 (s)	19.4*
13	0.95 (s)	28.6	0.93 (s)	28.56
14	1.55 (s)	19.8	0.90 (s)	28.6
15	1.77 (s)	16.2	1.47 (s)	27.1
16		138.2		113.5
17		151.2		178.5
18		182.9		158.8
19	5.82 (s)	102.2	5.78 (s)	105.3
20		161		181.3
21		181.5		151.9
OMe	3.84 (s)	56.7	3.79 (s)	56.4

^{1}H and ^{13}C NMR at 600 MHz and 150 MHz in $CDCl_3$, *Assignments may be interchanged

In order to determine the enantiomeric purity of compound **4-2**, chiral HPLC analysis was conducted.[42] Prior to the analysis of **4-2**, a racemic mixture of trimethoxychromenol **4-7** was prepared from **4-1** according to the Kobayashi's method.[43] HPLC separation (Chiral OJ-RH) of the racemic mixture of **4-7** afforded two peaks for each enantiomer (Figure 4-7). Generally, in the CD spectrum of chromenols, strong Cotton effect is observed around the 260-270 nm region due to the skewed

styrene chromophore. The right-handed helix shows strong negative Cotton effect and the left hand helix positive cotton effect.[44] In compound **4-7**, the bulky side chain generates steric hindrance to the chromenol ring and prefers the pseudoequatrial orientation.[45] Therefore, the absolute configuration of the chiral center at C9 in **4-7** could be deduced from the CD spectral data (Figure 4-7). Then, **4-2** was converted to **4-7**, and subjected to the chiral HPLC, which gave two pronounced peaks, suggesting that **4-2** was a racemic mixture (Figure 4-8). By altering the stationary phase to chiral OJ, **4-2** could be directly separated into enantiomers, confirming that **4-2** was a racemic mixture.

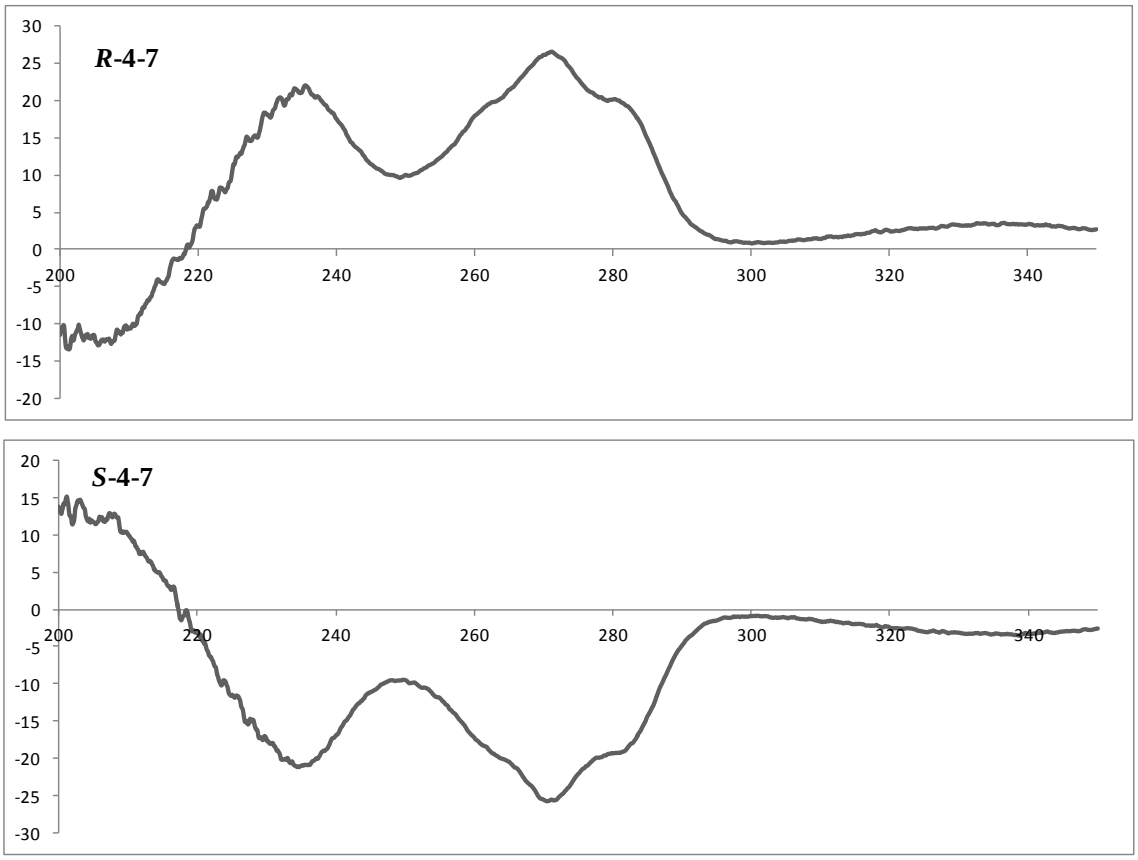

Figure 4-7. CD spectra of *R*-**4-7** and *S*-**4-7**.

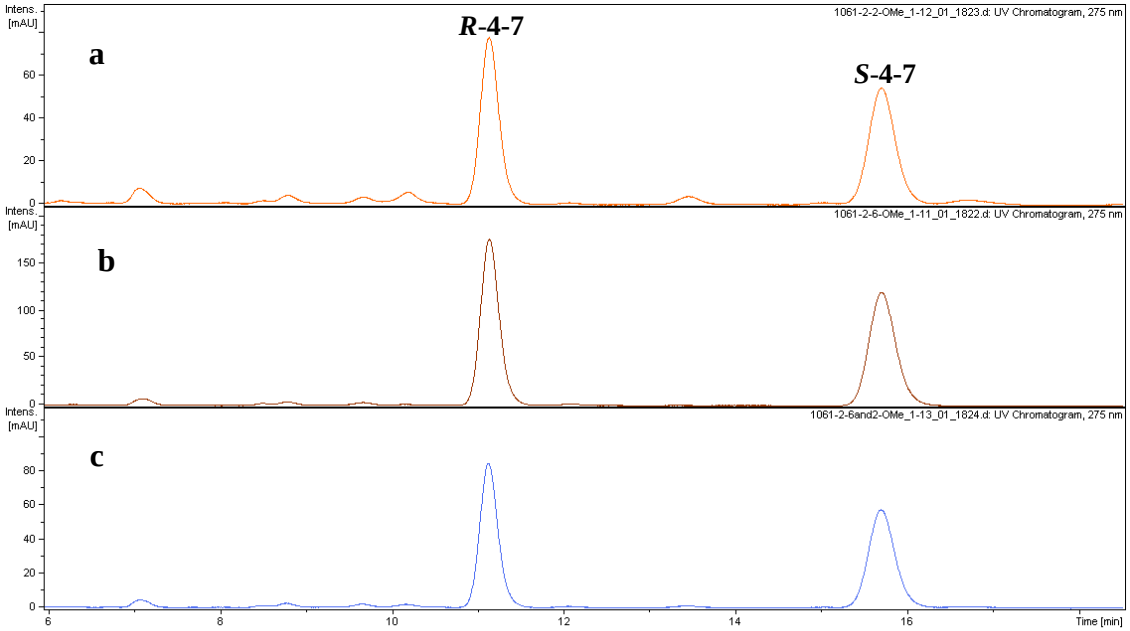

Figure 4-8. Chiral HPLC chromatograms of compound **4-7** prepared from (a) **4-1**, (b) **4-2**, and (c) coinjection of them.

Sesquiterpene quinones are characteristic matabolites of marine sponges. In particular, sesquiterpene quinones containing a decalin ring were intensively studied as to their structural diversity and biological activities.[46] A further investigation of the extract of another marine sponge led to the isolation of 5-*epi*-isospongiaquinone (**4-6**) from an unidentified marine sponge S13-013. **4-6** was first reported as the antibiotic compound isolated from an Australian sponge *Spongiabispida*, and consisted of the clerodane-type decalin ring.[47] With metachromins (**4-1** - **4-5**) and 5-*epi*-isospongiaquinone (**4-6**) in hand, their biological activity against HeLa/Fucci2 cells was evaluated. Compounds **4-1** - **4-6** exhibited moderate antiproliferative activity with IC_{50} values of 10, 21, 19, 12, 18, 6.3 μg/mL, respectively. Interestingly, enantiomers of **4-2** exhibited equipotent biological activity. Notably, time-lapse imaging of HeLa/Fucci2 cells revealed that compound **4-1**, **4-3**, and **4-6** induced cell cycle arrest at S and G2 phase, whereas other compounds did not induce mitotic arrest (Figure 4-9).

Terpene quinones were reported to exhibit a broad spectrum of biological activities, such as antitumor, antiviral, and anti-inflammatory. Their diverse biological activities were attributed to two general mechanism[46] 1) redox cycling of quinone causes the production of reactive oxygen species which damage mitochondria and biomolecules; 2) electron arylation of cellular nucleophiles which induce disorder of

cellular function. It is conceivable that reactive oxygen species produced through redox cycling of terpene quinones damaged DNA and induced cell cycle arrest, and/or terpene quinones broadly arylated cellular molecules regulating cell cycle progression, and induced cell cycle arrest. The results of this study implicate that the 2-hydroxy-5-methoxy-1,4-benzoquinone moiety is required for the mitotic arrest.

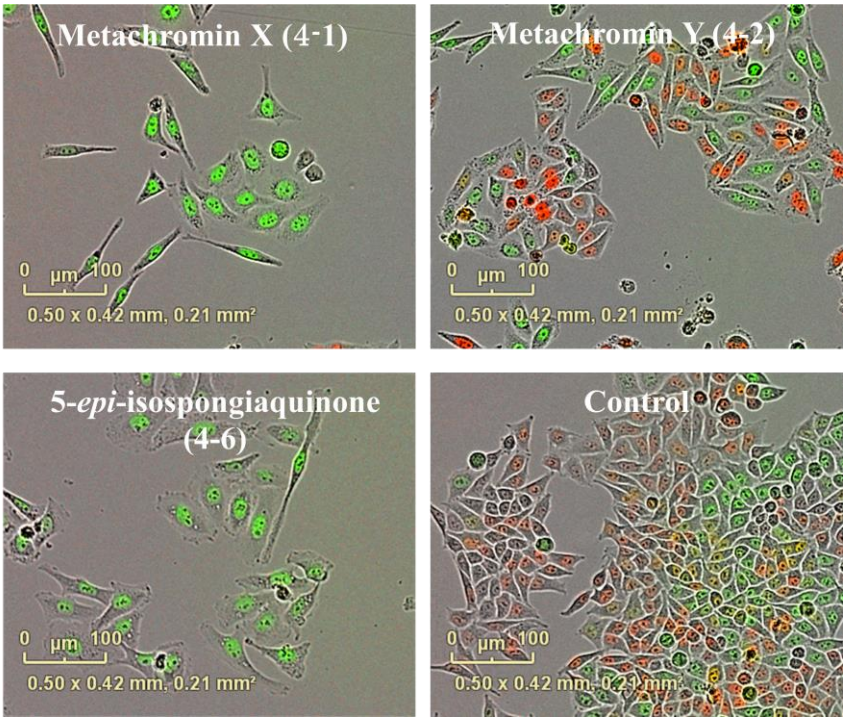

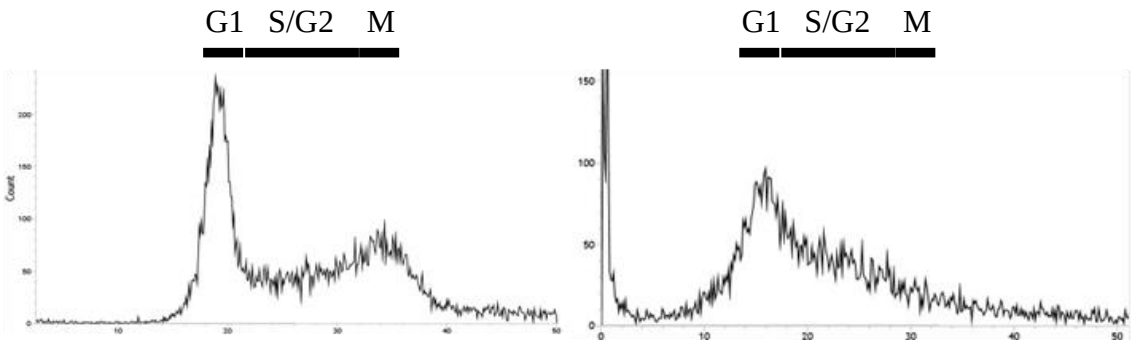

Control 20 μg/mL of **1**

Figure 4-9. Evaluation of biological activities of terpene quinones. (A) Fluorescent microscopy images of HeLa/Fucci2 cells treated with 20 μg/mL of **4-1**, **4-2**, and **4-6**, and MeOH as control. Red and green fluorescence represents cells at G1 and S/G2/M phase, respectively. Pictures were taken after 68 h incubation. (B) Flow cytometry of HeLa/Fucci2 cells. Distribution of the HeLa/Fucci2 cells in G1 phase was decreased by the treatment of **4-1**.

4.2.3. Conclusion

Herein, I report the time-lapse imaging assay using HeLa/Fucci2 cells to investigate bioactive marine natural products that induce mitotic arrest. As a result, two new metabolites, metachromins X (**4-1**) and Y (**4-2**), together with the known metachromins C (**4-3**), J (**4-4**), and T (**4-5**) were isolated from a marine sponge S09-1061-02. Additionally, another terpene quinine, 5-*epi*-isospongiaquinone (**6**) was isolated from a marine sponge S13-013. Compounds **4-1**, **4-3**, and **4-6** induced mitotic arrest of HeLa/Fucci2 cells. The structure activity relationship of these terpene quinones revealed that the 2-hydroxy-5-methoxy-1,4-benzoquinone ring was responsible for the inhibition of the cell cycle progression. The current results will encourage further studies on the activity and mechanism of the terpene quinones, leading to the fragment based drug design. Time-lapse imaging of HeLa/Fucci2 cells is a promising experimental means to identify natural products exhibiting biological activity concerned with cell cycle progression, offering opportunities for the development of new natural product derived antitumor agents.

4.2.4. Experimental Section

4.2.4.1. General Experimental Procedures.

UV spectra were measured on a Shimadzu Biospec 1600. NMR spectra were recorded on a JEOL alpha 600 NMR spectrometer. Chemical shifts were referenced to solvent peaks: δ_H7.24 and δ_c 77.0 for $CDCl_3$. ESI mass spectra were measured on a JEOL JMS-T100LC. HPLC was carried out on the Shimadzu LC 20AT with a SCL-10Avp controller and a SPD-10Avp detector. Time-lapse imaging of cells was conducted on the Essen bioscience IncuCyteZoom. DNA content was analyzed by flow cytometer BD FACSJAZZ.

4.2.4.2. Animal Material.

The sponge S09-1061-02 was collected at Miyako sea-knoll, southwestern Japan, at a depth of 415 m, during a cruise of R/V Natsushima, by using the Remotely Operated Vehicle ‘Hyper-Dolphin’ in October 2009. The sponge S13-013 was collected at the sea near Amami-Ohshima during the cruise of Toyoshio-maru in 2013.

4.2.4.3. Extraction and Isolation of metachromins.

The frozen marine sponge (80 g, wet weight) was homogenized and extracted with

EtOH (250 mL x 2) and mixture of MeOH and $CHCl_3$ (1:1, 300 mL). The combined extracts were evaporated *in vacuo* and partitioned between H_2O and $CHCl_3$. The organic layer was evaporated and partitioned between 90% MeOH and *n*-hexane. The aqueous MeOH layer was concentrated and subjected to the ODS column chromatography eluting with 50% MeOH, 70% MeOH, 90% MeOH, and $CHCl_3$/MeOH/H_2O (14:6:1). The 90% MeOH eluate was concentrated and purified by RP-HPLC (Cosmosil MS-II; 20 x 250 mm) with 80% MeCN containing 0.5% AcOH to afford **4-2** (8.5 mg), **4-4**, **4-5** and mixture of **4-1** and **4-3** (500 mg). One part of the mixture was further purified with RP-HPLC (Cosmosil MS-II; 20 mm x 250 mm) with 80% MeCN containing 0.5% AcOH to afford **4-1** and **4-3**.

4.2.4.3.1. Metachromin X (**4-1**): dark orange solid; UV (MeOH) λ_{max}(log ε) 210 (16 000), 287 (16 000), 424 (490); ^{1}H NMR and ^{13}C NMR data ($CDCl_3$), see Table 1; HRESIMS *m*/*z*[M+Na]$^+$381.2051 (calcd for $C_{22}H_{30}O_4Na^+$, 381.2042)

4.2.4.3.2. Metachromin Y (**4-2**): red solid; UV (MeOH) λ_{max}(log ε) 214 (9 900), 258 (6 000), 307 (7 100), 485 (420); ^{1}H NMR and ^{13}C NMR data ($CDCl_3$), see Table 1; HRESIMS *m*/*z*[M+Na]$^+$ 379.1869 (calcd for $C_{22}H_{28}O_4Na^+$, 379.1885). The accurate optical rotation could not be measured because the UV absorption of **2** interfered with the D line of a Na light.

4.2.4.4. Extraction and Isolation of 5-*epi*-isospongiaquinone.

The frozen marine sponge S13-013 (100 g, wet weight) was extracted with EtOH (300 m x 2) and mixture of MeOH/$CHCl_3$ (1:1, 300 mL). The combined extracts were combined and concentrated *in vacuo*, then partitioned between H_2O and $CHCl_3$. The organic layer was further partitioned between 90% MeOH and *n*-hexane. The 90 % layer was concentrated and subjected to ODS column chromatography eluting with 50% MeOH, 70% MeOH, 90% MeOH, and $CHCl_3$/MeOH/H_2O (14:6:1). The MeOH fraction was purified by ODS HPLC (Cosmosil AR-II; 20 mm x 250 mm) eluting with 78% MeCN to afford 35 mg of 5-*epi*-isospongiaquinone (**4-6**).

4.2.4.5. Preparation of 4-7 from 4-1.

To a solution of compound **4-1** (12.5 mg) in MeCN (3.5 mL) was added K_2CO_3 (240 mg) and MeI (100 μL). The reaction mixture was refluxed for 2 h. The reaction mixture was filtrated and dried *in vacuo*. Si gel column chromatography (*n*-hexane/EtOAc = 3:1) afforded methyl ether of **4-1** (12.5 mg). The methylated compound (10 mg) was dissolved in pyridine (3 mL) and heated at 110 ^oC overnight. The reaction mixture was concentrated *in vacuo*. To a solution of the resultant oil (10 mg) in MeCN (0.5 mL) was

added K_2CO_3 (100 mg) and MeI (60 μL) and refluxed for 3 h, then filtered and dried *in vacuo*. RP-HPLC purification afforded the racemic mixture of **7** (2.3 mg); ^{1}H NMR ($CDCl_3$); δ 6.64 (d, 10.0 Hz, 1H), 6.43 (s, 1H), 5.67 (d, 10.0 Hz, 1H), 3.82 (s, 3H), 3.80 (s,3H), 3.74 (s, 3H), 2.11 (t, 8.8 Hz, 2H), 1.83 (t, 6.2, 2H), 1.74-1.70 (m, 3H), 1.51-1.49 (m, 3H), 1.50 (s, 3H), 1.44 (s, 3H), 1.35 (m, 2H), 0.94 (s, 3H), 0.88 (s, 3H); LRESIMS *m/z* 387.6 $(M+H)^+$.

4.2.4.6. Preparation of 4-7 from 4-2.

To a solution of **4-2** (1.2 mg) in EtOAc (50 μL), H_2O (0.5 mL), and Et_2O (0.5 mL) was added $Na_2S_2O_4$ (20 mg). The reaction mixture was stirred vigorously for 20 min at room temperature. The reaction mixture was extracted with Et_2O (1 mL x 2) and dried over Na_2SO_4 and N_2 gas flushing. The resultant solid was then dissolved in DMSO (0.8 mL), and added K_2CO_3 (50 mg) and MeI (50 μL). The reaction mixture was stirred for 1h under the N_2 gas. The reaction mixture was filtered and dried *in vacuo*, and purified by RP-HPLC to afford compound **4-7** (0.9 mg).^{1}H NMR data and LRESIMS were superimposable on those of **4-7** prepared from **4-1**.

4.2.4.7. Cell Culture and MTT assay

HeLa/Fucci2 cells were cultured in DMEM (Wako) supplemented with 10% fetal bovine serum, and 100 units/mL penicillin and 0.1 mg/mL streptomycin at 37 ºC under an atmosphere of 5% CO_2. To each well of a 96-well microplate containing 200 μL of tumor cell suspension (1 x 10^4 cells/mL) was added a sample after overnight preincubation, and the plate was incubated for 72 h. After addition of 3-(4,5-dimethylthiazol-2-yl)-2,5-diphenyltetrazolium bromide (MTT) saline solution (1 mg/mL, 50 μL) to each well, the plate was incubated for 3 h. After the incubation, the supernatant was discarded and DMSO (150 μL) was added. The absorbance was measured to determine IC_{50} values.

4.2.4.8. Time-Lapse Imaging of HeLa/Fucci2 Cells

HeLa/Fucci2 cells were grown in FluoroBrite DMEM media (life technologies) supplemented with 10% fetal bovine serum, 4 mM L-glutamine, 100 units/mL penicillin and 0.1 mg/mL streptomycin. HeLa/Fucci2 cells were grown on six-well plates (100,000 cells in control groups and 300,000 cells in compound treated cells) and incubated for three days at 37 ºC with either 20 μg/mL of **4-1**, **4-2**, **4-6**, or 0.2% MeOH.

4.2.4.9. Cell cycle analysis of HeLa/Fucci2 cells by flow cytometer.

HeLa/Fucci2 cells were seeded in 6 well plate at concentrations of 10,000 cells/mL in control group and 30,000 cells/mL in **4-1** treated cells. After two days incubation with 0.2% of MeOH or 20 μg/mL of **4-1**, the cells were treated with 0.25% trypsin and collected. Cells were rinsed with PBS twice, and stained with hypotonic PI solution (50 μg/mL of PI, 0.1% of sodium citrate, 0.2% of NP-40, 0.25 mg/mL of RNase in distilled water). 20,000 cells were analyzed by flow cytometer at 585 nm.

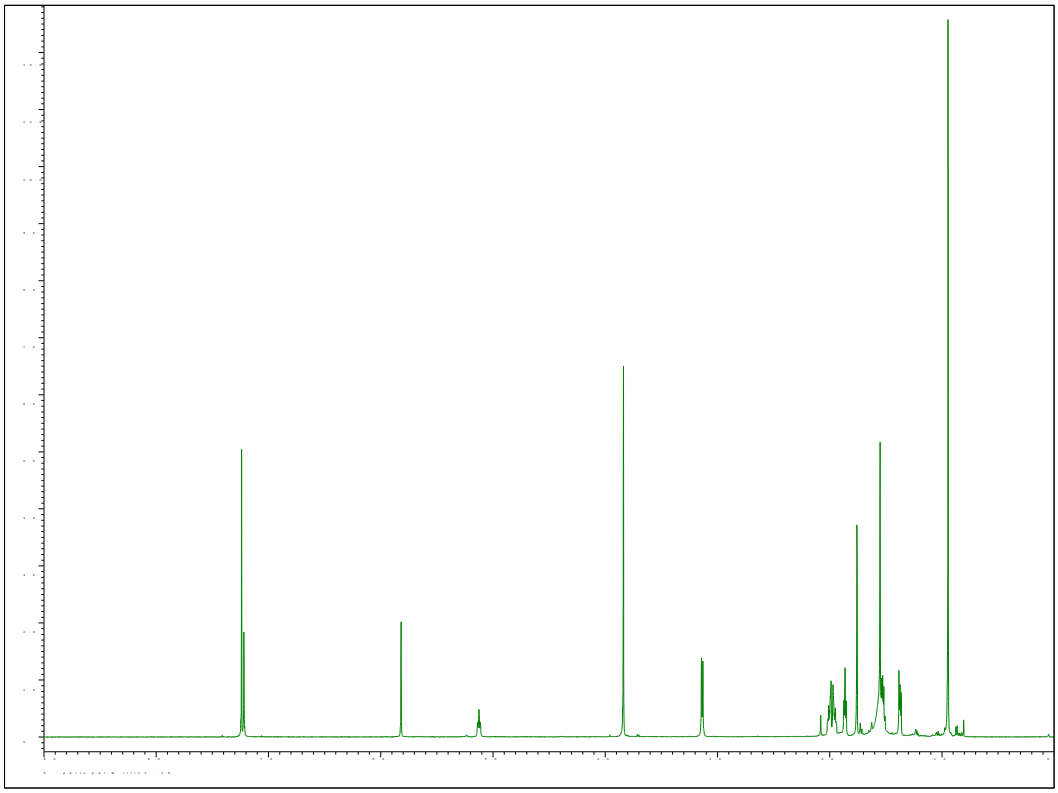

Figure S4-2-1. ^{1}H NMR spectrum of **4-1**

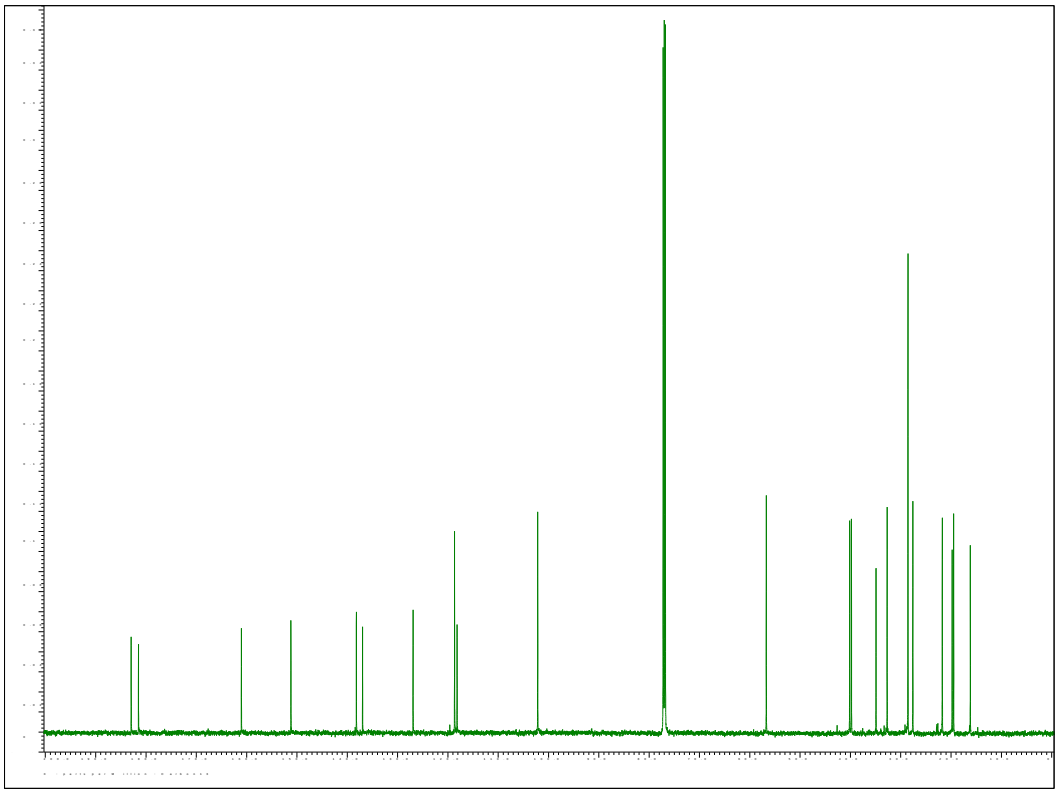

Figure S4-2-2. ^{13}C NMR spectrum of **4-1**

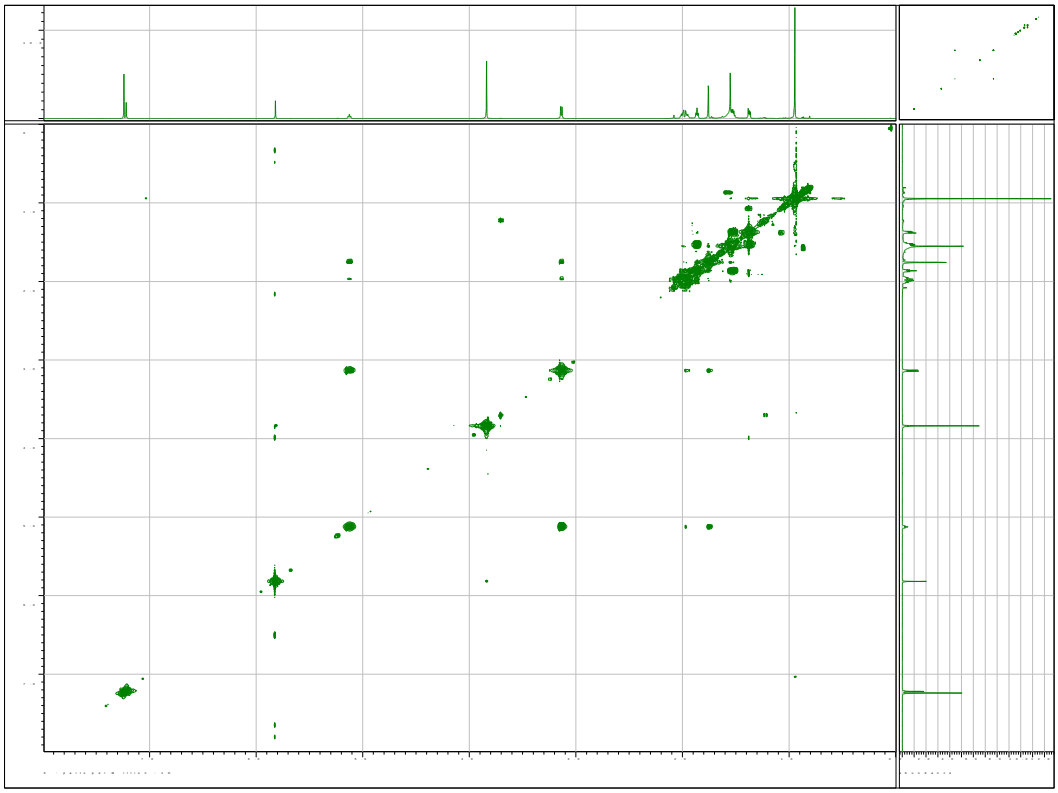

Figure S4-2-3. COSY spectrum of **4-1**

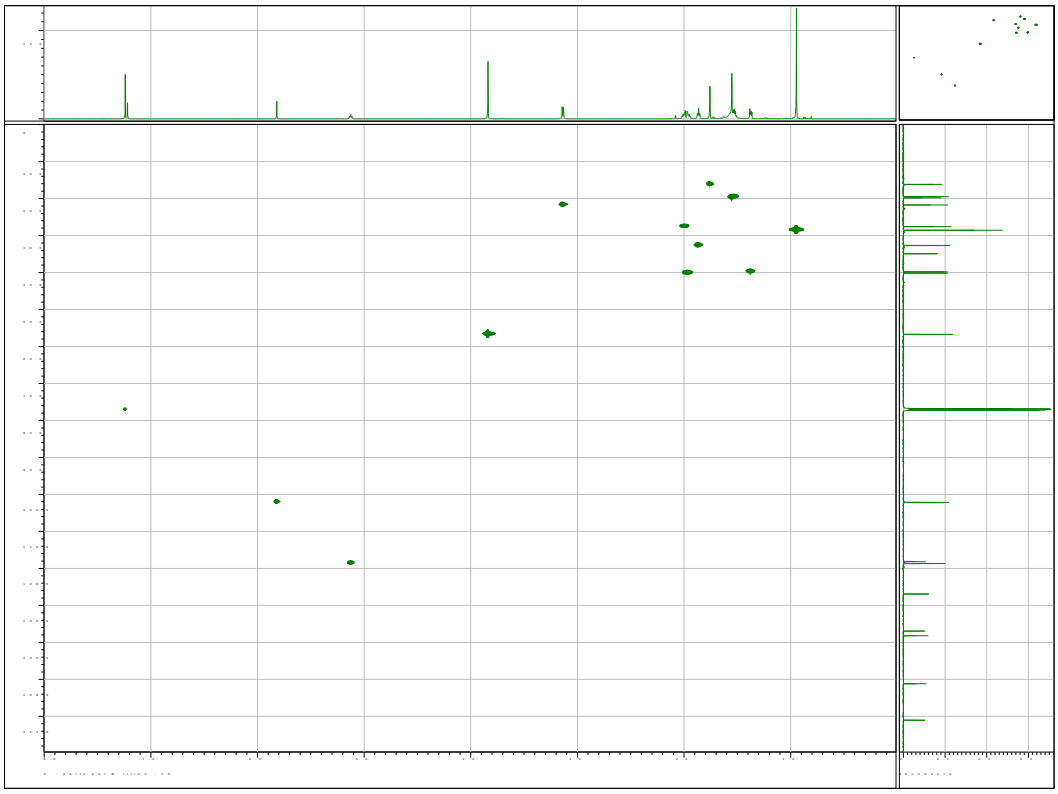

Figure S4-2-4. HSQC spectrum of **4-1**

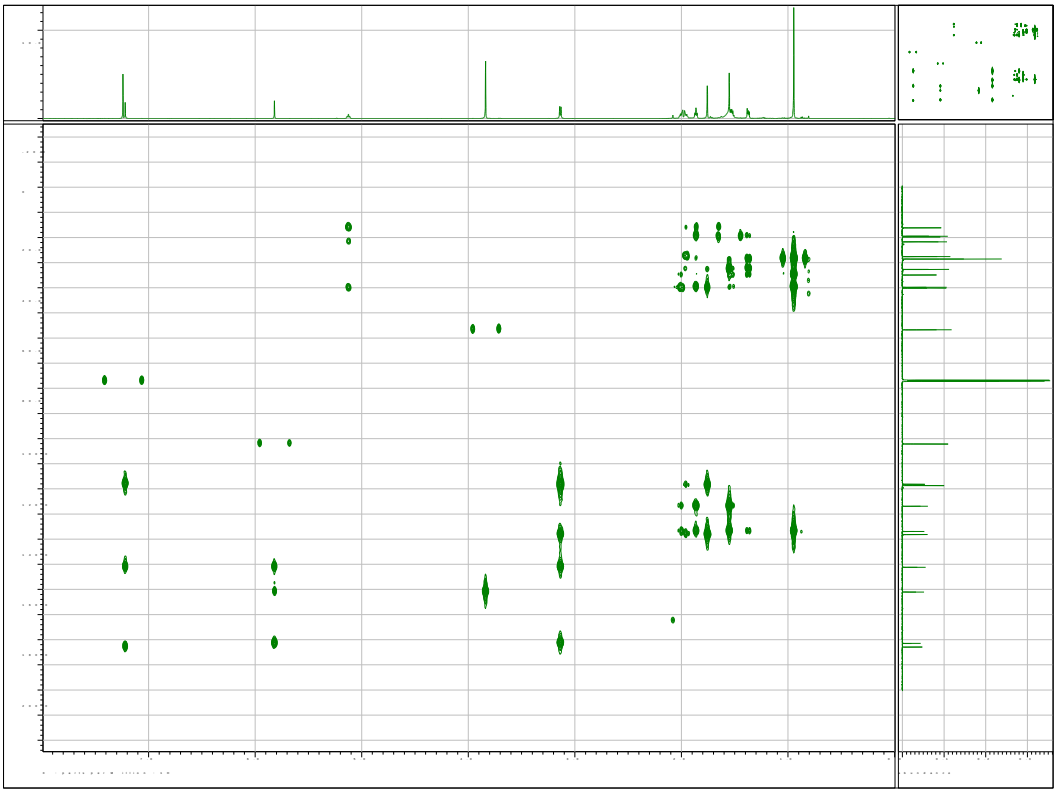

Figure S4-2-5. HMBC spectrum of **4-1**

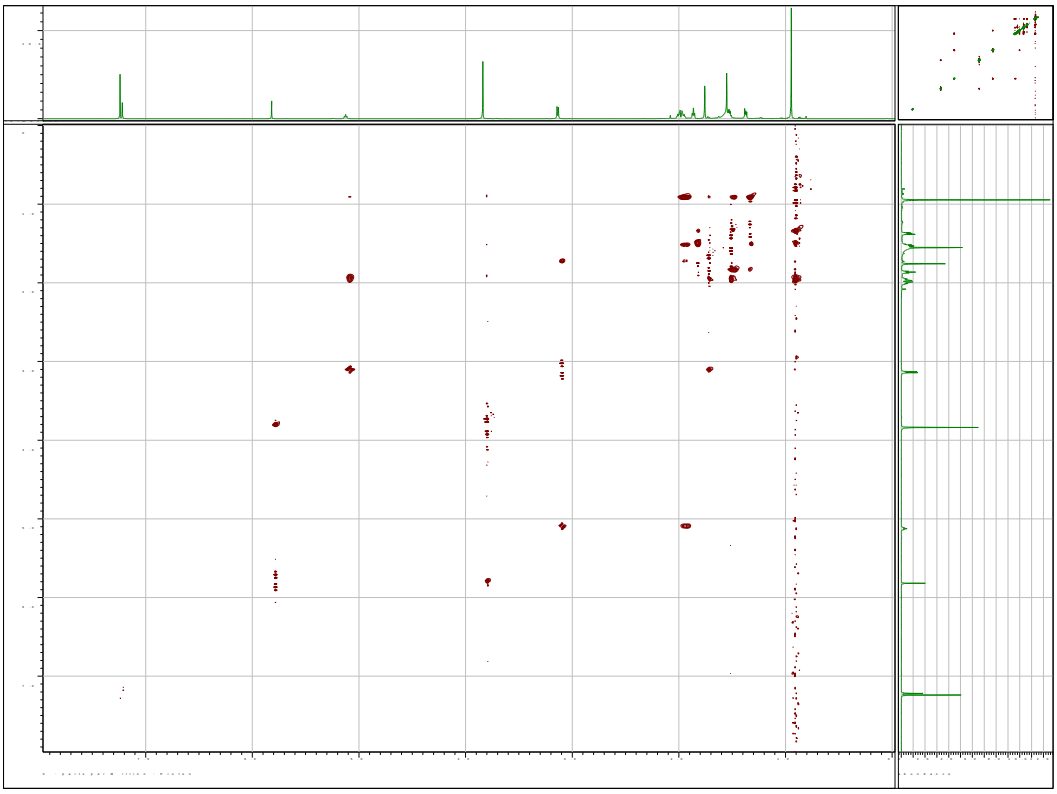

Figure S4-2-6. NOESY spectrum of **4-1**

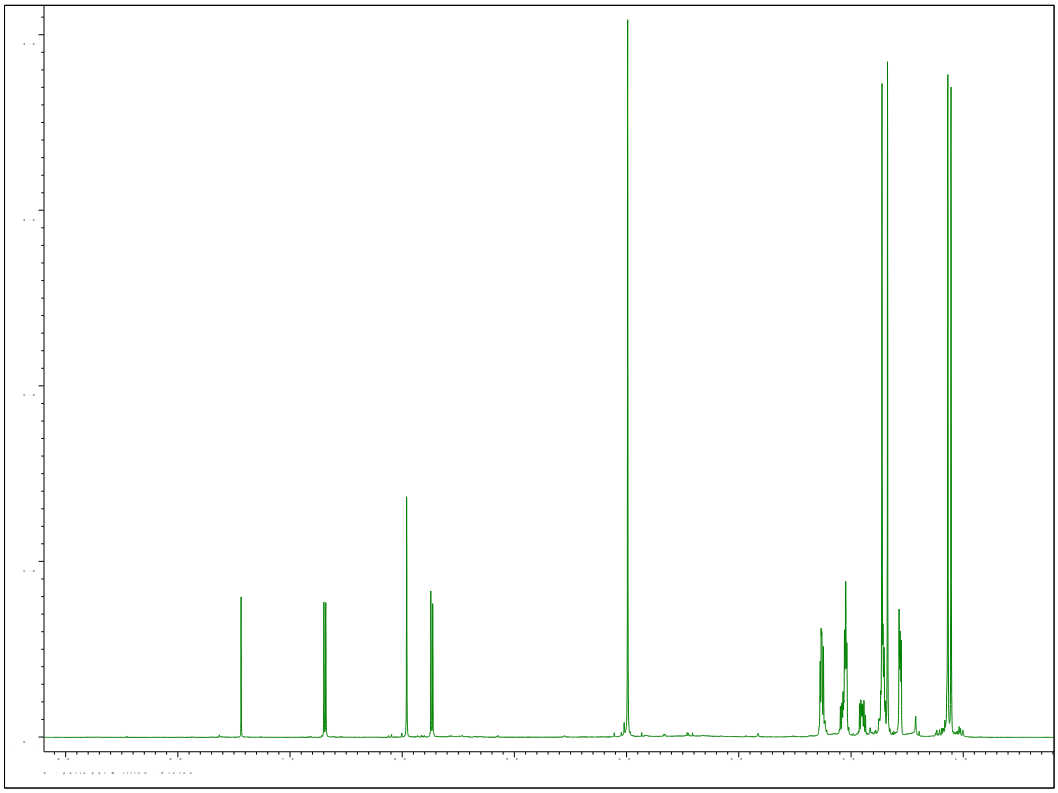

Figure S4-2-7. ^{1}H NMR spectrum of **4-2**

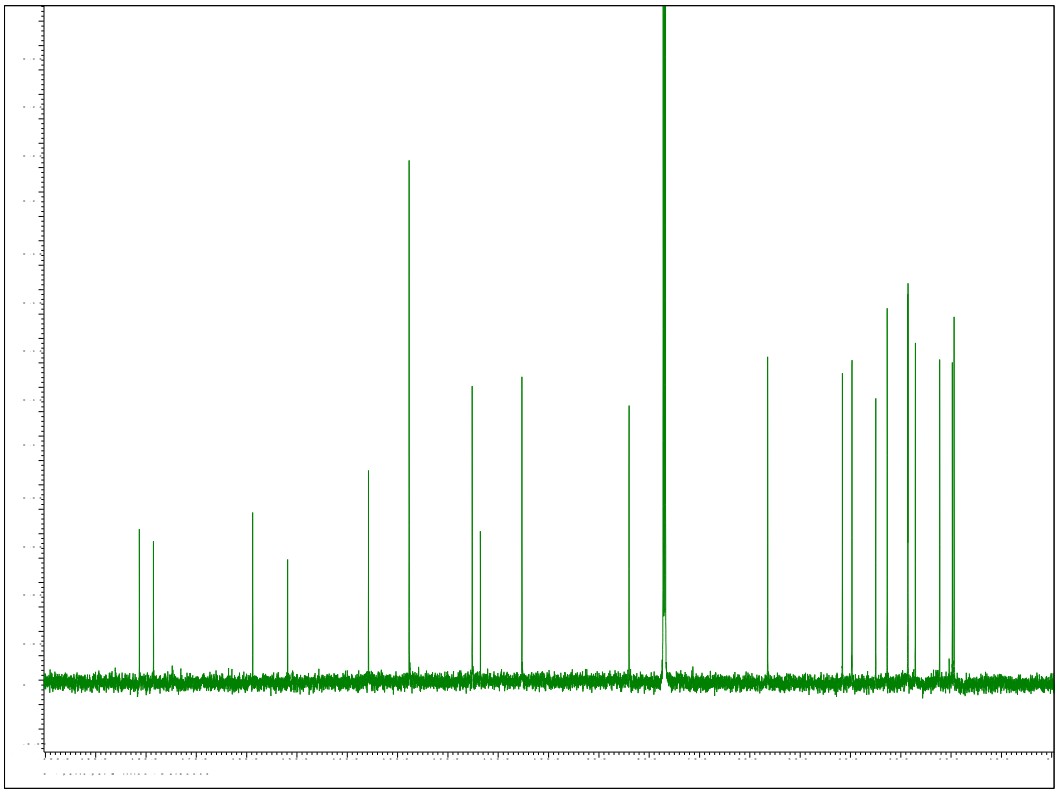

Figure S4-2-8. ^{13}C NMR spectrum of **4-2**

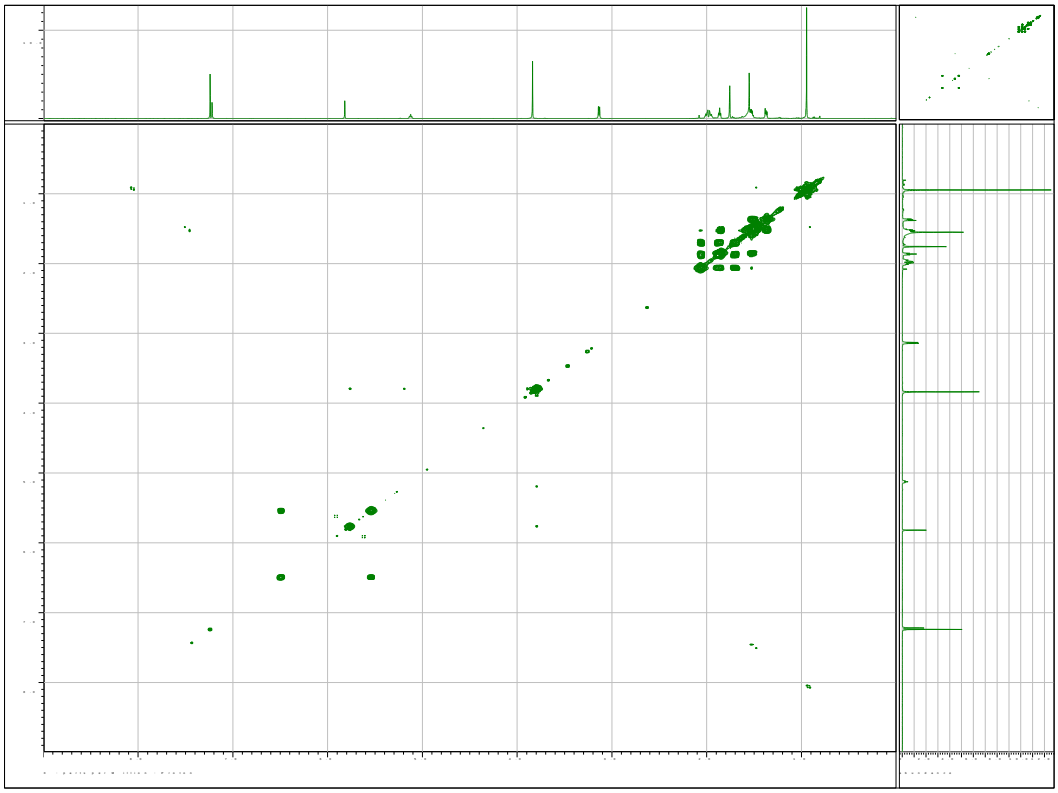

Figure S4-2-9. COSY spectrum of **4-2**

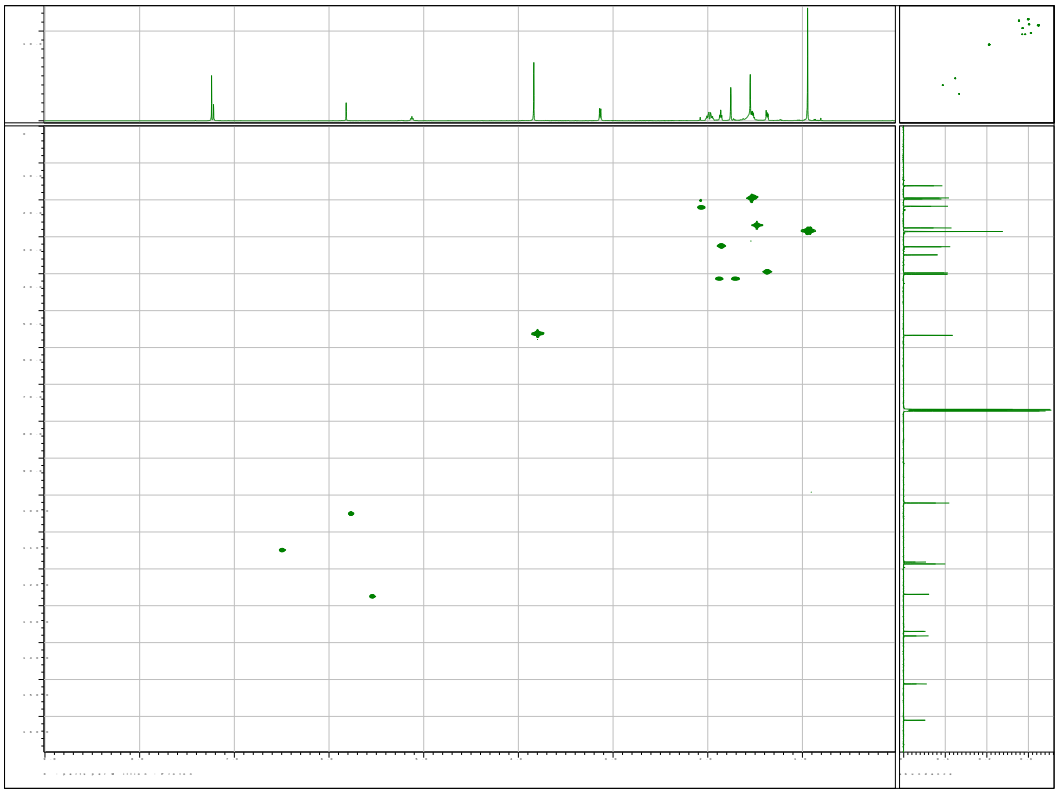

Figure S4-2-10. HSQC spectrum of **4-2**

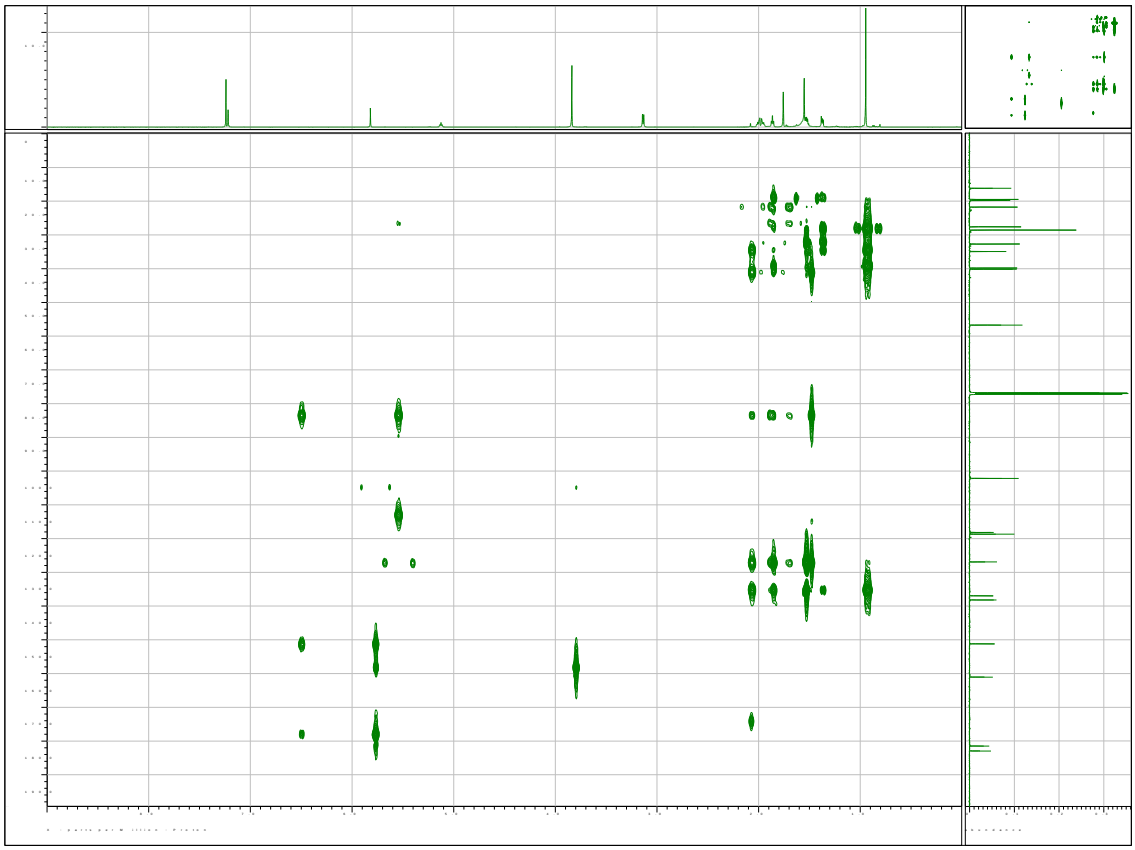

Figure S4-2-11. HMBC spectrum of **4-2**

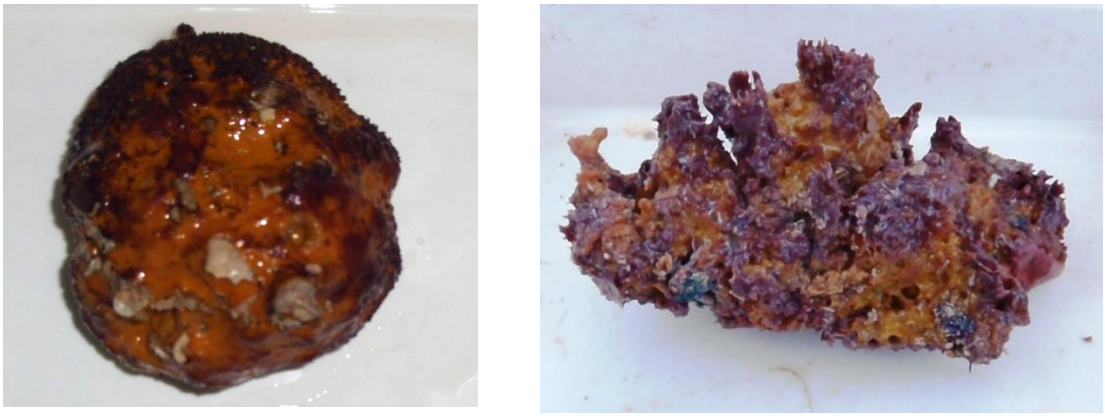

Figure S4-2-12. Photographs of unidentified marine sponges S09-1061-02 (left) and S13-013 (right).

Chapter 5. Conclusion

Marine organisms produce a vriety of secondary metabolites, and such marine natural products are important sources of the drug leads and research tools. Recent dramatic advances of scientific technologies are disclosing the molecular mechanisms, biosynthetic genes, and the true producers of bioactive marine natural products. Fundamental part of these translational researches is the discovery of bioactive compounds from the marine organisms.

In this study, we have investigated novel bioactive compounds from deep-sea marine sponges, and discovered several novel bioactive sponge metabolites by using cell-based assays.

We discovered two groups of acetylene compounds, (-)-durynes and miykosynes from the same marine sponge *Petrosia* sp. In combination of NMR spectroscopy and FAB-MS/MS measurements their chemical structures were determined. In particular, miyakosyne A was highlighted in the discussion over the determination of the absolute configuration at isolated chiral center.

Potent cytotoxic macrolide lactams, poecillastrins, were discovered from an unidentified marine sponge S09-1060-01. These molecules have complicated structures and a number of chiral centers. In spite of the limited amount of compounds, we partly assigned the relative configurations. Poecillastrins exhibited unique bioactivity and they are worthy to explore for their therapeutic potentials.

Fluorescent time-lapse imaging of HeLa/Fucci2 was applied for the evaluation of biological activities of marine natural products. This assay enabled us to select samples that induced cell cycle arrest and/or cellular morphological changes, resulting in the isolation of several active compounds. Metachromins are the first marine natural products identified through the time-lapse imaging assay of HeLa/Fucci2 cells. Structure activity relationship of these terpene quinones revealed that 2-hydroxy-5-methoxy-1,4-benzoquinone moiety is essential for inducing mitotic arrest.

By this study, we have confirmed that marine sponges are rich sources of bioactive metabolites. Investigation of novel marine natural products through cell-based assays will lead to the discovery of therapeutically promising metabolites.

References and Notes

Chapter 1.

1. a) Bergmann, W.; Feeney, R.J. *J. Am. Chem. Soc.***1950**, *72*, 2809–2810. b) Bergmann, W.; Freeney, R. J. *J. Org. Chem.* **1951**, *16*, 981–987.

2. Hu, G.P.; Yuan, J.; Sun, L.; She, Z.G.; Wu, J.H.; Lan, X.J.; Zhu, X.; Lin, Y.C.; Chen, S.P. *Mar. Drugs* **2011**, *9*, 514–525.

3. Mehbub, M. F.; Lei J.; Franco, C.; Zhang, W. *Mar. Drugs*, **2014**, *12*, 4539-4577.

4. Gerwick, W. H.; Fenner, A. M. *Microb. Ecol.* **2013**, *65*, 800-806.

5. a) Seger, C.; Sturm, S.; Stuppner, H. *Nat. Prod. Rep.* **2013**, *30*, 970-987. b) Molinski, T. F. *Natural Product Reports* **2010,** *27*, 321-329.

6. Rochfort, S. *J. Nat. Prod.***2005**, *68*, 1813-1820.

7. Guthals, A.:Watrous, J. D.;Dorrestein, P. C,;Bandeira, N. *Mol. Bio. Sys.* **2012**, *8*, 2535–2544.

8. Inokuma, Y.; Yoshioka, S.; Ariyoshi, J.; Arai, T.; Hitora, Y.; Takada, K.; Matsunaga, S.; Rissanen,K.; Fujita, M.*Nature* **2013**, *495*, 461-466.

9. Haefner, B. *Drug Discov. Today* **2003**, *8*, 536-544.

10. a) Milshteyn, A.; Schneider, J. S.; Brady, S. F. *Chem. Biol.* **2014**, *21*,1211-1223. b) Luo, Y.; Cobb, R. E.; Zhao, H. *Curr. Opin. Biotechnol.* **2014**, *30*, 230-237.

11. a) Li, J. W.-H.; Vederas, J. C. *Science*, **2009**, *325*, 161-165. b) Molinski, T. F.;Dalisay, D.S.; Lievens, S. L.; Saludes, J. P. *Nat. Rev. Drug Discov.* **2009**, *8*, 69-85.

12. a) Mayer, A. M. S.; Glaser, K. B.; Cuevas, C.; Jacobs, R. S.; Kem, W.; Little, R. D.; Mclntosh, J. M.; Newman, D. J.; Potts, B. C.; Shuster, D. E. *Trends in Pharmacol. Sci.* **2010**, *31*, 255-265. b) Nastrucci, C.; Cesario, A.; Russo, P. *Recent Pat. Anti-Canc.* **2012**, *7*,218-232.

13. a) Wright, A. E.; Forleo, D. A.; Gunawardana, G. P.; Koehn, F. E.; McConnell, O. J. *J. Org. Chem.* **1990**, *55*, 4508-4512. b) Rinehart, K. L.; Holt, T. G.; Fregeau, N. L.; Stroh, J. G.;Keifer, P. A.; Sun, F.; Li L. H.; Martin, D. G. *J. Org. Chem.* **1991**, *56*, 1676.

14. Hirata, Y.; Uemura, D. *Pure Appl. Chem.* **1986**, *58*, 701.

15. Pettit, G. R.; Kamano, Y.; Herald, C. L.; Fujii, Y.; Kizu, H.; Boyd,M. R.; Boettner, F. E.; Doubek, D. L.; Schmidt, J. M.; Chapuis J.-C., Michel C. *Tetrahedron* **1993**, *49*, 9151-9170.

16. Hamann, M. T.; Scheuer, P. J. *J. Am. Chem. Soc.* **1993,** *115*, 5825-5826.

17. a) Rinehart, K. L.; Gloer, J. B.; Cook, J. C.; Mizsak, S. A.; Scahill, T. A. *J. Am. Chem. Soc.* **1981,** *103*, 1857-1859. b) Urdiales, J. L.; Morata, P.; DeCastro, I. N.; SanchezJimenez, F. *Cancer Lett.* **1996,** *102*, 31-37.

18. Fontana, A.; Cavaliere, P.; Wahidulla, S.; Naik, C. G.; Cimino, G. *Tetrahedron* **2000,** *56*,

7305-7308.
19. Look, S. A.; Fenical, W.; Jacobs, R. S.; Clardy, J. *Proc. Natl. Acad. Sci. USA* **1986,** *83*, 6238-6240.
20. Pettit, G. R.; Herald, C. L.; Doubek, D. L.; Herald, D. L.; Arnold, E.; Clardy, J. *J. Am. Chem. Soc.* **1982,** *104*, 6846-6848.
21. Talpir, R.; Benayahu, Y.; Kashman, Y.; Pannell, L.; Schleyer, M. *Tetrahedron Lett.* **1994**, *35*, 4453–4456.
22. Feling, R. H.; Buchanan, G. O.; Mincer, T. J.; Kauffman, C. A.; Jensen, P. R.; Fenical, W. *Angew. Chem.-Int. Edit.* **2003,** *42*, 355-357.
23. a) Quinoa, E.; Adamczeski, M.; Crews, P.; Bakus, G. J. *J. Org. Chem.* **1986,** *51*, 4494-4497 b) Adamczeski, M.; Quinoa, E.; Crews, P. *J. Am. Chem. Soc.* **1989,** *111*, 647-654.
24. Gunasekera, S. P.; Gunasekera, M.; Longley, R. E.; Schulte, G. K. *J. Org. Chem.* **1990,** *55*, 4912-4915.
25. Cuadros, R.; de Garcini, E. M.; Wandosell, F.; Faircloth, G.; Fernandez-Sousa, J. M.; Avila, J. *Cancer Lett.* **2000,** *152*, 23-29.
26. Cohen, S. S. *Perspect. Biol. Med.***1963**, *6*, 215-227.
27. Rustum, Y. M.; Raymakers, R. A. *Pharmacol. Ther.* **1992**, *56*, 307-321.
28. Thomas, X. *Expert Opin. Pharmacother*. **2009**, *10*, 221-237.
29. Erba, E.; Bergaaschi, D.; Bassano, L.; Damia, G.; Ronzoni, S.; Faircloth, G. T.; D'lncalci, M. *Eur. J. Cancer* **2001**, *37*, 97-105.
30. Jin, S.; Scott, K. W. *Clin. Cancer Res.* **1999**, *5*, 3790.
31. Jordan, M. A.; Wilson, L. *Nature Reviews* **2005**, *4*, 253-265.
32. Cormier, A.; Knossow, M.; Wang, C. G.; Gigant B. *Methods in Cell Biology*, **2010**, *95*, 373-390.
33. Jackson, K. L.; Henderson, J. A.; Phillips, A. J. *Chem. Rev.* **2009**, *109*, 3044-3079.
34. McBride, A.; Butler, S. K. *Am. J. Health-Syst Pharm*. **2012**, *69*, 745-755.
35. a) Leusch, H.; Moore, R. E.; Paul, V. J.; Mooberry, S. L.; Corbett, T. H. *J. Nat. Prod.* **2001**, *64*, 907-910. b) Harrigan, G. G.; Yoshida, W. Y.; Moore, R. E.; Nagle, D. G.; Park, P. U.; Biggs, J.; Paul, V. J.; Mooberry, S. L.; Corbett, T. H.; Valeriote, F. A.*J. Nat. Prod.* **1998**, *61*, 1221-1225.
36. Pettit, G. R. *Fortschr. Chem. Org.Naturst.* **1997**,*70*, 1-79.
37. Francisco, J. A. ;Cerveny, C. G.; Meyer, D. L.; Mixan, B. J.; Klussman, K.; Chace, D. F.; Rejniak, R. X.; Gordon, K. A.; DeBlanc, R.; Toki, B. E.; Law, C.-L.; Doronina, S. O.; Siegall, C. B.; Senter, P. D.; Wahl, A. F. *Blood* **2003**, *102*, 1458-1465.
38. McKee, T. C.; Ireland, C. M.; Lindquist, N.; Fenical, W. *Tetrahedron Lett.***1989**, *30*, 3053-3056.
39. Munoz-Alonso, M. J.; Gonzalez-Santiago, L.; Zarich, N.; Martinez, T.; Alvarez, E.; Rojas, J. M.; Munoz,A. *J.Pharmacol. Exp.Ther.* **2008**, *324*, 1093-1101.

40. Pettit, G. R.; Herald, C. L.; Doubek, D. L.; Herald, D. L.; Arnold, E.; Clardy, J. *Journal of the American Chemical Society* **1982,** *104*, 6846-6848.
41. Kuznetsov, G.; TenDyke, K.; Towel, M. J.; Cheng, H.; Liu, J.; Marsh, J. P.; Schiller, S. E. R.; Spyvee, M. R.; Yang, H.; Seletsky, B. M.; Shaffer, C. J.; Marceau, V.; Yao, Y.; Suh, E. M.; Campagna, S.; Fang, F. G.; Kowalczyk, J. J.; Littlefield, B. A. *Mol. Cancer Ther.* **2009**,*8*, 2852–2860
42. Rocha-Lima, C. M.; Bayraktar, S.; Macintyre, J.; Raez, L.; Flores, A. M.; Ferrell, A.; Rubin, E. H.; Poplin, E. A.; Tan, A. R.; Lucarelli, A.; Zojwalla, N. *Cancer* **2012**, *17*, 4262-4270.
43. Bucar, F.;Wube, A.; Schmid, M. *Nat. Prod. Rep.* **2013**, *30*, 525-545.
44. a) Henrich, C. J.; Beutler, J. A. *Nat. Prod. Rep.* **2013**, *30*, 1284-1298. b) Kepp, O., Galluzzi, L.; Lipinski, M.; Yuan, J.; Kroemer, G. *Nat. Rev. Drug Discov.* **2011**, *10*, 221-237.
45. Michelini, E.; Cevenini, L.; Mezzanotte, L.; Coppa, A.; Roda, A. *Anal. Bioanal. Chem.* **2010,** *398*, 227-238.
46. a) Johnson, J. I.; Decker, S.; Zaharevitz, D.; Rubinstein, L. V.; Venditti, J.; Schepartz, S.; Kalyandrug, S.; Christian, M.; Arbuck, S.; Hollingshead, M.; Sausville, E. A. *British Journal of Cancer* **2001,** *84*, 1424-1431. b) Yamori, T. *Cancer Chemother. Pharmacol.* **2003**, *52*, 74-79.
47. Blees, J. S.; Schmid, T.; Thomas, C. L.; Baker, A. R.; Benson, L.; Evans, J. R.; Goncharova, E. I.; Colburn, N. H.; McMahon, J. B.; Henrich, C. J. *J. Biomol. Screen.* **2010,** *15*, 21-29.
48. a) Futamura, Y.; Kawatani, M.; Kazami, S.; Tanaka, K.; Muroi, M.; Shimizu, T.; Tomita, K.; Watanabe, N.; Osada,H. *Chem. Biol.* **2012**, *19*, 1620-1630. b) Schulze, C. J.; Bray, W. M.; Woerhmann, M. H.; Stuart, J.; Lokey, S.; Linington, R. G. *Chem. Biol.* **2013**, *20*, 285-295.

Chapter 2.

1. Minto, R. E.; Blacklock. B. J. *Prog. Lipid Res.* **2008**, *47*, 233-306.
2. Van Soest, R. W. M.; Fusetani, N.; Andersen, R. J. In *Sponge Sciences*; Watanabe, Y.; Fusetani, N., Eds.; Springer-Verlag: Tokyo, 1998; p 3-30.
3. Wright, A. E.; McConnell, O. J.; Kohmoto, S.; Lui, M. S.; Thompson, W.; Snader, K. M. *Tetrahedron Lett.* **1987**, *28*, 1377-1380.
4. Gung, B. W.; Omollo, A. O. *J. Org. Chem.* **2008**, *73*, 1067-1070.
5. Ohtani, I.; Kusumi, T.; Kashman, Y.; Kakisawa, H. *J. Am. Chem. Soc.* **1991**, *113*, 4092-4096.
6. We named **2-6** as (-)-durynes B-F by considering that the duryne was well-recognized.
7. Breitmaier, E.; Voelter, W. In *Carbon-13 NMR Spectroscopy*; VCH Verlagsgesellschaft: Weinheim, 1987; p192-194. The C-4 carbons of (*E*)- and (*Z*)-2-octene resonate at 33.0 and 27.1 ppm, respectively.
8. Fusetani, N.; Shiragaki, S.; Matsunaga, S.; Hashimoto, K. *Tetrahedron Lett.* **1987**, *28*, 4313-4314.

9. Wright, A. E.; McConnell, O. J.; Kohmoto, S.; Lui, M. S.; Thompson, W.; Snader, K. M. *Tetrahedron Lett.* **1987**, *28*, 1377-1380.
10. Gross, M. L. *Int. J. Mass Spectrom.* **2000**, *200*, 611-624.
11. Sui, B.; Yeh, E. A.-H.; Curran, D. P. *J. Org. Chem.* **2010**, *75*, 2942-2954.
12. DiDonato, G. C.; Busch, K. L. *Biomed. Mass Spectrom.***1985**, *12*, 364-366.
13. Fusetani, N.; Shiragaki, T.; Matsunaga, S.; Hashimoto, K. *Tetrahedron Lett.* **1987**, *28*, 4313-4314.
14. Ochi, M.; Ariki, S.; Tatsukawa, A.; Kotsuki, H.; Fukuyama, Y.; Shibata, K. *Chem. Lett.* **1994**, 89-92.
15. Kobayashi, M.; Mahmud, T.; Tajima, H.; Wang, W.; Aoki, S.; Nakagawa, S.; Mayumi, T.; Kitagawa, I. *Chem. Pharm. Bull.* **1996**, *44*, 720-724.
16. Guo, Y.; Gavagnin, M.; Trivellone, E.; Cimino, G. *Tetrahedron* **1994**, *50*, 13261-13268.
17. Ueoka, R.; Ise, Y.; Matsunaga, S. *Tetrahedron* **2009**, *65*, 5204-5208.
18. Kim, J. S.; Lim, Y. J.; Im, K. S.; Jung, J. H.; Shim, C. J.; Lee, C.-O.; Hong, J.; Lee, H. *J. Nat. Prod.* **1999**, *62*, 554-559.
19. Sui, B.; Yeh, E. A.-H.; Curran, D. P. *J. Org. Chem.* **2010**, *75*, 2942-2954.
20. Okamoto, C.; Nakao, Y.; Fujita, T.; Iwashita, T.; van Soest, R. W. M.; Fusetani, N.; Matsunaga, S. *J. Nat. Prod.* **2007**, *70*, 1816-1819.
21. Dai, J.-R.; Hallock, Y. F.; Cardellina, J. H. II.; Gray, G. N.; Boyd, M. R. *J. Nat. Prod.* **1996**, *59*, 860-865.
22.Seo, Y.; Cho, K. W.; Rho, J.-R.; Shin, J.; Sim, C. J. *Tetrahedron* **1998**, *54*, 447-462.
23. Kim, J. S.; Im, K. S.; Jung, J. H.; Kim, Y.-L.; Kim, J.; Shin, C. J.; Lee, C.-O. *Tetrahedron* **1998**, *54*, 3151-3158.
24. Behl, C.; Davis, J. B.; Lesley, R.; Schubert, D. *Cell* **1994**, *77*, 817-827.
25. Mori. K. *Bioorg. Med. Chem.* **2007**, *15*, 7505-7523.
26. (a) Lee, J.; Kobayashi, Y.; Tezuka K.; Kishi, Y.; *Org. Lett.* **1999**, *1*, 2181-2184; (b) Kobayashi, Y.; Hayashi, N.; Kishi, Y. *Org. Lett.* **2001**, *3*, 2253-2255.; (c) Higashibayashi, S.; Czechtizky, W.; Kobayashi, Y.; Kishi, Y. *J. Am. Chem. Soc.* **2003**, *125*, 14379-14393
27. Matsumori, N.; Kaneno, D.; Murata, M.; Nakamura, H.; Tachibana K. *J. Org. Chem.* **1999**, *64*, 866-876.
28. Curran, D. P.; Zhang, Q.; Lu, H.; Gudipati, V. *J. Am. Chem. Soc.* **2006**, *128*, 9943-9956.
29. Mori, K. Determination of Structure Including Absolute Configuration of Bioactive Natural Products, Comprehensive Natural Products II Chemistry and Biology,; Mander, L.; Liu H.-W., Ed.; Elsevier: Oxford, 2010; Vol. 9, pp 147-167.
30. Hitora, Y.; Takada, K.; Okada, S.; Matsunaga, S.; *Tetrahedron* **2011**, *67*, 4530-4534.

31. Inokuma, Y.; Yoshioka, S.;Ariyoshi, J.; Arai, T.;Hitora, Y.; Takada, K.; Matsunaga, S.;Rissanen, K.; Fujita, M. *Nature* **2013**, *495*, 461-466.
32. Inokuma, Y.; Yoshioka, S.;Ariyoshi, J.; Arai, T.;Hitora, Y.; Takada, K.; Matsunaga, S.;Rissanen, K.; Fujita, M. *Nature* **2013**, *501*, 262.
33. Imaizumi, K.; Terasima, H.; Akasaka, K.; Ohrui, H.; *Anal. Sci.* **2003**, *19*, 1243-1249.
34. The inability to HPLC separation of diastereomeric linear acetylenes with remote stereogenic centers are discussed in Sui, B.; Yeh, E. A.-H.; Curran, D. P. *J. Org. Chem.* **2010**, *75*, 2942-2954.
35. Grieco, P. A.; Gilman, S.; Nishizawa, M. *J. Org. Chem.* **1976**, *41*, 1485-1486.

Chapter 3.

1. Skropeta, D.; Wei, L. *Nat. Prod. Rep.* **2014**, *31*, 999-1025.
2. Skropeta, D. *Nat. Prod. Rep*. **2008**, *25*, 1131-1166.
3. Cantrell, C. L.; Gustafson, K. R.; Cecere, M. R.; Pannell, L. K.; Boyd, M. R. *J. Am. Chem. Soc.* **2000,** *122*, 8825-8829.
4. Rashid, M. A.; Cantrell, C. L.; Gustafson, K. R.; Boyd, M. R. *J. Nat. Prod.* **2001,** *64*, 1341-1344.
5. Rashid, M. A.; Gustafson, K. R.; Boyd, M. R. *Tetrahedron Lett.* **2001,** *42*, 1623-1626.
6. Rashid, M. A.; Gustafson, K. R.; Crouch, R. C.; Groweiss, A.; Pannell, L. K.; Van, Q. N.; Boyd, M. R. *Org. Lett.* **2002,** *4*, 3293-3296.
7. Takada, K.; Choi, B. W.; Rashid, M. A.; Gamble, W. R.; Cardellina, J. H., II; Van, Q. N.; Lloyd, J. R.; McMahon, J. B.; Gustafson, K. R. *J. Nat. Prod.* **2007,** *70*, 428-431.
8.Takemoto, D.; Takekawa, Y.; Van Soest, R. W. M.; Fusetani, N.; Matsunaga, S. *Bios. Biotechnol. Biochem.* **2007,** *71*, 2697-2700.
9. Plaza, A.; Baker, H. L.; Bewley, C. A. *J. Nat. Prod.* **2009,** *72*, 324-324.
10. Bowman, E. J.; Gustafson, K. R.; Bowman, B. J.; Boyd, M. R. *J. Biol. Chem.* **2003,** *278*, 44147-44152.
11. Kobayashi, Y.; Tan, C. H.; Kishi, Y. *J. Am. Chem. Soc.* **2001,** *123*, 2076-2078.
12. Ohtani, I.; Kusumi, T.; Kashman, Y.; Kakisawa, H. *J. Am. Chem. Soc.* **1991**, *113*, 4092-4096.

Chapter 4.

1. a) Brown, J. M.; Wouters, B. G *Cancer Res.* **1999,***59*, 1391-1399. b) Stewart, Z. A.; Westfall, M. D.; Pietenpol, J. A. *Trends in Pharmacol. Sci.* **2003,** *24*, 139-145.
2. Sherwood, S. W.; Schimke, R. T. *Methods Cell Biol.* **1995,** *46*, 77-97.

3. Sakaue-Sawano, A.; Kurokawa, H.; Morimura, T.; Hanyu, A.; Hama, H.; Osawa, H.; Kashiwagi, S.; Fukami, K.; Miyata, T.; Miyoshi, H.; Imamura, T.; Ogawa, M.; Masai, H.; Miyawaki, A. *Cell* **2008,** *132*, 487-498.

4. Sakaue-Sawano, A.; Kobayashi, T.; Ohtawa, K.; Miyawaki, A. *Bmc Cell Biol.* **2011,** *12:2*.

5. Wohlschlefel, J. A.; Dwyer, B. T.; Dhar, S. K.; Cvetic, C.; Walter, J. C.; Dutta, A. *Science* **2000**, *290*, 2309-2312.

6. Fusetani, N.; Sugawara, T.; Matsunaga, S.; Hirota, H. *J. Org. Chem.* **1991,** *56*, 4971-4974.

7. Yagi, H.; Matsunaga, S.; Fusetani, N. *Tetrahedron* **1993,** *49*, 3749-3754.

8. Matsunaga, S.; Fusetani, N. *J. Org. Chem.* **1995,** *60*, 1177-1181.

9. Fusetani, N.; Sugano, M.; Matsunaga, S.; Hashimoto, K. *Experientia* **1987,** *43*, 1234-1235.

10. Matsunaga, S.; Fusetani, N.; Hashimoto, K. *Experientia* **1986,** *42*, 84-84.

11. Sharma, G. M.; Burkhold.Pr. *J. Chem. Soc. D-Chem. Commun.* **1971**, 151-152.

12. Fusetani, N.;Yasumuro, K.; Matsunaga, S.; Hashimoto, K. *Tetrahedron Lett.* **1989**, *30*, 2809-2812.

13. a) Sakemi, S.; Ichiba, T.; Kohmoto, S.; Saucy, G.; Higa, T. *J. Am. Chem. Soc.* **1988,** *110*, 4851-4853. b) Nishimura, S.; Matsunaga, S.; Yoshida, M.; Hirota, H.; Yokoyama, S.; Fusetani, N. *Bioorg. Med. Chem.* **2005,** *13*, 449-454. c) Mosey, R. A.; Floreancig, P. E. *Nat. Prod. Rep.* **2012,** *29*, 980-995.

14. a) Tanaka, J.; Higa, T.; Kobayashi, M.; Kitagawa, I. *Chem. Pharmac. Bull.* **1990,** *38*, 2967-2970. b) Terry, D. R.; Spector, I.; Higa, T.; Bubb, M. R. *J. Biol. Chem.* **1997,** *272*, 7841-7845.

15. Sata, N. U.; Wada, S.; Matsunaga, S.; Watabe, S.; van Soest, R. W. M.; Fusetani, N. *J. Org. Chem.* **1999,** *64*, 2331-2339.

16. Fusetani, N.; Matsunaga, S.; Konosu, S. *Tetrahedron Lett.* **1981,** *22*, 1985-1988.

17. Tsukamoto, S.; Yamashita, T.; Matsunaga, S.; Fusetani, N. *J. Org. Chem.* **1999,** *64*, 3794-3795.

18. Fusetani, N.; Warabi, K.; Nogata, Y.; Nakao, Y.; Matsunaga, S.; van Soest, R. R. M. *Tetrahedron Lett.* **1999,** *40*, 4687-4690.

19. Warabi, K.; Nakao, Y.; Matsunaga, S.; Fukuyama, T.; Kan, T.; Yokoshima, S.; Fusetani, N. *Comp. Biochem. Physiol. –B:Biochem. Mol. Biol.* **2001,** *128*, 27-30.

20. Nakao, Y.; Maki, T.; Matsunaga, S.; van Soest, R. W. M.; Fusetani, N. *Tetrahedron* **2000,** *56*, 8977-8987.

21. Matsunaga, S.; Fusetani, N.; Konosu, S. *Tetrahedron Lett.* **1984,** *25*, 5165-5168.

22. Hamada, T.; Sugawara, T.; Matsunaga, S.; Fusetani, N. *Tetrahedron Lett.* **1994,** *35*, 719-720.

23. Matsunaga, S.; Fusetani, N.; Kato, Y.; Hirota, H. *J. Am. Chem. Soc.* **1991,** *113*, 9690-9692.

24. Tsukamoto, S.; Kato, H.; Hirota, H.; Fusetani, N. *Tetrahedron Lett.* **1996,** *37*, 5555-5556.

25. a) Li, H. Y.; Matsunaga, S.; Fusetani, N. *J. Nat. Prod.* **1994,** *57*, 1464-1467. b) Takada, K.; Okada, S.; Matsunaga, S. *Fisheries Sci.* **2014,** *80*, 1057-1064.

26. Ciminiello, P.; Costantino, V.; Fattorusso, E.; Magno, S.; Mangoni, A.; Pansini, M. *J. Nat. Prod.* **1994,** *57*, 705-712.
27. Tsuda, M.; Ishibashi, M.; Agemi, K.; Sasaki, T.; Kobayashi, J. *Tetrahedron* **1991,** *47*, 2181-2194.
28. Nakao, Y.; Matsunaga, S.; Fusetani, N. *Tetrahedron Lett.* **1993,** *34*, 1511-1514.
29. Fusetani, N.; Shiragaki, T.; Matsunaga, S.; Hashimoto, K. *Tetrahedron Lett.* **1987,** *28*, 4313-4314.
30. Garcia, E. E.; Benjamin, L. E.; Fryer, R. I. *J. Chem. Soc.-Chem. Commun.* **1973**, 78-79.
31. Kanazawa, S.; Fusetani, N.; Matsunaga, S. *Tetrahedron Lett.* **1993,** *34*, 1065-1068.
32. Lee, K. H.; Nishimura, S.; Matsunaga, S.; Fusetani, N.; Horinouchi, S.; Yoshida, M. *Cancer Sci.* **2005,** *96*, 357-364.
33. a) Saito, S.; Watabe, S.; Ozaki, H.; Fusetani, N.; Karaki, H. *J. Biol. Chem.* **1994,** *269*, 29710-29714. b) Burres, N. S.; Clement, J. J. *Cancer Res.* **1989,** *49*, 2935-2940. c) Hori, M.; Saito, S. Y.; Shin, Y. Z.; Ozaki, H.; Fusetani, N.; Karaki, H. *Febs Lett.* **1993,** *322*, 151-154.
34. a) Schmitz, F. J.; Deguzman, F. S.; Hossain, M. B.; Vanderhelm, D. *J. Org. Chem.* **1991,** *56*, 804-808. b) McCarthy, P. J.; Pitts, T. P.; Gunawardana, G. P.; Kellyborges, M.; Pomponi, S. A. *J. Nat. Prod.* **1992,** *55*, 1664-1668.
35. Hande, K. R. *BBA-Gene Struct. Expr.* **1998,** *1400*, 173-184.
36. Marshall, K. M.; Barrows, L. R. *Nat. Prod. Rep.* **2004,** *21*, 731-751.
37. Nurse, P.; Masui Y.; Hartwell, L. *Nat. Med.* **1998**, 4, 1103-1106.
38. Lampson, M. A., Kapoor, T. M. *Nat. Chem. Biol.* **2006**, *2*, 19-27.
39. Kobayashi, J.; Murayama, T.; Ohizumi, Y. *J. Nat. Prod.* **1989**, *52*, 1173-1176.
40. Takahashi, Y.; Tsuda, M.; Fromont, J.; Kobayashi, J. *Heterocycles* **2006**, *67*, 791-796.
41. Takahashi, Y.; Yamada, M.; Kubota, T.; Fromont, J.; Kobayashi, J. *Chem. Pharm. Bull.* **2007**, *55*, 1731-1733.
42. The accurate optical rotation of **2** cannot be obtained because the UV absorption of **2** interfered with the D line of a Na light.
43. Ishibashi, M.; Ohizumi, Y.; Cheng, J.-F.; Nakamura, H.; Hirata, Y.; Sasaki, T.; Kobayashi, J. *J. Org. Chem.***1988**, *53*, 2855-2858.
44. Crabbe, P.; Klyne, W. *Tetrahedron* **1967**, *23*, 3449-3503.
45. Kikuchi, T.; Mori, Y.; Yokoi, T.; Nakazawa, S.; Kuroda, H.; Masada, Y.; Kitamura, K.; Kuriyama, K. *Chem. Pharm. Bull.* **1983**, *31*, 106-113.
46. (a) Tsoukatou, M.; Marechal, J. P.; Hellio, C.; Novakovic, I.; Tufegdzic, S.; Sladic, D.; Gasic, M. J.; Clare, A. S.; Vagias, C.; Roussis, V. *Molecules* **2007**, *12*, 1022-1034. (b) Sladic, D.; Gasic, M. J. *Molecules***2006**, *11*, 1-33. (c) Gordaliza, M. *Mar. Drugs* **2010**, *8*, 2849-2870.
47. Urban, S.; Capon, R. J. *J. Nat. Prod.* **1992**, *55*, 1638-1642.